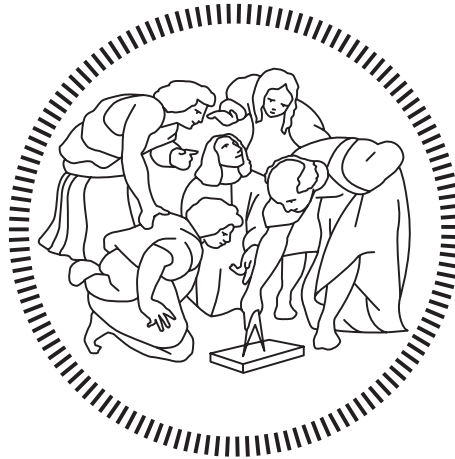


Politecnico di Milano

SCHOOL OF INDUSTRIAL AND INFORMATION ENGINEERING

Master of Science – Biomedical Engineering



White matter damage and brain atrophy anticipate
delayed functional impairments in repetitive mild
traumatic brain injured mice

Supervisor

Prof. Filippo Rossi

Co-Supervisor

Dott.ssa Elisa Roncati Zanier

Candidate

Elisa Pisu – 927627

Academic Year 2020 – 2021

Abstract

Background. Repetitive mild TBI (rmTBI) is highly common in contact sports such as American football and especially boxing, where repetitive head impacts are an inherent part of the game. Participating in contact sports is thought to increase an individual's risk for later-life impairments and neurodegeneration due to rmTBI, with neuropsychological sequelae involving changes in cognition, mood, and motor control.

To date there are no diagnostic tools that can be used to monitor the long-term consequences of rmTBI since brain structural changes are so subtle that cannot be seen on computed tomography (CT) or conventional magnetic resonance imaging (MRI) exams.

By using a mouse model of closed head rmTBI we investigate the possibility to use structural MRI and diffusion tensor imaging (DTI) analysis to monitor brain damage before the onset of functional impairment.

Methods. Anaesthetised adult C57BL/6J mice were subjected to 1 or 5 injuries every 48 hours by electromagnetic controlled impact device while sham mice underwent the same procedure without the delivery of any injury. Sensorimotor deficits were evaluated up to 12 months post injury by neuroscore and SNAP tests. Locomotor activity and cognitive function were evaluated by open field and novel object recognition tests at 6 and 12 months after injury. DTI and structural MRI were done at 6 and 12 months to examine microscopic changes, such white matter damage, and macroscopic changes, as structural damage and brain atrophy, respectively.

Results. A reduction of fractional anisotropy (FA) was evident at 6 months in the corpus callosum and other white matter fibers of rmTBI but not smTBI mice. In the rmTBI these differences persist up to 12 months post injury. The reduction in FA was associated to an increase in radial and mean diffusivity and a reduction in axial diffusivity. Cortical thickness was reduced underneath the injury site and was associate to brain atrophy in cortical and subcortical areas.

Conclusions. rmTBI but not smTBI produced white matter pathology and brain atrophy detectable by MRI analysis before the appearance of sensorimotor and cognitive impairment in adult male and female mice.

Estratto

Introduzione. Il trauma cranico lieve ripetuto (*repetitive mild traumatic brain injury*: rmTBI) è molto comune negli sport di contatto, tra cui il football Americano, il rugby, e in particolare il pugilato, in cui i pugni rivolti alla testa del giocatore fanno parte del gioco stesso. Praticare sport di contatto, a causa degli impatti ripetuti alla testa, aumenta il rischio di sviluppare processi neurodegenerativi a lungo termine, i quali possono portare ad alterazioni neuropsicologiche tra cui cambiamenti della cognizione, dell'umore e del controllo motorio. A causa delle sue dimensioni e della sua natura viscoelastica, il cervello umano (in particolare la materia bianca, per la sua struttura anisotropica e altamente organizzata) è particolarmente vulnerabile alle forze accelerative/decelerative impartite durante un urto alla testa. Proprio per la sua natura viscoelastica, esso subisce deformazioni quando sottoposto a graduali accelerazioni in condizioni di carico quotidiano, mentre risponde rigidamente a seguito di deformazioni dinamiche molto rapide, conseguenti ad un impatto. Nel primo caso gli assoni sono capaci di deformarsi, raggiungendo una lunghezza pari al doppio rispetto alla lunghezza di riposo, e tornare allo stato iniziale senza deformazioni residue; nel secondo, il citoscheletro assonale può essere danneggiato, provocando un danno assonale diffuso (*diffuse axonal injury*: DAI). Il DAI è un danno microscopico che avviene in assenza di evidenti alterazioni a livello del tessuto cerebrale ed è un'importante causa di morbidità nei pazienti rmTBI. Ad oggi non esistono strumenti diagnostici che permettano di monitorare le conseguenze a lungo termine del rmTBI, in quanto i danni strutturali al cervello sono così limitati da non essere evidenziati con esami di tomografia computerizzata (*computed tomography*: CT) o con tecniche convenzionali di risonanza magnetica per immagini (*magnetic resonance imaging*: MRI), essendo capaci di rilevare alterazioni anatomiche a livello millimetrico, e quindi solo le manifestazioni macroscopiche di una patologia. L'imaging a tensore di diffusione (DTI) è una tecnica avanzata di neuroimaging che fornisce informazioni quantitative sul DAI. Il suo principio di funzionamento è basato sulla misura della diffusione delle molecole d'acqua all'interno della materia bianca, nella quale, avendo essa una struttura anisotropica altamente organizzata, le molecole d'acqua diffondono in maniera direzionale e ordinata. Nei normali fasci assonali quindi, la libera diffusione dell'acqua è limitata radialmente; negli assoni danneggiati dal DAI, la diffusione delle molecole d'acqua è alterata, causando metriche di diffusione anomale. In particolare, le misure di DTI più utilizzate sono l'anisotropia frazionaria (FA), la diffusività media (MD), la diffusività radiale (RD) e la diffusività assiale (AD). La FA definisce il grado di direzionalità della diffusione e fornisce il vettore principale di diffusione delle molecole d'acqua. La FA è altamente sensibile ai cambiamenti nella microstruttura dell'assone: valori intorno ad 1 indicano un'elevata direzionalità della diffusione delle molecole d'acqua e quindi un assone sano; valori intorno a 0 indicano una bassa direzionalità della diffusione delle molecole d'acqua, suggerendo un danno assonale. La MD fornisce informazioni sulla diffusività media dell'acqua e quantifica la densità cellulare e di membrana: un suo aumento

indica la presenza di processi patologici come edema e necrosi. La RD valuta la diffusione perpendicolare al vettore principale: rivela patologie della mielina e il suo valore aumenta in presenza di processi di demielinazione. La AD valuta la diffusione parallela al vettore principale: rivela la presenza di degenerazione assonale e il suo valore tende ad aumentare con l'invecchiamento. In pazienti che hanno subito il rmTBI, sono stati osservati valori di FA diminuiti e di MD aumentati in numerosi tratti della materia bianca, alcuni dei quali erano correlati con la persistenza e la gravità dei sintomi. Studi su modelli animali hanno mostrato una corrispondenza diretta tra la patologia DAI e la diminuzione di anisotropia della materia bianca.

Oltre ad alterazioni microscopiche, a seguito del rmTBI, il cervello può andare incontro ad alterazioni macroscopiche quali perdita di volume e atrofia. L'encefalopatia traumatica cronica (CTE) è una tauopatia progressiva che si verifica come conseguenza della rmTBI, causata dagli impatti alla testa che subiscono gli atleti durante l'attività sportiva. La CTE è caratterizzata da atrofia cerebrale globale con corpo calloso assottigliato, ventricoli dilatati e cavum septum pellucidum, e ha un profilo clinico e neuropatologico che diventa sintomatico 8-10 anni dopo aver sperimentato rmTBI, con manifestazioni che includono sintomi di irritabilità, impulsività, aggressività, depressione, perdita di memoria a breve termine e maggiore tendenza al suicidio. Tali sintomi sono stati associati ad atrofia cerebrale in numerosi studi condotti su atleti dopo anni dal termine della carriera sportiva. L'utilizzo della MRI strutturale per valutare le variazioni volumetriche del cervello a seguito del rmTBI rappresenta un'opzione ottimale, grazie al suo diffuso utilizzo in ambito clinico e alla sua elevata risoluzione e specificità nel rilevare atrofia cerebrale.

Attraverso l'utilizzo di un modello murino di rmTBI a scatola cranica intatta (*closed head injury*: CHI), abbiamo investigato la possibilità di utilizzare analisi di MRI strutturale e di DTI per monitorare il danno cerebrale prima della comparsa di compromissioni funzionali a lungo termine. Lo scopo del nostro lavoro è stato quello di identificare due importanti biomarcatori di rmTBI, quali: i) alterazioni microstrutturali, come il DAI, tramite analisi di DTI e ii) alterazioni macrostrutturali, come atrofia cerebrale e assottigliamento corticale, tramite scansioni di MRI pesate in T2. Tali biomarcatori sono stati valutati a 6 e 12 mesi dall'ultimo impatto.

Metodi. Topi C57BL/6J maschi e femmine anestetizzati sono stati sottoposti ad un singolo impatto (*single mild TBI*: smTBI) o 5 impatti (rmTBI), tramite un dispositivo elettromagnetico ad impatto controllato con un intervallo tra gli impatti ripetuti di 48 ore. I topi controllo sono stati sottoposti alle stesse procedure ma senza ricevere alcun impatto. La comparsa di deficit sensorimotori sono stati valutati dopo 1 e 5 settimane, 3, 6 e 12 mesi dall'ultimo impatto tramite i test *SNAP* e *neuroscore*. Il test *SNAP* valuta i parametri neurologici quali vista, propiocezione, forza degli arti e postura; un topo che non presenta deficit neurologici ottiene un punteggio pari a 0. Il test *neuroscore* valuta i riflessi del topo e il corretto utilizzo degli arti: un topo neurologicamente intatto ottiene un punteggio pari a 12. L'attività locomotoria e le funzioni cognitive sono state valutate a 6 e 12 mesi dopo l'ultimo impatto attraverso i test *open field* (OF), che misura l'attività locomotoria e il livello

di ansia del topo posizionato all'interno di un'arena aperta, e *novel object recognition* (NOR), il quale valuta l'apprendimento e la memoria del topo tramite l'utilizzo di diversi oggetti, che il topo sarà capace di ricordare in assenza di deficit della memoria. Le analisi di DTI (tramite la sequenza di eccitazione *echo-planar imaging* (EPI)) e MRI strutturale (tramite la sequenza 3D *fast low-angle shot* (FLASH)) sono state effettuate dopo 6 e 12 mesi per esaminare i danni microscopici cerebrali, come il danneggiamento della materia bianca, e i danni macroscopici strutturali, come l'atrofia cerebrale e l'assottigliamento corticale.

Risultati. La funzionalità sensorimotoria esaminata tramite i test *SNAP* e *neuroscore* ha mostrato la presenza di deficit nel gruppo rmTBI dopo 1 settimana e dopo 12 mesi dall'ultimo impatto. Dopo 1 settimana tali deficit non erano invece presenti nel gruppo smTBI, suggerendo che impatti multipli siano necessari per causare compromissioni funzionali nel nostro modello murino. Il test NOR ha rivelato la presenza di deficit di memoria nel gruppo rmTBI sia soggetta ad una evoluzione temporale, infatti mentre a 6 mesi non si osservavano differenze tra i topi controllo e i rmTBI a 12 mesi è emerso un impairment cognitivo solo nei topi esposti a traumi ripetuti.

Una riduzione nel valore di FA è stata evidente nei topi sottoposti ad impatti ripetuti nel corpo calloso e in altre fibre della materia bianca già a 6 mesi dall'ultimo impatto, ma non nei topi sottoposti ad un singolo impatto. Nei topi sottoposti a rmTBI tale riduzione si è mantenuta fino a 12 mesi. Solo nel gruppo rmTBI la riduzione in FA era associata ad un aumento della MD e della RD ed a una diminuzione della AD sia a 6 che a 12 mesi. La valutazione dello spessore corticale ha mostrato una riduzione al di sotto del sito di impatto. Inoltre era presente atrofia cerebrale che coinvolgeva non solo aree corticali quali la corteccia frontale, occipitale, parietotemporale, ma anche aree sottocorticali quali corpo calloso e ippocampo, e tali alterazioni strutturali erano già evidenti a 6 mesi dal trauma.

Conclusioni. Ad oggi non esistono validi biomarcatori diagnostici per il monitoraggio delle conseguenze a lungo termine del rmTBI negli atleti, e le linee guida per il ritorno alla pratica sportiva a seguito di un urto alla testa sono esclusivamente basate sulla valutazione dei sintomi. Il nostro studio dimostra che il trauma cranico lieve ripetuto, ma non singolo, causa atrofia e danno alla sostanza bianca, rilevabili attraverso analisi di DTI e di MRI strutturale prima dello sviluppo di compromissioni sensorimotorie e cognitive in topi adulti. Traducendo questa situazione negli atleti, l'obiettivo è quello di poter identificare danni cerebrali macrostrutturali e microstrutturali con l'uso di tecniche avanzate di MRI per agire terapeutamente prima della comparsa di alterazioni nella cognizione, nell'umore e nel controllo motorio dell'atleta. Ciò sarebbe estremamente utile in quanto, fino ad ora, tali danni possono essere diagnosticati solo post-mortem. Inoltre, trovare biomarcatori prognostici mediante tecniche di MRI sarebbe di fondamentale importanza anche per valutare l'efficacia di nuovi approcci terapeutici in grado di prevenire le gravi disabilità fisiche, psichiatriche, emotive e cognitive causate dal rmTBI alleggerendo inoltre l'enorme onere procurato dagli effetti a lungo termine del rmTBI sul sistema sanitario.

Sono attualmente in corso le analisi istopatologiche dei cervelli murini, che serviranno a comprendere le cause delle alterazioni misurate mediante le analisi di MRI.

Table of contents

Abstract	1
Estratto	2
Table of contents	5
List of figures	7
List of tables	12
Chapter 1 Introduction	13
1.1 Mild traumatic brain injury.....	13
1.1.1 Traumatic brain injury: epidemiology and current concerns.....	13
1.1.2 Mild TBI: definition and diagnostic criteria.....	15
1.2 Sport-related TBI.....	18
1.2.1 General recognition of the acute and chronic effects of repeated mild TBI..	19
1.2.2 Pathophysiology associated with repetitive mild TBI.....	21
1.2.2.1 Acute stages after mild TBI – window of vulnerability.....	22
1.2.2.2 Chronic stages and neurodegenerative sequelae after repetitive mild TBI ...	25
1.3 Animal models of repetitive mild TBI.....	29
1.3.1 Translational challenges.....	29
1.3.2 Translational strategies.....	31
1.3.3 Closed head repetitive mild TBI model in mice.....	34
1.3.4 Novel closed-head model using a piston-controlled impact.....	34
1.4 Neuroimaging of mild TBI.....	37
1.4.1 Traditional neuroimaging in clinical mild TBI and limitations.....	37
1.4.2 Advanced magnetic resonance neuroimaging for mild TBI.....	39
1.4.2.1 MRI signal.....	40
1.4.2.2 Structural T2 weighted imaging.....	44
1.4.2.3 Diffusion tensor imaging.....	45
1.5 Imaging biomarkers for repetitive mild TBI.....	54
1.5.1 Microscopic changes: diffuse axonal injury – DTI analysis.....	54
1.5.2 Macroscopic changes: brain atrophy – Volumetric analysis.....	56
Chapter 2 Aim	59
Chapter 3 Materials and methods	60
3.1 Ethics statement.....	60
3.2 Animals.....	60
3.3 Injury Protocol.....	61

3.4	Experimental Design	63
3.5	Assessment of consciousness	64
3.6	Behavioural tests	64
3.6.1	Simple Neuroassessment of Asymmetric Impairment	64
3.6.2	Neuroscore	66
3.6.3	Open Field	68
3.6.4	Novel Object Recognition	69
3.7	MRI acquisition and analysis	72
3.7.1	Acquisition	72
3.7.2	Analysis	72
3.8	Statistics	74
Chapter 4	Results	75
4.1	Assessment of consciousness following repetitive mild TBI.....	75
4.2	Effects of repetitive mild TBI on behavioural outcome.....	76
4.3	White matter damage assessed by DTI	78
4.4	Brain atrophy assessed by structural MRI	83
Chapter 5	Discussion and conclusions	87
Acronyms	91
Bibliography	93

List of figures

Figure 1 - Different types of TBI. (A) Sheared brain: axonal injury on CT (upper panel) and MRI using SWI (lower panel) in an adult patient with TBI. Note the greater sensitivity of MRI for detection of microbleeds (green arrows), which are commonly associated with DAI, a common form of brain injury, particularly in high-velocity road traffic incidents, in which traumatic axonal injury (damage to WM tracts) occurs over a widespread area. (B) Bruised brain: contusional brain injury (green arrows) on CT in two patients with TBI, located in the frontal and temporal regions. (C) Brain under pressure: epidural haematoma (bleeding between the skull and outer coverings of the brain; green arrows) on CT in two patients with TBI. (D) Disconnected brain: WM tracts measured with DTI and visualised by MRI tractography in an adult patient with TBI 12 days after the injury (upper panel) and at 6-month follow-up (lower panel)..... 14

Figure 2 - Historical timeline of developments and the cumulative number of published cases of dementia pugilistica and CTE. 21

Figure 3 - Typical imaging findings of SIS. (A, B) Admission noncontrast axial CT images, and (C) artists rendition demonstrate a small heterogeneous left frontal subdural hematoma (white arrows), that causes complete effacement of the basal cisterns and brainstem distortion. Note the subtle linear increased density in the region of the circle of Willis (black arrow), consistent with pseudo-subarachnoid hemorrhage, resulting from the marked elevation in intracranial pressure. Although there is preservation of the gray-white matter differentiation, there is asymmetric enlargement of the left hemisphere, consistent with hyperemic cerebral swelling (dysautoregulation). Note how side A is smaller than side B, even though the left hemisphere is mildly compressed by the overlying subdural hematoma. The extent of mass effect and midline shift is disproportional to the volume of the subdural hematoma..... 24

Figure 4 - Gross pathology of CTE. (A) The coronal section of normal brain, showing the expected size and relationship of the cerebral cortex and ventricles. (B) The brain from a retired professional football player, showing the characteristic gross pathology of CTE with severe dilatation of (1) ventricles II and (2) III, (3) cavum septum pellucidum, (4) marked atrophy of the medial temporal lobe structures, and (5) shrinkage of the mammillary bodies. 29

Figure 5 - In general, real-life TBI is a complex mixture of injury mechanisms, such as impact and rotational forces. Animal models can be used to study these mechanisms more separately, with better control of physical parameters. 31

Figure 6 - Pubmed searches. (A) Number of studies published about single severe TBI models. 22 from 2001 to 2010, 117 from 2011 to 2021. (B) Number of studies published about repetitive mild TBI models, 20 from 2001 to 2010, 215 from 2011 to 2021. 32

Figure 7 - (A) Weight drop model. (B) Piston driven model, which can use an electromagnetic driven impactor device (left) or a pneumatic driven impactor (right). 33

Figure 8 - (A) FPI model: a rapid fluid pulse injection is used to cause injury directly onto the surface of the dura. (B) Blast-injury model: injury is caused by primary injury of blast. 33

Figure 9 - Typical imaging findings of second-impact syndrome (SIS). A: Head CT obtained after second impact. *Arrows* point to thin bilateral subdural hematomas. B: Sagittal T1-weighted brain MR image. *Arrows* point to downward descent of the midline structures. C: Axial T2-weighted MR image. *Arrows* point to thalamic injury. D: Axial DWI. *Arrow* points to left thalamic injury. Restricted diffusion was proven by calculation of apparent diffusion coefficient (not shown).
..... 39

Figure 10 - Graph shows the number of articles found in PubMed from 1990 to the year indicated on the x-axis, with search terms as specified in the legend. An increase in rate of publication is demonstrated with all search parameters after 2005. 40

Figure 11 - (a) Spin orientation in absence and (b) in presence of an external magnetic field. M_z is the net magnetization representing the contribution of all spins. (c) Precessional motion of a spin.41

Figure 12 - Net magnetization (a) under normal conditions and (b) after the effect of the external electromagnetic wave..... 41

Figure 13 - Relaxation process. Spins reversed in the transverse plane start precessing around the main direction of the magnetic field causing. The sum of these spins (M_{xy}) decrease with a time called T2 relaxation time..... 42

Figure 14 - Relaxation recovery process. Relaxation process. Once the effect of external 90° RF pulse end, spins reversed in the transverse plane start recovering their original magnetization (M_z) with a recovery time called T1..... 42

Figure 15 - Left: Temporal evolution of the net magnetization. Right: free induction decay obtained by reading the transverse magnetization. 43

Figure 16 - Spin refocusing with a 180° EM pulse. 43

Figure 17 - Spin-echo sequence. 44

Figure 18 - Generation of a series of echoes using a train of consecutive 180° pulses, following. Repetition time (TR) is the time between 90° pulses..... 44

Figure 19 - Simulation that shows how tissues intensities can be modulated varying TR and TE. . 45

Figure 20 - The origin of DTI contrast. (A) Contrast and signal levels in the DWI of a human brain (left) reflect water diffusion behavior (random walk) (right). Diffusion behavior is modulated by tissue structure at the cellular level: For instance, diffusion can be restricted within cells, water may escape when cell membranes are permeable and might then experience a tortuous pathway in the extracellular space (hindrance). (B) In the presence of a magnetic field gradient, magnetized water molecule hydrogen atoms are dephased. The amount of dephasing is directly related to the diffusion distance covered by water molecules during measurement. The overall effect of this dephasing is an interference, which reduces MRI signal amplitudes. In areas with fast water diffusion (e.g., within ventricles), the signal is deeply reduced, while in areas of slow water diffusion (e.g., WM bundles), the signal is only slightly reduced. This differential effect results in a contrast in the DWI, which is not visible in standard MRI images..... 48

Figure 21 - From diffusion anisotropy to diffusion tensor. (a) An ideal phantom composed by ordered (upper part) and random (lower part) structures. The image intensity is high when the structures have the same orientation as the diffusion gradient applied (represented by the hand). (b) Diffusion tensors visualized as ellipsoids and rendered as anisotropy and orientation-encoded color maps. 50

Figure 22 - DTI contrasts in the mouse brain. The CSF in the ventricle is indicated by the white arrow. The CC is indicated by yellow arrows. The unit for mean, axial, and radial diffusivity is $\mu\text{m}^2/\text{ms}$. FA and RA are unitless. In the DEC image, major white-matter tracts characterized by high anisotropy are shown with color-coded orientations. The color scheme is: red, left–right; green, rostral–caudal; and blue, superior–inferior. 51

Figure 23 - Schematic diagrams illustrating how complex neuropathology can affect DTI results. (a) Normal myelinated axons and the corresponding diffusion tensor and axial and radial diffusivity (λ_{\parallel} and λ_{\perp} , respectively). The diffusion tensor is represented by the ellipsoid here and is shown in subsequent plots as a grey ellipsoid with dashed lines. (b,c) Axon and myelin injury with and without cell infiltration. (d,e) Axon and myelin injury with axonal loss, with and without cell infiltration. 52

Figure 24 - In 30 mTBI patients, vestibular disturbances correlated with (a) decreased FA in cerebellar regions and (b) increased mean diffusivity in vermian lobules of the spinocerebellum, while convergence insufficiency in 25 mTBI patients correlated with (c) increased FA in the right anterior thalamic and right geniculate nucleus optic radiations. Images were derived from tract-based spatial statistics (TBSS) results and rendered on T1-weighted images from the Montreal Neurologic Institute in (a) coronal, (b) sagittal, and (c) axial projections. Significant voxels ($P<.05$, corrected for multiple comparisons) were thickened by using TBSS fill function into local tracts (red) and overlaid on WM skeleton (blue). 56

Figure 25 - Areas of significant volume loss are demonstrated by projecting coregistered data from (a) medial and (b) lateral projections in 28 mTBI patients and (c) medial and (d) lateral projections in 22 control subjects onto right cerebral hemisphere templates after 1 year (Bonferroni-corrected $P<0.05$). 59

Figure 26 - Mice were anesthetized with isoflurane inhalation (induction 3%; maintenance 1.5%) in an N2O/O2 (70%/30%) mixture and placed in a stereotaxic frame on a heating pad to maintain their body temperature at 37 °C. MTBI was induced using a 5 mm diameter rigid impactor driven by an electromagnetic controlled impact device (impactOne, Leica), rigidly mounted at an angle of 20° to the vertical plane and applied to the intact scalp, between bregma and lambda, over the left parieto-temporal cortex (antero-posteriority: -2.5 mm, laterality: -2.5 mm), at impactor velocity 5 m/s and deformation depth 1 mm. 62

Figure 27 - Schematic representation of the experimental design. mTBI was induced by electromagnetic controlled impact device on the left parietal bone in anesthetised mice. Mice subjected to repeated mTBI (rmTBI) received 5 injuries 2 days apart, over a period of 8 days. Mice subjected to a single head impact (smTBI) received one injury the 8th day.
w, week; m, month; MRI, magnetic resonance imaging; DTI, diffusion tensor imaging; T2-WI, T2-weighted imaging; SNAP, Simple Neuroassessment of Asymmetric Impairment; NOR, novel object recognition. 63

Figure 28 - Description of score system assigned to the SNAP test. 65

Figure 29 - Graphical representation of the test to perform on the animal.	65
Figure 30 - Graphical representation of the position of the objects inside the arena.	71
Figure 31 - Workflow followed to create the in-house atlases. Acquired images are corrected and averaged to create an in-house Template. This is normalized over an ex vivo template and masked. The template mask is projected to the reference images that are subsequently masked and averaged to create an in-house skull stripped template. This brain template is again normalized over the ex-vivo template and reference atlases obtained back-projecting the ex-vivo atlas.....	73
Figure 32 - Automatic parcellation procedure. Firstly, the brain extraction is performed (yellow arrows). Subsequently the normalization of the reference images to the subject brain (red arrows) allowed the projection and the fusion of all the reference atlases to the subject space (blue arrows).	74
Figure 33 - Effect of rmTBI on apnea, righting reflex and percentage of weight change on sham, smTBI and rmTBI groups. (A) Righting reflex in smTBI (n=12), rmTBI (n=17), and sham (n=22) group. (B) Righting reflex in rmTBI mice (n=17). (C) Apnea duration in rmTBI mice (n=17). (D) Percentage of weight change between sham group (n=26) and rmTBI group (n=18) at all time points. Note: the 12m time point for the smTBI group was not recorded for any of the parameters. Data are presented as mean \pm standard deviation. **P<0.01; ***P<0.001 versus sham by a 2-way ANOVA followed by Tukey's multiple comparison test.	76
Figure 34 - Behavioural deficits. Sensorimotor deficits were longitudinally rated at 1 and 5 weeks, 3 and 6 months after the last smTBI, and 1 and 5 weeks, 3, 6 and 12 months after the last rmTBI (n=18) or sham (n=26) by Simple Neuroassessment of Asymmetric Impairment (SNAP) (A) and Neuroscore (B). RmTBI had a significantly worst SNAP score and Neuroscore at 1 week that emerged again with SNAP test at 12 months. No differences were found between smTBI (n=12) and sham mice at all time points in both tests. Data are presented as mean \pm standard deviation. **P<0.01; ***P<0.001 versus sham by a mixed-effect model followed by Sidak's post hoc multicomparison test. Open Field (OF) test for measuring locomotor activity and Novel Object Recognition (NOR) test for the investigation of learning and memory were performed at 6 months for smTBI (n=12), rmTBI (n=18) and sham (n=26) (C) and at 12 months (D) after the last repetitive mTBI (rmTBI, n=18) or sham (n=14). The OF test revealed that the rmTBI moved significantly more compared to shams both at 6 and 12 months. The NOR test showed no differences between sham and rmTBI at 6 months, while a significant difference emerged at 12 months. Data are presented as mean \pm standard error of the mean deviation. *P<0.05 versus sham by unpaired t-test.	77
Figure 35 - DTI analysis of WM. (A) Voxel-based analysis evaluated at 6 months post rmTBI with red-yellow voxels showing a significant FA reduction (p<0.05 by unpaired t-test) in rmTBI (n=18) compared to sham (n=14-16) mice. (B) Schematic representation of the ROI of WM tracts.....	79
Figure 36 - ROI based analysis of ipsilateral (il) and contralateral (cl) WM showing mean FA values longitudinally assessed at 6 and 12 months post rmTBI. Data are presented as mean \pm standard deviation. **P<0.01, ***P<0.001 rmTBI vs sham by a mixed-effect model followed by Sidak's post hoc multicomparison test. EC: external capsule, BCC: body of the corpus callosum, GCC: genu of the corpus callosum; SCC: splenium of the corpus callosum.....	80

Figure 37 - ROI based analysis of ipsilateral (il) and contralateral (cl) WM showing mean AD, RD, MD values longitudinally assessed at 6 and 12 months post rmTBI. (A-D) AD was reduced at both time points compared to sham values in the il-EC (p<0.001), il-SCC (p<0.001) and il-BCC at 12m (P<0.001) and cl-EC (p<0.05), cl-SCC(p<0.01) and cl-BCC at 12m (p<0.01). (E-H) RD was increased at both time points compared to sham values in the il-EC (p<0.001), il-SCC (p<0.01), il-BCC (P<0.001), il-GCC at 6m (P<0.001) and cl-EC (p<0.05), cl-SCC(p<0.01), cl-BCC (P<0.01), cl-GCC at 6m (p<0.5). (I-M) MD was increased only in the il-GCC at 6 m (P<0.05) and il-BCC at 12 m (p<0.01). Data are presented as mean ± standard deviation. **P<0.01, ***P<0.001 rmTBI vs sham by a mixed-effect model followed by Sidak's post hoc multicomparison test.

EC: external capsule, BCC: body of the corpus callosum, GCC: genu of the corpus callosum; SCC: splenium of the corpus callosum..... 81

Figure 38 - ROI based analysis in smTBI (n=9) and sham (n=9) mice. Data are presented as mean ± SEM. *P<0.05 versus sham by unpaired t-test.

EC: external capsule, BCC: body of the corpus callosum, GCC: genu of the corpus callosum; SCC: splenium of the corpus callosum..... 82

Figure 39 - Structural MRI analysis. (A) Representative image showing cortical thickness in sham and rmTBI mice. (B) Voxel-based analysis of the cortical thickness showing red-yellow voxels in which the thickness was reduced in rmTBI (n=18) compared to sham (n=15-16) mice (p<0.05 by unpaired t-test). 84

Figure 40 - Semi-automatic quantification of ipsilateral (il) and contralateral (cl) volumes of the frontal-cortex (A), occipital cortex (B), parietotemporal cortex (C), hippocampus (D) and corpus callosum (E) longitudinally assessed at 6 and 12 months post rmTBI. *P<0.05, **P<0.01, ***P<0.001 rmTBI vs sham by a mixed-effect model followed by Sidak's post hoc multicomparison test. 85

Figure 41 - Comparing smTBI with sham mice at 6 months the quantification of brain volumes in (A) frontal, (B) occipital, (C) parieto-temporal cortex, (D) hippocampus and (E) corpus callosum. Data are presented as mean ± SEM. Unpaired t-test. 86

List of tables

Table 1 - Summary of pathological changes proposed by McKee.....	26
Table 2 - Summary of clinical features according to McKee.....	27
Table 3 - ROI based analysis at 6 months revealed no differences were found in AD, RD, MD between smTBI and sham. *P<0.05 versus sham by unpaired t-test.	83

Chapter 1

Introduction

1.1 Mild traumatic brain injury

1.1.1 Traumatic brain injury: epidemiology and current concerns

Traumatic brain injury (TBI) is defined as an alteration in brain function, or other evidence of pathology, caused by an external force¹ exceeding regular exposure from normal body movement which the brain normally can accommodate². In other words, TBI is a neurological event marked by structural, cellular, molecular pathology, and/or functional disturbances in the central nervous system (CNS) triggered by head trauma³. TBI is a major cause of death and disability worldwide, and accounts for a significant proportion of life-years with disability⁴. TBI is classified as mild (e.g., brief change in mental status), moderate, or severe (e.g., extended unconsciousness, coma). Severe TBI has a mortality rate estimated at 30–40%⁵, with survivors experiencing a substantial burden of physical, psychiatric, emotional, and cognitive disabilities⁶. However, such disabilities are not restricted to severe cases, but also occur frequently after mTBI (mTBI)⁶. Population-based studies show that 50–60 million people worldwide (including at least 3.5 million in the US, and 2.5 million in Europe) are affected by a new TBI each year^{7,8}, of which the great majority (60–95%) are mTBI⁹. Across all ages TBI represents 30–40% of all injury-related deaths, and it is projected to remain the most important cause of disability from neurological disease until 2030 (2–3 times higher than the contribution from Alzheimer’s disease (AD) or cerebrovascular disorders)^{10,11}. The incidence of TBI in high income countries has increased in the elderly to a greater extent than might be expected from demographic aging, whereas increased use of motorised vehicles in low-income and middle-income countries has led to a rise in TBI from road traffic incidents¹⁰. It has been estimated that TBI costs the global economy approximately \$US400 billion annually, that represents about 0.5% of the entire annual global output¹⁰. Deficiencies in prevention, care, and research urgently need to be addressed to reduce the huge burden and societal costs of TBI.

TBI is a complex condition, characterized by wide variations in the clinical manifestations which are attributable to the complexity of the brain, and to the high variability of the damage that depend on type, intensity, direction, and duration of the external forces¹⁰. Following the primary damage inflicted at the time of injury, the secondary damage evolves over hours, days or even over a lifetime in some cases, and it is strongly dependent on host responses to the primary injury. TBI is best viewed as a collection of different disease processes (Figure 1), with different clinical patterns and outcomes, each requiring different approaches to

diagnosis and management¹⁰. For this reason, treatment strategies, should aim to the needs of the individual patient.

TBI might confer a long-term risk for cognitive impairment and dementia^{12,13}, stroke^{14,15}, parkinsonism^{16,17}, and epilepsy¹⁸, and is associated with an increased long term mortality rate compared with rates for the general population¹⁰. These risks also occur in milder forms of TBI, especially after repetitive mild injuries, with a vast majority of TBI patients suffering from mTBI. Clinical progress has not kept pace with the rising global burden of TBI and the recognition of the prolonged effects of injury. Since the introduction of computed tomography (CT) scanning into routine care more than 40 years ago, there have been no major improvements in outcome prediction after TBI in high income countries with developed trauma systems¹⁰. Promising advances in disease characterisation and monitoring of disease evolution are coming thanks to more sensitive methods for the detection of TBI-related blood biomarkers and to new magnetic resonance imaging (MRI) techniques. Among these, there are: a) susceptibility-weighted imaging (SWI), a MRI sequence that is particularly sensitive to compounds that distort the local magnetic field, like microbleeds resulting from microvascular shearing, as seen in diffuse axonal injury (DAI) (Figure 1A, lower panel); b) diffusion tensor imaging (DTI), a MRI method in which the directional movement of water molecules is used to estimate the location, orientation, and connectivity of white matter (WM) tracts; c) MR tractography, a three-dimensional modelling technique in which a visual representation of the location, orientation, and connectivity of neural tracts is constructed using data collected by diffusion MR sequences, such as DTI (Figure 1D)¹⁰.

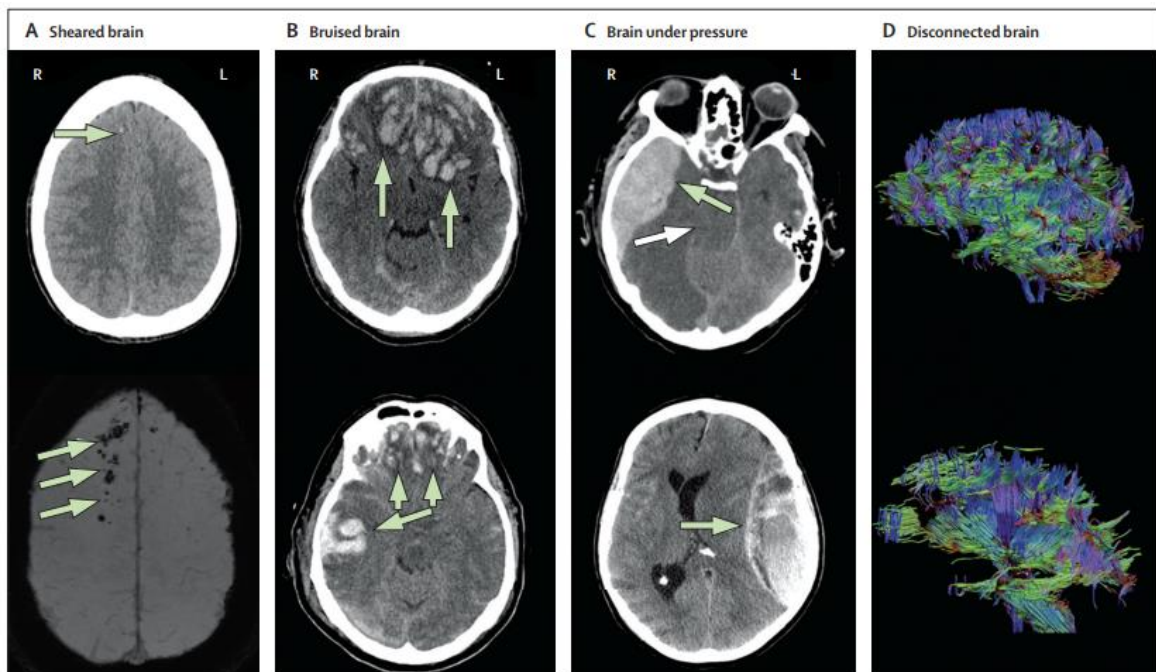


Figure 1 - Different types of TBI. (A) Sheared brain: axonal injury on CT (upper panel) and MRI using SWI (lower panel) in an adult patient with TBI. Note the greater sensitivity of MRI for detection of microbleeds (green arrows), which are commonly associated with DAI, a common form of brain injury, particularly in high-velocity road traffic incidents, in

which traumatic axonal injury (damage to WM tracts) occurs over a widespread area. (B) Bruised brain: contusional brain injury (green arrows) on CT in two patients with TBI, located in the frontal and temporal regions. (C) Brain under pressure: epidural haematoma (bleeding between the skull and outer coverings of the brain; green arrows) on CT in two patients with TBI. (D) Disconnected brain: WM tracts measured with DTI and visualised by MRI tractography in an adult patient with TBI 12 days after the injury (upper panel) and at 6-month follow-up (lower panel).¹⁰

Clinical research has, until recently, focused mainly on more severe TBI. Although the individual impact of mTBI is less, the category makes the largest contribution to the global burden of disability. Timely intervention and structured follow-up in this group could deliver substantial gains in public health and societal costs¹⁰. In particular, the greatest efforts should be aimed at finding ways to characterise the currently under-recognised risk of long-term disabling sequelae in patients with relatively mild injuries. The need for further development, validation, and implementation of prognostic models in TBI for the mild category is urgent¹⁰.

1.1.2 Mild TBI: definition and diagnostic criteria

Now labeled the “silent epidemic”, recognition of mTBI as a growing problem has prompted new research and insight into its diagnosis and management¹⁹. MTBI is typically caused by blunt non-penetrating closed-head injury (CHI) resulting in transient symptoms with no evident structural abnormalities on a routine CT scan of the brain²⁰. It has been reported that 28% of mTBI patients with normal CT have lesions on an MRI scan done within 2 weeks after the trauma, with lesions (contusions and/or multiple foci of haemorrhagic axonal injury) being associated with worse outcome²¹. While moderate and severe TBIs mainly are a neurosurgical and intensive care problem, at least in the acute phase, many cases of mTBI do not even undergo structural brain imaging analysis²⁰. Diagnostic assessment is often based on a single post-injury evaluation that, firstly, does not consider the dynamic nature of neurological processes following TBI, and secondly, does not adequately rule out rare cases of potentially life-threatening sequelae (e.g., intracranial hemorrhage, second impact syndrome (SIS))³.

Symptoms in mTBI are highly variable, and may, except for loss of consciousness (LOC) (which is not a mandatory sign), include physical (e.g., nausea and vomiting, dizziness, headache), cognitive (e.g., poor concentration and memory problems) and behavioural (e.g., irritability and emotional lability) symptoms²².

There is a wide variety of definitions for mTBI: the World Health Organization Collaborating Centre Task Force on Mild Traumatic Brain Injury found 38 different definitions used in the international literature, as well as a variety of terminologies (mild TBI, minor TBI, concussion, etc.)²³. By clinical convention, mTBI is diagnosed in patients who have sustained a CHI that results in a Glasgow Coma Scale (GCS) score of 13-15,

indicating minimal or no change in mental status²⁴. The GCS was developed in 1974 for the evaluation of severity of TBIs: it measures a person's level of consciousness after a brain injury, based on eye, verbal and motor behaviours, with a higher total score indicating a higher level of consciousness of the patient. The total score for the best eye opening, verbal response and motor response ranges from 3 to 15, with a sum score of 3 indicating total unresponsiveness and 15 indicating the best response (totally conscious)²⁵. Although the focus was on more severe brain traumas, the GCS also included a classification for "minor head injuries", with scores falling between 13 and 15 in the early phases of recovery, indicative of mild head injuries²⁶. With all the focus on severe TBI, the fact that 60-95% of all TBIs were mild went virtually unnoticed, being viewed as insignificant: at those times, patients were typically discharged within an hour, and no follow-up was recommended²⁶. Toward the end of the 1980s, Povlishock and Coburn published the first book devoted exclusively to minor head injury²⁷, where they provided compelling evidence from both animals and humans that axonal injury is the most consistent feature of mild to moderate injury²⁶. Studies by Gennarelli et al. were among the first that induced mTBI in monkeys and provided objective evidence that diffuse axonal shearing was more pronounced when rotational forces were applied²⁶. Like the studies on monkeys, the histological finding in humans yielded microscopic damage caused by mTBI. Thus, the scientific evidence that emerged up to the end of the 1980s supported that microscopic brain damage can be caused even by a minor TBI. This was especially relevant because traditional neuroimaging lacked the sensitivity to identify DAI in most cases. This objectified microscopic evidence led to the inference that there likely exists a neurogenic basis for the persistence of post-concussive symptoms²⁶.

A significant advance in the diagnosis of mTBI was achieved in 1993 when the American College of Rehabilitation Medicine (ACRM) published the diagnostic criteria for mTBI²⁸ in the *Journal of Head Trauma Rehabilitation*. Prior to this definition being published, most neurologists diagnosed a mTBI only if LOC was observed. ACRM authors suggested that LOC is not essential for diagnosing a mTBI and that post-traumatic amnesia (PTA) or neurological symptoms are sufficient to render a diagnosis, with this intuition being still supported by ongoing research. The inclusion criteria to diagnose a mTBI according to the ACRM were: 1) any period of LOC lasting 0-30 minutes; 2) any loss of memory for events immediately before and after the accident (PTA), lasting less than 24 h; 3) any alteration of mental state at the time of accident, which includes any sort of confusion, disorientation, or slowed thinking; 4) focal neurological deficits that may or may not be transient; 5) GCS score of 13-15 at 30 minutes post-injury. The exclusion criteria were: 1) LOC exceeding 30 minutes; 2) PTA persisting longer than 24 hours; 3) after 30 minutes, the GCS falling below 13²⁸.

The US Centers for Disease Control and Prevention (CDC) in 2003 defined mTBI as an insult to the head due to blunt contact or acceleration-deceleration of the head that results in one or more of the following clinical features: 1) transient confusion, disorientation, or impaired consciousness; 2) amnesia or memory dysfunction around the time of injury; 3)

neurological or neuropsychological dysfunction (in adults: seizure, headache, dizziness, irritability, fatigue, or poor concentration; in infants and young children: irritability, lethargy, or vomiting); and 3) any period of LOC lasting 0-30 minutes^{3,29}.

The World Health Organization (WHO) definition of mTBI came in 2004, and it generally follows the 1993 ACRM criteria but does not include alterations in mental status for diagnosis^{30,31}. Note that the 1993 ACRM and 2004 WHO definitions of mTBI include GCS and PTA criteria, whereas the CDC does not require either component; in addition, none require LOC³.

More recently, in 2009, the US Department of Veteran Affairs issued a Clinical Practice Guideline for the management of concussion and mTBI. This guideline established similar criteria to that of 1993 ACRM for diagnosis of brain injury in combat soldiers, with the additional neuroimaging requirement of structural imaging to be normal³.

Importantly, all these definitions are consistent with classifying TBI as a neurological event. Defining TBI as “an alteration in brain function, or other evidence of brain pathology, caused by an external force”¹, makes explicit the link between the functional alteration or structural pathology in the brain with an inciting insult. In these terms, TBI can be compared to other common diagnostic formulations that connote sudden onset of tissue pathology, such as “cerebrovascular accident” (CVA, commonly called “stroke”) and “acute myocardial infarction” (AMI, “heart attack”). Each of these conditions are diagnosed through a specific set of clinical signs, symptoms, and test results without reference to the underlying etiology or mediating pathophysiology, as they are medical events, not diseases *per se*³. However, while workups for CVA and AMI are based on established clinical definitions and validated medical protocols accepted around the world, the situation for TBI remains challenging and highly variable across geographic areas, institutions, and even between providers, especially at the mild end of the TBI spectrum. Diagnosing mTBI is particularly challenging since the majority are diagnosed hours, days, or even months after the accident. In these cases, the GCS lacks utility, because the scale cannot be administered retrospectively. Even though it is possible to retrospectively assess mTBI by evaluating if the patient experienced a gap in memory caused by LOC or PTA, these often come from the patient, family members, or witnesses, and collected during a single examination; therefore, are incomplete and unreliable. Moreover, other confounding factors such as recent substance use, neuropsychiatric comorbidities, psychogenic and/or psychosocial stress may further complicate the interpretation^{3,26}. Finally, the diagnosis is currently conferred without reference to validated biomarkers that are sensitive and specific for TBI, especially when mild, making diagnosis clinically challenging³.

1.2 Sport-related TBI

Perhaps the form of TBI that has garnered the greatest interest recently is repetitive mild TBI (rmTBI), as principally occurring in contact sports such as ice hockey, American football, rugby, and especially boxing^{32,33}, where repetitive head impacts are an inherent part of the game. rmTBI has been found to be highly common also among military personnel in Iraq and Afghanistan, with TBI accounting for about 28% of all combat casualties, of which approximately 88% are mild CHI³⁴. It appears that the terms mTBI and concussion have been used synonymously, the latter being more common in sports medicine and mTBI in general medical contexts. Concussion is a neurological syndrome defined by an inciting head injury that triggers abrupt onset of a clinically defined constellation of transient signs and symptoms that spontaneously resolves over a typical course of minutes to hours³. The term ‘concussion’ is used only to describe clinical symptoms after blunt impacts and not as an indicator of pathophysiological changes in the brain². Defining concussion as a syndrome highlights the link between an incident head injury with onset of a set of signs (observed by others) and symptoms (reported by the subject) that fall into four major categories: 1) somatic, which include headaches, nausea, vomiting, balance and/or visual problems, sensitivity to light and noise; 2) emotional, like sadness (until depression), nervousness and irritability; 3) sleep disturbance; 4) cognitive, including difficulty in concentrating or impaired memory³⁵.

It is estimated that 5–35% of more than 1.6 million American service personnel have sustained a concussion³⁶, and the number of sport-related concussion in the United States ranges from 300,000 to 3.8 million^{37,38}. Persistent accounts of rmTBI suffered by athletes have directed much needed attention to this growing and significant problem. Epidemiological studies reveal that about 60% of retired professional football players sustained at least one concussion during their careers³⁹ and approximately 25% experienced repeated injuries^{39,40}, with young athletes being more vulnerable to their effects than adults⁴¹. Football players and boxers, particularly those who make it to the professional level, are exposed to thousands of blows to the head over the course of many years. Clinical studies have shown that sport athletes with a history of previous concussions are more likely to have future concussive injuries than those with no history⁴². Defining clinically practical ways to measure the number of blows to the head among contact sport athletes is among the major challenges in the field of TBI. Up to now, the “gold standard” for determining a lifetime history of TBI is retrospective self-reports³⁵ through questionnaires developed to obtain athletes athletic and concussion histories and to provide meaningful and accurate estimates of overall repetitive TBI exposure^{43–45}. Although there are inherent limitations in retrospective self-reports, numerous studies have demonstrated their usefulness in evaluating the association between long-term rmTBI exposure and latent impairments with an acceptable level of reliability^{46,47}. Alternatively, other ways for measuring a subject’s cumulative trauma exposure are number of fights, fights per year, number of knockouts and years of fighting, that have already been utilized in studies with boxers. Among football

players, the total number of seasons, primary position and level achieved (high school, college, professional) have been considered as well. Frequency of fighting may be a complementary variable that requires consideration; fighting more frequently may reduce the time the brain has to fully recover from prior trauma and may be a risk factor that interacts with number of fights. However, each of these variables may have a slightly different influence on the development of long-term impairments and underlying neuropathology³⁵. MTBI does not typically cause structural changes seen on routine imaging studies, such as CT scan, but rather exert its pathological changes at the microscopic level⁴⁸. Most clinicians recognize post concussive syndrome (PCS) as the persistence of concussive symptoms beyond a month³⁵. Individuals at increased risk for PCS include athletes exposed to multiple concussions in close proximity to each other and athletes subjected to a double hit such as a direct helmet-to-helmet hit and then the head hitting the ground as the athlete falls⁴⁹. An athlete who experiences an additional head trauma while they are symptomatic from a prior concussion through the course of the same game or match is even at higher risk of suffering PCS³⁵. Reports of PCS resolution in symptomatic patients range from 10% at 1 week to 50% at 1-year post-injury^{50,51}. Although rare, there are reports where PCS take as long as 5 years to clear up after trauma⁴⁹.

1.2.1 General recognition of the acute and chronic effects of repeated mild TBI

In recent years, there has been an increasing interest about the potential long-term impact of repetitive head injuries in athletes playing high-impact sports and in military personnel. Participating in contact sports is thought to increase an individual's risk for later-life impairments and neurodegeneration due to rmTBI, with neuropsychological sequelae involving changes in cognition, mood, and motor control⁵².

Figure 2 shows the long history associated with the recognition of sport-related TBI's effects⁵³. In 1928, Martland termed the chronic neuropsychiatric sequelae in boxers the "punch drunk" syndrome, describing the symptoms as "a dragging of the leg and a general slowing down in muscular movements, hesitancy in speech, tremors of the hands and nodding movements of the head", and in more severe cases reporting "a peculiar tilting of the head, a marked dragging of one or both legs, a staggering, propulsive gait with the facial characteristics of the parkinsonian syndrome, or a backward swaying of the body, tremors, vertigo and deafness"⁵⁴, with a marked mental deterioration taking place finally. Martland assumed as pathophysiological event of the punch-drunken syndrome the formation of traumatic multiple haemorrhages deep in the brain⁵⁴. Then, dementia pugilistica evolved as another term in these boxers⁵⁵. The clinical picture of boxers affected by dementia pugilistica included psychiatric symptoms, emotional lability, personality changes, memory impairment and dementia, pyramidal and extrapyramidal dysfunction, and cerebellar impairment⁵³. Two decades later the first description of dementia pugilistica, Corsellis and

colleagues⁵⁶, in a landmark autopsy study of former professional and amateur boxers, described stereotypical neuropathological findings as neurofibrillary tangles (NFTs) accumulation in the superficial grey matter, especially at the base of the sulci, with prominent perivascular and periventricular pathology⁵⁷. In a re-examination of dementia pugilistica cases originally examined by Corsellis, with further cases added, 19 of 20 former boxers were found to have diffuse amyloid- β (A β) plaques in addition to NFTs⁵⁸. While dementia pugilistica had been recognized for decades, reports of a similar phenomenon in football emerged only in the early 1990's⁵⁷. The recognition that sports other than boxing were associated with the development of symptoms showing years after the initial trauma, characteristic of dementia pugilistica, lead to the preferred use of terms such as progressive traumatic encephalopathy and, later, chronic traumatic encephalopathy (CTE), which describes a more severe trauma-induced latent neurodegeneration⁵⁵. The first autopsy report on football players appeared in the literature only recently from Omalu and colleagues⁵⁹, which noted a pathology indistinguishable from that of dementia pugilistica, with frequent diffuse neocortical A β plaques and sparse NFTs pathology. This was the first time that CTE pathology was observed in a former NFL player. Whereas monitoring of head hits in boxing derives from records of knockouts, concussion histories in football players have been notoriously poor, due to both the absence of meticulous records and the culture of the sport, in which injuries are ignored by both players and coaching staff to keep players in the game. In a clinical study a general health questionnaire was completed by 2552 retired professional football players with an average age of 53.8 (\pm 13.4) years and an average professional football playing career of 6.6 (\pm 3.6) years; a second questionnaire focusing on memory and issues related to mild cognitive impairment was then completed by a subset of 758 retired professional football players (>50 year of age). Retired American football players with three or more reported concussions were found to have fivefold increased prevalence of mild cognitive disorders and threefold increased prevalence of substantial memory problems compared with retirees without a history of concussion³⁹.

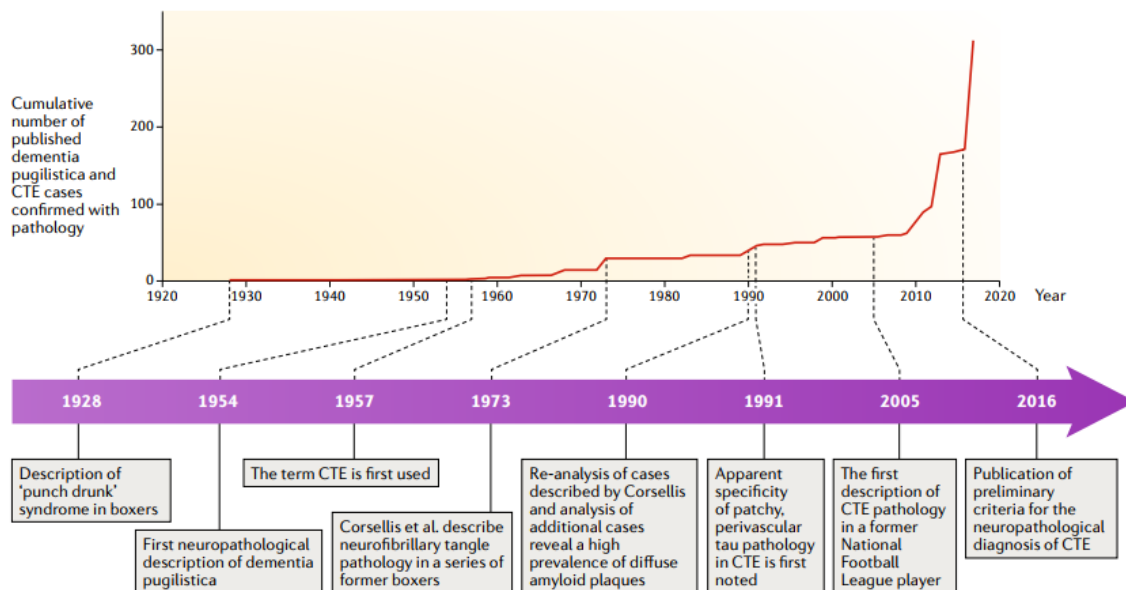


Figure 2 - Historical timeline of developments and the cumulative number of published cases of dementia pugilistica and CTE.⁵³

1.2.2 Pathophysiology associated with repetitive mild TBI

Brain trauma is an acute biomechanical event characterized by multiple pathophysiological processes that develop over time in a continuum. TBI survivors are affected by a “polypathology” whose main features are WM degradation, neuronal loss, protein misfolding, and persistent neuroinflammation. Interestingly, in addition to toxic processes, TBI also induces neurorestorative events that include neurogenesis, gliogenesis, angiogenesis, synaptic plasticity, and axonal sprouting. These processes are stimulated by endogenous growth-related factors and may persist for weeks to months, contributing to recovery after TBI⁶. The adult brain retains neurogenic zones with neural stem cells that can differentiate into functional neurons and migrate toward the site of injury^{6,60,61}. However, all the spontaneous brain restorative processes are short-lived^{6,62,63}.

After a mTBI a series of pathophysiologic processes including changes in metabolism, cerebral blood flow, and neurotransmission take place⁶⁴. Primary insult is the initial biochemical traumatic process as a result of linear acceleration/deceleration and/or rotational forces on the brain⁵⁵, with rotational forces being the most injurious⁶⁵. The biochemical response initiates a chain of neurometabolic and neurochemical reactions that include the activation of an inflammatory response, an imbalance of ionic concentrations, an increase in excitatory amino acids, a dysregulation of neurotransmitter release and synthesis, an imbalance of mitochondrial functions and energy metabolism, the production of free radicals, alterations in regional cerebral blood flow and metabolism^{66,67}. To lessen the primary traumatic impact on the brain, novel helmet designs, neck-strengthening exercises,

techniques to limit head contact and rule changes have been proposed^{9,68}. Secondary injury is the ensuing process that “occurs at some time after the primary impact and is largely preventable and treatable”⁶⁹, which includes neuroinflammation, excitotoxicity, axonal injury, metabolic derangements, blood-brain barrier disruption and cerebral edema⁵⁵. Both primary and secondary injury phases contribute to the extent of damage⁷⁰. However, in mTBI and rmTBI there is no clear spatial separation between primary and secondary injury, and mechanisms of pathology remain insufficiently characterized⁷¹. While in a single mild TBI (smTBI), a dynamic restorative process likely underpins the transient alteration in brain function, the long-term sequelae of rmTBI are more reminiscent of moderate–severe injuries, albeit to a reduced degree and in a starkly different temporal progression^{64,72}. It remains to be elucidated whether this worsening of long-term outcome is due to a cumulative effect of subsequent mTBIs or the independent or synergistic action of secondary processes exacerbating outcome⁷¹. Among the numerous potential acute pathological mechanisms of mTBI that could trigger progressive neuropathological changes², accumulating evidence suggests an altered neuroinflammatory state, that may persist for many years following a period of repetitive head impacts⁷³. The inflammatory response in mTBI includes local cerebral production of cytokines and chemokines, endothelial activation, microglial activation, and migration of systemic neutrophils, lymphocytes, and monocytes into the injured brain, spreading from the site of injury to remote regions in the brain⁶. Within a group of former American football players, the cellular density of CD68 immunoreactivity, a marker that labels phagocytic/activated microglia, was significantly increased in subjects with a history of football participation with or without CTE, when compared to noncontact sport athlete controls. Consistent with increased density of CD68 immunoreactive cells, microglia also exhibited a phenotypic change⁵⁴. In addition, a study demonstrated that duration of American football career was significantly associated with both increased activated microglia cell density (CD68) and with increased tau pathology⁷⁴. Experimental studies show that aspecific suppression of the inflammatory response may protect the injured tissue early on but harm the brain at chronic stages, suggesting that therapeutic strategies should aim at modulation, rather than inhibition, of the inflammatory response⁶. Overall, the association in human brain between neuroinflammation and tau pathology in CTE is also supported by mouse models, demonstrating possible mechanistic links^{2,75,76}. In summary, the inflammatory response plays a major role in the underlying pathophysiology in both acute and chronic mTBI: it has both detrimental and beneficial properties and activates CNS resident cells as well as inflammatory cells from the systemic circulation. Further development of biomarkers targeting the inflammatory response will likely be crucial for monitoring the clinical and pathological sequelae of TBI during life. Thus far, no anti-inflammatory trials in human TBI have shown an improvement in outcome. Improved understanding of the pathobiology of TBI will be crucial for the development of both diagnostics and eventual therapeutic agents².

1.2.2.1 Acute stages after mild TBI – window of vulnerability

It has been hypothesized that mTBI leads to transient functional impairments and is associated with specific neurometabolic and neurochemical events that may lead to a state of enhanced vulnerability in which a secondary insult may exacerbate the damage^{66,67,77,78}. In the acute phase following a mTBI, the most dangerous sequela is a second impact, which could bring to two different devastating outcomes. The first and more common outcome when a person's head receives a further hit within a certain time window of brain vulnerability, is the accumulation of damages which can bring to cumulative long-term consequences, such as the development of chronic cognitive impairments, as seen in boxers or football players, associated with accelerated and/or increased neurodegeneration in specific brain regions⁶⁷. Results from both human and animal studies illustrate a vulnerability period during which there is an increased symptom severity with slower recovery of neurological function if a further hit follows a previous mTBI⁷⁹. There is a lack of experimental evidence about the timing of brain vulnerability after a concussion⁸⁰ and what cause this vulnerability. Some suggest as causative factor the metabolic changes taking place after a mTBI⁷⁹. Following a mTBI neuronal membrane disruption causes a release of neurotransmitters (glutamate), and, consequently, an influx of excitatory amino acids (sodium and calcium) and an efflux of potassium. The disruption of the ionic equilibrium requires activation of cellular pumps to push ions back across their membrane gradients: being these pumps energy dependent, there is an immediate increase in glucose uptake, followed by a period of glucose metabolic depression. Questions about if this period may coincide with the time window of brain vulnerability remain open⁷⁹.

Another possible outcome, although rare, is the so-called SIS (Figure 3), which occurs when an athlete who sustains a head injury sustains a second injury before symptoms associated with the first have resolved, which may be even remarkably minor, and perhaps only involving a blow to the chest that jerks the athlete's head and indirectly imparts accelerative forces to the brain⁸¹. The pathophysiology of the SIS is thought to involve a loss of autoregulation of the brain's blood supply. Autoregulation is the process by which our brain normally maintains a constant blood flow: when the brain's blood pressure rises, there is a concurrent restriction in the diameter of arterioles. When SIS occurs, autoregulation disrupts: instead of constricting when blood pressure is normal or elevated, arterioles dilate and allow blood to rush through. The result is a massive inflow of blood within the cranium, and being the brain contained within the rigid skull, the result is a markedly increase in intracranial pressure. This phenomenon may result in herniation of the uncus of the temporal lobe below the tentorium, or in herniation of the cerebellar tonsils through the foramen magnum. The usual time from the second impact to brainstem failure is rapid, taking 2 to 5 minutes. Once brain herniation and brainstem compromise occur, ocular involvement and respiratory failure precipitously ensue, bringing to death^{35,81}. Each year, a few athletes lose their lives due to SIS, although the exact number is unclear.

A research study by Boden et al.⁸² reviewed 94 head incidents in high school and college football players reported to the National Centre for Catastrophic Sports Injury Research during 13 academic years (1989-2002). The injuries resulted in subdural hematoma in 75 athletes, subdural hematoma with diffuse brain edema in 10 athletes, diffuse brain edema in 5 athletes, and arteriovenous malformation or aneurysm in 4 athletes. What is noteworthy is that 59% of the contacts reported that the athletes had a history of a previous head injury, of which 71% occurred within the same season as the catastrophic event, and 39% of the athletes were playing with residual neurologic symptoms from the prior head injury. There were 9% deaths because of the injury, 51% athletes with permanent neurologic injuries, and 40% with serious injuries which fully recovered. What emerged from the study is that an unacceptably high percentage of high school players were playing with residual symptoms from a prior head injury. With a greater commitment from coaches, athletes, athletic trainers, and medical personnel to keep players with concussion symptoms off the field, deaths from SIS could be drastically reduced or eliminated⁸².

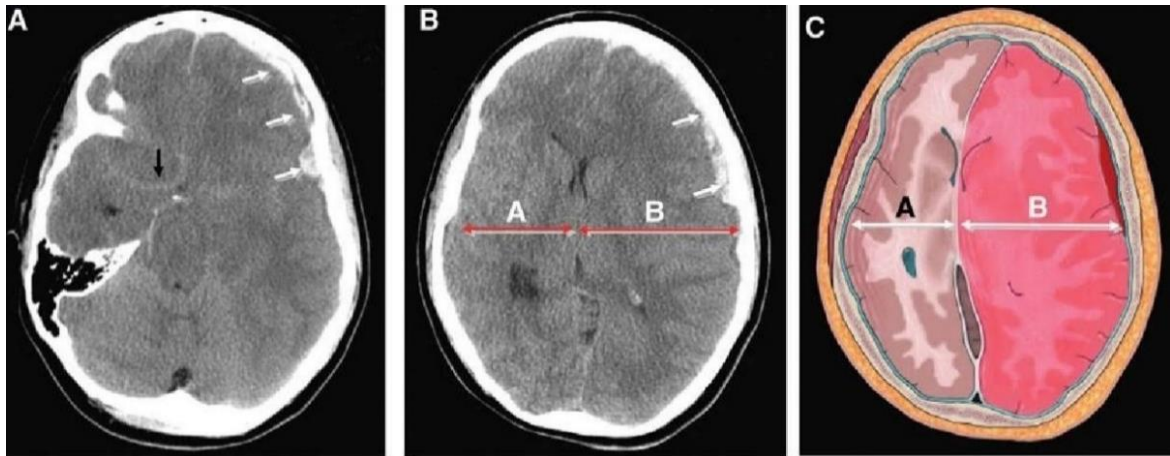


Figure 3 - Typical imaging findings of SIS. (A, B) Admission noncontrast axial CT images, and (C) artist's rendition demonstrate a small heterogeneous left frontal subdural hematoma (white arrows), that causes complete effacement of the basal cisterns and brainstem distortion. Note the subtle linear increased density in the region of the circle of Willis (black arrow), consistent with pseudo-subarachnoid hemorrhage, resulting from the marked elevation in intracranial pressure. Although there is preservation of the gray-white matter differentiation, there is asymmetric enlargement of the left hemisphere, consistent with hyperemic cerebral swelling (dysautoregulation). Note how side A is smaller than side B, even though the left hemisphere is mildly compressed by the overlying subdural hematoma. The extent of mass effect and midline shift is disproportional to the volume of the subdural hematoma.⁸³

1.2.2.2 Chronic stages and neurodegenerative sequelae after repetitive mild TBI

CTE is a progressive tauopathy that occurs as a consequence of rmTBI, most commonly caused by sport-related head injuries or military-related blast exposure, characterized by the widespread deposition of hyperphosphorylated tau (p-tau) as NFTs⁸⁴ within brain regions that correspond to the symptomatology⁸⁵. CTE has a distinct clinical and neuropathological profile that becomes symptomatic usually 8–10 years after experiencing rmTBI, with manifestations which include symptoms of irritability, impulsivity, aggression, depression, short-term memory loss and heightened suicidality⁸⁶. With advancing disease, more severe neurological changes develop, such as dementia, gait and speech abnormalities and parkinsonism; up to late stages, when CTE may be clinically mistaken for AD or frontotemporal dementia⁸⁷. However, the neuropathological changes of CTE are clearly distinctive from other tauopathies, including AD, corticobasal degeneration, frontotemporal lobar degeneration, and variant disorders³.

The spectrum of tau pathology within CTE suggests stages of disease severity that increase with age and years of contact sport participation^{74,84,85}. Tau is a protein normally expressed in neurons, which binds to and stabilizes microtubules, and promotes tubulin assembly. Aberrantly phosphorylated tau proteins interfere with these functions and are prone to pathogenic proteins aggregation, neurotoxicity, and progressive neurodegeneration³. Focal injury induces local tau protein phosphorylation, aggregation, and miscompartmentalization that lead to neuronal dysfunction through a characteristic pattern of regional spread throughout the brain³ in a prion-like manner^{88–90}. Zanier and colleagues^{91,92} induced severe TBI in wild-type mice and found progressive and widespread tau pathology, replicating their same findings in humans, in which a single severe brain trauma is associated with the emergence of widespread p-tau pathology late after injury. The earliest stage of CTE neuropathology manifests as isolated focal lesions within neocortical sulcal depths, typically in frontal cortex, that may be clinically asymptomatic or accompanied by minor neuropsychiatric impairment. The localization of early lesions likely reflects the effects of mechanical stress concentration at the base of cortical sulci, around small blood vessels, and along gray–white matter interfaces^{93,94}. Then, the neuropathological features of CTE extend to include multiple patchy foci within temporal and parietal cortices². They progress in 1) extensive p-tau immunoreactive NFTs and astrocytic tangles in the frontal and temporal cortices, in a patchy, superficial distribution, particularly around small cerebral vessels and at the depths of cerebral sulci, but also in limbic regions, diencephalon and brainstem nuclei; 2) extensive degeneration of axons and WM fibre bundles; 3) TAR DNA-binding protein 43, immunoreactive intraneuronal and intragial inclusions and neurites in most cases; 4) a relative paucity of A β deposits, although diffuse plaques are present in roughly one-half of the cases⁸⁴. Although tau-positive astrocytes, including thorn-shaped astrocytes, may be present, the presence of neuronal tau distinguishes CTE from age-related tau astroglipathy².

Many cases are associated with A β deposition; however, the distribution of abnormal tau is distinct from that seen in AD².

In advanced disease, there are also macroscopic abnormalities: generalized cerebral atrophy and enlarged ventricles; atrophy of the medial temporal lobe structures and mammillary bodies; cavum septi pellucidi, often with fenestrations; pallor of the substantia nigra^{84,87} (Table 1). These stages of CTE tau pathology correlate with age, clinical symptoms, duration of contact sports or repetitive head impact exposure, and length of survival after exposure². Notably, the progression of tauopathy in CTE is distinct from that of AD, in which tau pathology begins in the brainstem, progresses to the medial temporal lobe, and only in the later stages involves the neocortex^{2,95}. In addition to tauopathy, increased Lewy Body Disease pathology is observed in CTE in subjects of contact sports⁹⁶.

While other neuropathological features, as just mentioned, may be present, the diagnosis of CTE requires evidence of deep sulcal perivascular tau pathology⁹⁷.

Table 1 - Summary of pathological changes proposed by McKee.⁸⁴

Stage	Pathological changes
1	Tauopathy solely in the depths of the sulci in the frontal cortex
2	Tau aggregation in the cerebral cortex spreads to multiple layers.
3	Dispersed tauopathy not only affecting the frontal and temporal cortices but also degeneration of the insula, amygdala, and hippocampus
4	Neuronal loss and a widespread tauopathy across the cerebral cortex

In 2008, the Centre for the Study of Traumatic Encephalopathy (CSTE) at Boston University School of Medicine established the CSTE brain bank at the Bedford VA Hospital to analyse the brain and spinal cords after death of athletes, military veterans and civilians who experienced rmTBI⁸⁴. Through this effort, McKee et al.⁸⁴ analysed post-mortem brains obtained from a cohort of 85 subjects with histories of rmTBI and found evidence of CTE in 68 subjects (76%), including athletes and military veterans. Within the cohort, CTE correlated with increased duration of football play, survival after football and age at death. Moreover, CTE was not the sole diagnosis in 37% of cases, of which 12% were diagnosed with motor neuron disease, 11% with AD, 16% with Lewy body disease and 6% with frontotemporal lobar degeneration, in addition to CTE. The frequent association of CTE with other neurodegenerative disorders suggests that repetitive brain trauma and p-tau protein deposition promote the accumulation of other abnormally aggregated proteins including TAR DNA-binding protein 43 (identified as the major disease protein in amyotrophic lateral sclerosis), A β protein (involved in AD) and alpha-synuclein (involved in Parkinson's disease).

Out of a group of 202 former football players who have died and donated their brains to research, the percentage of players who have pathologically confirmed CTE is remarkably high (>87%), with the frequency increasing from high school to college to professional player²: 0 of 2 pre-high school players, 3 of 14 in high school (21%), 48 of 53 college athletes (91%), 9 of 14 semiprofessional athletes (64%), 7 of 8 Canadian Football League athletes (88%), and 110 of 111 National Football League (99%) players. Neuropathological severity of CTE was distributed across the highest level of play, with all 3 former high school players having mild pathology and the majority of former college (27 [56%]), semiprofessional (5 [56%]), and professional (101 [86%]) players having severe pathology. Among 27 participants with mild CTE pathology, 26 (96%) had behavioral or mood symptoms or both, 23 (85%) had cognitive symptoms, and 9 (33%) had signs of dementia. Among 84 participants with severe CTE pathology, 75 (89%) had behavioral or mood symptoms or both, 80 (95%) had cognitive symptoms, and 71 (85%) had signs of dementia⁹⁸ (Table 2).

Table 2 - Summary of clinical features according to McKee.⁸⁴

Stage	Clinical presentation
1	Headache, inattention, loss of concentration
2	Depression, explosivity, impairment of short-term memory
3	General cognitive impairment
4	Dementia, language impairment

Considerable heterogeneity between the mechanisms of injury between sports, mainly depending on force and direction of the impact, also exists, leading to different clinical symptoms. In boxing, the impacts are less strong but occur frequently, whereas, in football, the impacts usually occur less periodically but have a superior impact⁹⁹. Further differences exist within each sport. In football, injury mechanics can vary depending on position which can result in both linear helmet-to-helmet and rotational impacts. Injury in boxing can occur from countercoup injuries, which come from a linear impact resulting from a jab, or from torque injuries, which are rotational impacts that result from an uppercut or hook. Viano et al. demonstrated that the rotational forces that boxers absorb can cause axonal damage, which is mainly located in the WM tracts¹⁰⁰. Viano et al. also compared the inertial forces produced by boxers and football players and concluded that the forces produced by football players can be up to 30% greater than those by boxers¹⁰⁰. The clinical presentations of CTE vary depending on the contact sport practiced by each individual. It has been previously observed that boxers tend to have more motor-related symptoms due to an increased number of torque injuries (rotational or twist force), while motor-related symptoms are infrequently seen in football players⁹⁹.

However, 20% of patients with a history of rmTBI did not show pathological evidence of CTE, and a high rate of mood disturbance was also seen in these non-CTE patients, of which 56% died by suicide or overdose⁸⁴. It is important to consider that genetic risk factor may also play an important role in the development of CTE and other neurodegenerative diseases. Among these, apolipoprotein E allele (which is a risk factor for AD)¹⁰¹, and polymorphisms in the gene encoding neprilysin, an A β -degrading enzyme which probably influence the rate of A β degradation and clearance after TBI¹⁰², have been proposed. In 2017, Cao et al. demonstrated that the apolipoprotein E4 allele contributes to the development of p-tau post-TBI¹⁰³. In 2018, Cherry et al. examined the association between CTE and gene variation TMEM106B, a transmembrane protein previously associated with TAR DNA-binding protein 43 related diseases and neuroinflammation¹⁰⁴. Cherry found an association between the minor allele and reduced tau pathology and neuroinflammation in the dorsolateral frontal cortex. Additionally, Cherry noted associations between minor allele and increased synaptic density and reduced ante-mortem dementia. While promising, current research on the relationship between CTE development and gene variations in apolipoprotein E4 and TMEM106B remains inconclusive and further studies are needed⁹⁹.

Whole-genome sequencing of patients with CTE may provide comprehensive genetic profiles of those who develop CTE as well as those who experience identical lifelong TBI histories but remain cognitively intact⁵⁷.

The role of repeated concussions in the development of CTE, including the epidemiology and the link between neuropathological characteristics and its clinical manifestations, is poorly understood². Douglas and colleagues⁵³ pointed out some controversies associated to CTE and the confusion arose around this pathology. According to them, the actual incidence of CTE is unknown, and the evidence linking participation in sports and later development of CTE or other neurodegeneration remains unsettled, despite some reports suggest that degenerative brain disease is almost inevitable for participants in some sports⁹⁸. They highlighted how in a study considering 438 former high school football players from 1946 to 1956 compared to 140 age-matched controls, Savica et al.¹⁰⁵ found no increased risk of dementia, Parkinson disease, or amyotrophic lateral sclerosis. Moreover, current consensus neuropathological criteria are acknowledged as only preliminary, partly because these criteria are based on a limited number of selected cases, and, additionally, the clinical diagnostic criteria have not yet agreed upon⁵⁷.

At present, definitive diagnosis of CTE can only be made by post-mortem neuropathological examination² (Figure 4). The cellular pathobiology and molecular mechanisms underpinning CTE tau proteinopathy and spread, as well as all the mechanism associated to human mTBI and its heterogeneity, are poorly understood and under intensive investigation. Animal modeling is a critical and irreplaceable component that can be used for the discovery of new biomarkers in a controlled setting¹⁰⁶.

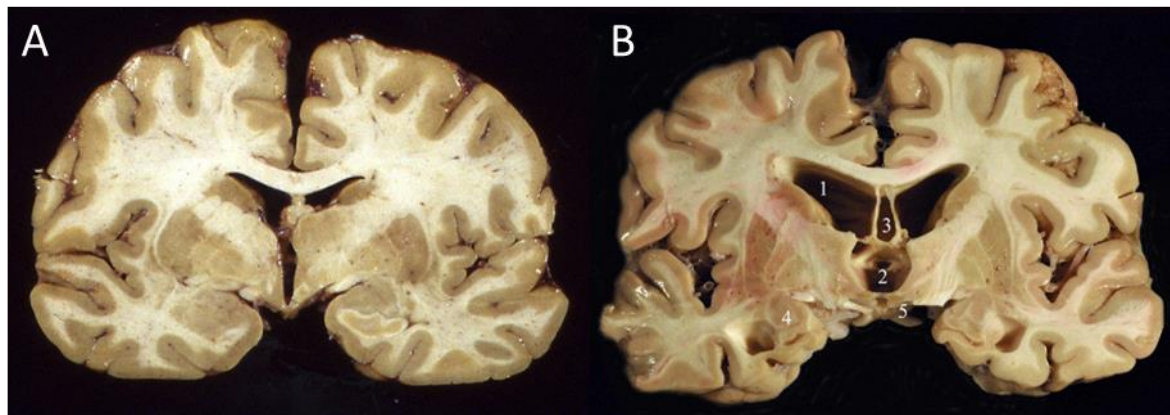


Figure 4 - Gross pathology of CTE. (A) The coronal section of normal brain, showing the expected size and relationship of the cerebral cortex and ventricles. (B) The brain from a retired professional football player, showing the characteristic gross pathology of CTE with severe dilatation of (1) ventricles II and (2) III, (3) cavum septum pellucidum, (4) marked atrophy of the medial temporal lobe structures, and (5) shrinkage of the mammillary bodies.¹⁰⁷

1.3 Animal models of repetitive mild TBI

1.3.1 Translational challenges

There are many challenges when studying the effects, pathophysiology, biomarkers, and treatment of mTBI in the clinical setting. Among these, the tremendous variability and heterogeneity in human mTBI, including mechanisms of injury, biomechanical forces, injury severity, spatial and temporal pathophysiology, genetic factors, pre-injury vulnerability, and clinical outcomes. Physical impact leading to TBI results in a rapid transfer of energy to the brain, while the resulting energy dissipation generates complex situations that are drastically dissimilar from case to case and are complicated to analyse². Another drawback related to the possibility to have a deep insight into human mTBI is that invasive studies to investigate underlying molecular and cellular changes in the brain are not ethically feasible, and mTBI patients may be unavailable to participate in detailed, serial, and longitudinal studies when they are no longer presenting symptoms, which typically occur within days, weeks, or months following injury. In addition, the possible long-term effects of rmTBI may progress over time and not fully appear until years after the injuries occurred. Therefore, the studies required to monitor these progressive changes in humans are extremely difficult, expensive, could take decades to complete, and may be affected by selection biases, genetics, and socioeconomic and lifestyle factors (e.g., alcohol/drug use)¹⁰⁶. These considerations highlight the need to integrate mechanistically directed preclinical mTBI research. On this perspective animal models are highly helpful, reducing the variability and heterogeneity found in human mTBI, and providing a means to study mTBI in a rigorous, controlled, and

efficient manner. In evolutionary terms, human and mouse lineages diverged from a common ancestor ~75 million years ago. Therefore, virtually, all human coding genes have homologous counterparts in the mouse genome¹⁰⁸. Gene homologs code for proteins with identical or closely related physiological functions in both species. This implies that mice and humans share similar anatomical organization of cells, tissues, organs, including brain, and even neurophysiology and behavior³. In addition to genotypic and anatomical similarities with humans, mice afford many practical advantages, including experimental malleability, ease of breeding and housing, straightforward genetic manipulation, making the mouse an unparalleled model organism to investigate mechanisms of human diseases and allowing to fill the gap between experimental science and clinical medicine³. Rodent models are time- and cost-efficient, and they allow researchers to examine cellular and molecular responses using histological assessment, which can give important insights on the neurophysiological changes associated with the evolution of brain injury¹⁰⁹. This is particularly important for the assessment of biomarkers of mTBI, as human studies aimed at finding them would take decades to complete and would be confounded by several factors. On the contrary, animal models can assess them in a relatively efficient and well-controlled manner, by administering repeated mild impacts with the inter-injury times guided by biomarker recovery¹⁰⁶.

However, there are still some concerns regarding the possibility to fully reproduce the complexity of mTBI in animal models. The lack of a universal clinical definition of clinical mTBI²³ creates challenges in establishing what is the most appropriate animal model and to what extent do experimental results apply to the human condition¹⁰⁶. Consequently, although the term “mild” TBI is used often in the preclinical literature, clearly defined criteria for mild, moderate, and severe TBI in animal models have not been agreed upon¹⁰⁶. For this reason, it is essential to establish objective indicators of injury severity and injury recovery into studies, in order to improve reproducibility among laboratories. This could be done by including details of the injury parameters, as well as serial measures of the presence or absence of any pathophysiological, structural, and functional changes induced by the model¹⁰⁶.

Moreover, modeling TBI in rodents will always lack some components of the human condition. In fact, it is unlikely that a single model can capture all the aspects of mTBI given the heterogeneity of underlying pathology associated with it (Figure 5). In addition, there are inter-species differences between humans and rodents regarding the duration of mTBI-associated deficits and the temporal profile of pathophysiological changes in the rodent brain¹⁰⁶.

Another important consideration is that human brain is characterized by an extensive convoluted fold (gyri and sulci) of the cerebral cortex, differentiating it from lower species as rodents, which have a lissencephalic brain (e.g., the surface of the brain appears smooth). There are several indications that the gyri and sulci complicate the energy distribution during rotational injuries and the large mass of the human brain makes it particularly vulnerable⁶. This is peculiarly relevant for the development of CTE pathology as computational

modelling suggests that axons located in the depths of the sulci at the interface between the gray and white matter are the most susceptible to shearing forces^{94,110}, although this has not been directly demonstrated neuropathologically. In fact, CTE pathology typically manifests itself in the depths of these folds in humans, which cannot be modeled in rodents because of their smooth brain surface. Consequently, although rodent models have considerably contributed to our knowledge of the pathological features and related mechanisms of rmTBI, such as glial activation, vascular damage, and axonal injury, there are some challenges and inherent limitations in using them when modeling human CTE-like pathology¹¹¹. In spite of this, animal models, especially mice, provide time-tested tools to establish causal mechanisms of disease, to enable systematic exploration of pathophysiology, and conduct rigorously controlled “proof of concept” experiments in order to evaluate new diagnostics and therapeutics that would be impractical or unethical in humans³.

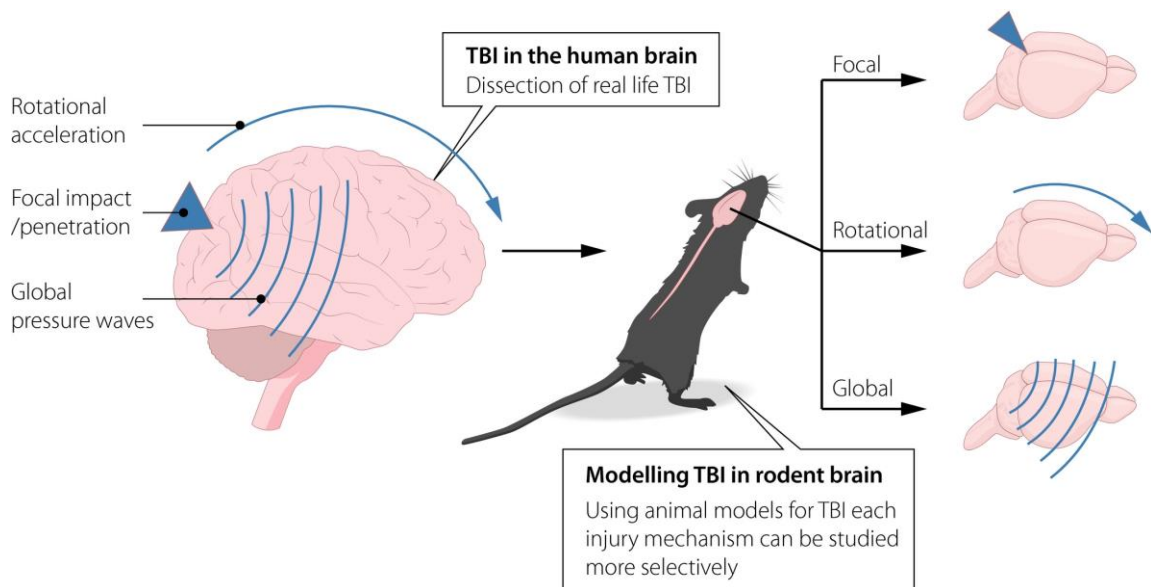


Figure 5 - In general, real-life TBI is a complex mixture of injury mechanisms, such as impact and rotational forces. Animal models can be used to study these mechanisms more separately, with better control of physical parameters.²

1.3.2 Translational strategies

The use of animal models in TBI research is crucial. Many animal models have been developed over the last 80 years to replicate the different unique features of mTBI (e.g., emotional or cognitive symptoms), including neurological and pathological aspects, as well as biomechanical forces (e.g., impact or rotational). However, compared to preclinical models of moderate-to-severe TBI, the number of publications attempting to model mTBI is much smaller in number. Fortunately, during the last decades the overall number of experimental mTBI studies are steadily increasing at a rate reflecting the public’s

acknowledging of the seriousness of mTBI, caused by the alarming number of people that suffer a mTBI and the appreciation that rmTBI can have a lasting negative impact on the health of the brain¹¹² (Figure 6).

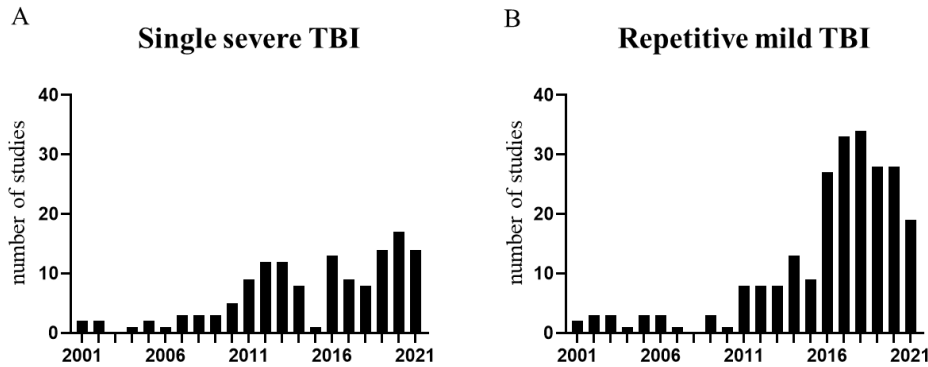


Figure 6 - Pubmed searches. (A) Number of studies published about single severe TBI models, 22 from 2001 to 2010, 117 from 2011 to 2021. (B) Number of studies published about repetitive mild TBI models, 20 from 2001 to 2010, 215 from 2011 to 2021.

The most common experimental methods used to produce a mTBI in mice are the weight-drop, the piston-controlled impact, the fluid percussion injury (FPI) and the blast-injury methods. In general, the injury can be performed after craniotomy of the mouse's skull (open-head models), directly impacting the brain surface, or without executing craniotomy, so as CHI models. In the weight-drop model (Figure 7A) the gravitational force of a free-falling weight from a specific height is used to produce focal or diffuse brain injury. The impact of the free-falling weight can be delivered to the exposed skull (closed-head) or to the intact dura (open-head), and the severity of head trauma can be varied by using different weights and/or heights of the weight-drop, which affect the force to the head at the time of impact. When the impact is delivered to the exposed skull, generally soft tips, e.g., silicon-covered, reduce the risk of skull fractures. For inducing focal brain injury, the animals are placed on non-flexible platforms to minimize dissipation of energy; while to induce a diffuse brain injury, the impact has to be widely distributed over the skull, and this is made by using flexible platforms allowing the head to accelerate, e.g., foam-type platforms or platforms with elastic springs^{109,112,113}. In the piston-controlled impact model (Figure 7B) a pneumatic or electromagnetic driven rod is fired either directly onto the exposed cortex (requires craniotomy and it is called controlled cortical impact or CCI) or onto the closed skull, either with or without scalp retraction, with the head often immobilized in a stereotaxic frame. In piston-controlled impact, the impact parameters (e.g., impact angle, impact velocity) can be precisely set and adjusted through the electromagnetic or pneumatic driven impactor device, enabling a high impact reproducibility¹⁰⁹.

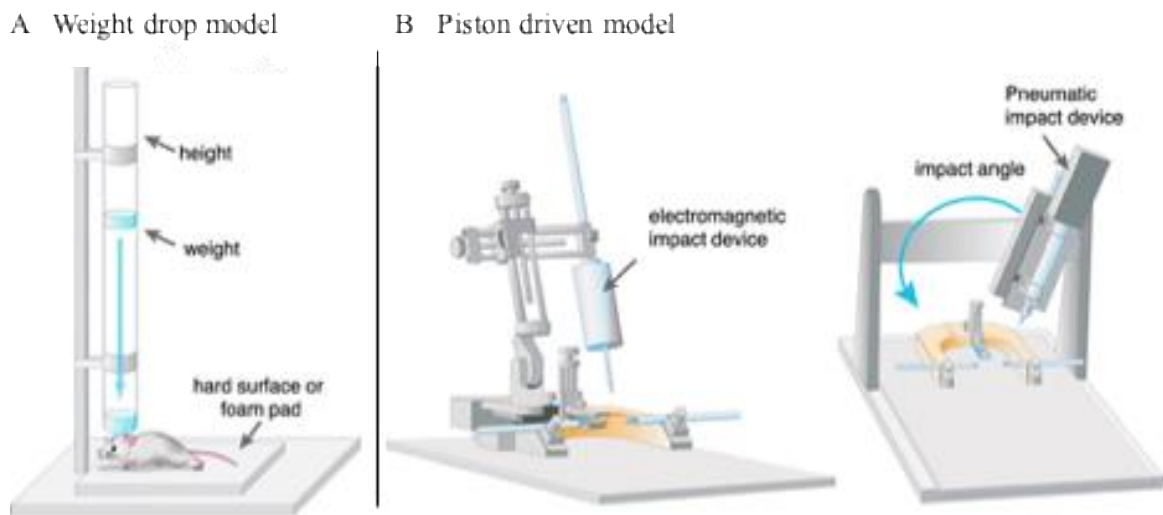


Figure 7 - (A) Weight drop model. (B) Piston driven model, which can use an electromagnetic driven impactor device (left) or a pneumatic driven impactor (right).¹¹²

In the FPI model (Figure 8A) brain injury is produced by rapidly injecting fluid volumes into the cranial cavity, after craniotomy, onto the intact dural surface, causing a pressure pulse that produces elastic deformation of the brain, which is thought to resemble brain deformation after head impact. The craniotomy is made either centrally, over the sagittal suture midway between bregma and lambda, or laterally, over the parietal cortex. Graded levels of injury severity can be achieved by adjusting the force of the fluid pressure pulse¹¹³. In the blast-injury model (Figure 8B), that simulates the blast-induced TBI occurring in military personnel, which is caused by improvised explosive devices in combat areas, with blast waves producing substantial oscillating acceleration-deceleration cycles on the head. In the blast-injury model, the animals are inserted in a tube and subjected to the pressure caused by the displacement of an air mass or an explosion, to simulate the waves produced by the detonation of an explosive charge.



Figure 8 - (A) FPI model: a rapid fluid pulse injection is used to cause injury directly onto the surface of the dura. (B) Blast-injury model: injury is caused by primary injury of blast.¹¹⁴

1.3.3 Closed head repetitive mild TBI model in mice

Clinical mTBI is typically characterized by direct-impact, non-penetrating head injury, that is, closed-skull or CHI. Consequently, clinically relevant models of experimental mTBI should use minimally invasive head impact methods, induce mild injury and exhibit symptoms in the absence of gross neuropathology¹¹⁵.

Techniques such as CCI and FPI require craniotomy, an invasive method which have shown to generate profound inflammatory, morphological and behavioral damage closer to the severe TBI scene instead of mTBI^{116–118}. In particular, the CCI model, in which the exposed dura is impacted, causes a focal brain injury which produces cortical contusion, hemorrhage, and brain edema and may cause severe neurological condition such as post-traumatic epilepsy. In FPI models, a high mortality rate due to apnea and high variability in injury parameters between laboratories are evident¹¹³. One crucial factor determining the outcome severity in this model seems to be the positioning of the craniotomy, as it is sufficient a small shift in the craniotomy site to cause marked differences in neurological outcome, lesion location and size^{113,119,120}. Thus, establishing a FPI model necessitates extensive methodological fine-tuning to obtain a standardized outcome in respect to its severity and pathophysiology¹²⁰. The weight-drop model presents several advantages, including: a low mortality rate, making it suitable for therapeutic evaluation; it involves a mild injury to a closed head, fitting the requirements for a mTBI; it efficiently induces clinically relevant behavioral outcomes representative of post-concussion symptomatology. On the other hand, disadvantages of the weight-drop model are the high variability of the injury severity and the inherent heterogeneities of the model because of the lack of a highly precise trauma impact and the lack of animal's head fixation, which bring to a scarce reproducibility of experiments¹²¹. As regards the blast-injury model, it is a model specifically suited to simulate military-related mTBI rather than sports-related mTBI.

It has recently been suggested that CHI animal models may more closely approximate clinical mTBI than FPI or CCI models^{122,123}. A suitable model resembling the clinical setting of mTBI and ensuring a high reproducibility of outcomes is the CHI model using a piston-controlled impact, with the head fixed on a stereotaxic frame.

1.3.4 Novel closed-head model using a piston-controlled impact

A novel mTBI model developed at the Roskamp Institute¹¹⁸ by Mouzon et al. delivers a total of 5 multiple impacts above the closed skull at a 48-hour inter-injury interval. The criteria for a mild injury were as follows: (1) a short period of post-traumatic apnea <30 seconds (recognized as an animal analog to human LOC¹²⁴) (2) a short period of righting reflex <6 minutes, (3) no sign of skull fractures at the time of euthanasia, and (4) no history of major hemorrhage(s)¹¹⁸. The model is particularly suitable to impart repeated head trauma as, in

terms of reproducibility, incorporates an electromagnetic coil-based delivery device, which delivers consistent strike velocities.

Mouzon and colleagues' purpose was to develop a reliable and robust mouse model of mTBI to investigate the chronic neurobehavioral and neuropathological outcomes following smTBI and rmTBI at time points from 6 to 18 months following injury¹²³.

In fact, the majority of existing animal models of rmTBI are very severe, using only 2-3 impacts that cause extensive neuronal cell loss, skull fracture and loss of brain tissue. This extent of injury is not occurring after rmTBI in humans, demonstrating the need for a new model of single and repetitive mild head impacts¹²⁵.

Before Mouzon et al. studies, published mouse models of CHI have only investigated the effect of a single mild head injury or two mild head injuries with an inter-injury interval of 24 h, where a single injury was shown to cause subtle and transient behavioral and immunohistochemical abnormalities, whereas two such injuries 24 h apart worsened the outcome¹²⁶⁻¹²⁹. This novel model can investigate the cumulative consequence of more than two brain injuries at multiple time intervals, as investigations of this nature are scarce and have predominantly employed the weight drop model¹¹⁸.

Moreover, only few studies have been designed to adequately evaluate the chronic effects of rmTBI, to which mice models are particularly suitable, as they have a relatively short life span (2–3 years), facilitating exploration of the chronic effects of rmild TBI. This gap in the investigation of long-term consequences of rmTBI was filled by Mouzon and colleagues¹²³. Before their searches, neuropathological changes and neurobehavioral deficits were only reported up to 3 months after injury, with only one work from Mannix and colleagues considering a time point of analysis at 12 months after injury, reporting neurobehavioral deficits although with little accompanying neuropathology^{130,131}. Mouzon et al. reported the consequences of smTBI and rmTBI with survival times up to 18 months after injury and observed less favorable behavioral outcome following rmTBI compared to smTBI, associated with characteristic neuropathological features¹²³.

1.3.4.1 Behavioral and neuropathological evidence associated to the model

The acute phase following human mTBI is associated with a complex and mixed neuroinflammatory response involving activation of resident microglia and astrocytes that express inflammatory mediators locally. However, this acute phase response likely contributes to immediate pathology, while persistent inflammation might trigger longer term neurodegenerative consequences. In support of this, autopsy-derived tissues from athletes demonstrate persistent neuroinflammation many years after rmTBI. Increasingly, neuroinflammation is proposed as contributing to development of neurodegenerative diseases, perhaps representing an early event in their pathogenesis¹²³.

In the acute phase, experimental results from Mouzon et al. work using a novel CHI mouse model¹¹⁸, reveal that a smTBI is associated with transient motor and cognitive deficits,

whereas rmTBI results in more significant deficits in both paradigms. In repetitively injured animals, histology revealed no overt cell loss in the hippocampus, although a reactive gliosis did emerge in hippocampal sector CA1 and in the deeper cortical layers beneath the injury site, where evidence of focal injury was also observed in the brainstem and cerebellum. Axonal injury, manifesting as amyloid precursor protein immunoreactive axonal profiles, was present in the corpus callosum (CC) of both injury groups, though more evident in the rmTBI animals. These data demonstrate that in the acute phase this mouse model of mTBI causes behavioral impairment after a single injury and increasing deficits after multiple injuries accompanied by increased focal and diffuse pathology¹¹⁸.

In the chronic stage, results reveal that for cognitive performance, the single injury animals have recovered to the same level of performance as corresponding sham animals by 6 months after injury, remaining at comparable levels at subsequent 12- and 18-month evaluations. These findings are consistent with observations in the human population in which those suffering from a single mild head injury often return to their pre-concussive status within a week^{132,133}. In contrast, in mice exposed to repetitive injuries, the acute cognitive deficit persisted at 6 months and continued to evolve through the 12- and 18-month time points. Altogether, these data provide evidence that cognitive impairments following a smTBI may be transient, whereas cognitive deficits following repetitive injuries not only persist but continue to evolve up to 18 months after injury. At all time points examined, the behavioral performance of repetitively injured animals was diminished when compared to the other groups. The main difference between both injury groups at 18 months was in learning performances. Animals from the rmTBI group were unable to learn the task, reinforcing the finding that repetitive insults worsen cognitive performance at chronic time points after injury. Overall, these results are consistent with observations in human patients, where residual impairments in learning strategy and/or a lack of executive function have been reported after injuries^{64,134}. The prevalence of mild cognitive impairment and significant memory problems is 5X greater in former athletes who suffered multiple concussions compared with retirees without a history of concussion¹¹⁸.

Importantly, in this model, these deficits arise in parallel with several neuropathological abnormalities, including progressive neuroinflammation and continuing WM degradation up to 12 months following repetitive injury. In particular, the single injury animals displayed evident pathology, manifest as a degree of neuroinflammation and WM loss (CC thinning), which peaked at 6 months and remained static at the 12-month evaluation. In contrast, not only did the repetitively injured mice show greater pathological changes at all time points when compared to the single injury animals, there was also evidence of a continued progression of neuropathology up to 12 months after injury. WM degradation appeared to continue some considerable months from the original injuries, with evidence of further callosal thinning between 6 and 12 months corresponding to evidence of ongoing axonal degradation manifest as amyloid precursor protein immunoreactive axonal profiles. Imaging studies have demonstrated that WM integrity is correlated with executive function, attention, and memory¹³⁵. Given that the most significant pathological changes were observed in the

CC rather than the hippocampus, it appears likely that the WM pathology is responsible for the neurobehavioral deficits. This correlates with the impairments in strategy learning that are frequently observed in human subjects in the absence of overt lesions in gray matter following TBI¹³⁶. The chronic inflammation observed is in line with autopsy reports from former athletes with history of rmTBI⁵⁶. Given the proposed pathophysiological role for chronic neuroinflammation in neurodegenerative disease¹³⁷, these data suggest that the progressive neuroinflammation in the rmTBI model may be a key contributor to the neurobehavioral deficits and, as such, represents a valid therapeutic target.

Notably, neither smTBI nor rmTBI was associated with elevated brain levels of A β or abnormal p-tau at 6 or 12 months after injury. This suggests that the cognitive deficits observed occurred independently of soluble A β or tau accumulation. The significance and role of A β and tau in TBI are the cause of an ongoing debate in the field, and rigorous evaluation of clinical populations and autopsied tissue is warranted¹¹⁰.

Despite the limitations when translating from laboratory mTBI models to human populations¹²², in this model Mouzon et al. describe components that are clinically relevant. The WM degradation, axonal injury, and neuroinflammation they observed in the CC in the injury groups at 6 and 12 months after injury are now recognized to be important aspects of long-term human rmTBI sequelae^{110,138}.

Importantly, these data provide evidence that while a smTBI produces a clinical syndrome and pathology that remain static in the period following injury, repetitive injuries produce behavioral and pathological changes that continue to evolve many months after the initial injuries. As such, this model recapitulates many aspects described in human studies of rmTBI, providing a suitable platform on which to investigate the evolving pathologies following rmTBI and potential strategies for therapeutic intervention¹²³.

1.4 Neuroimaging of mild TBI

1.4.1 Traditional neuroimaging in clinical mild TBI and limitations

The advent of cross-sectional neuroimaging, first using CT and later MRI, revolutionized the assessment of TBI by permitting rapid non-invasive detection and localization of intracranial hemorrhage, contusion, and edema, to categorize the degree of damage, and, therefore, to help in triaging patients for acute interventions and for prognosis¹³⁹. However, conventional CT and MRI are only able to configure anatomical images with millimeter resolution, meaning that they detect gross pathology at a similar level¹⁴⁰. As it is unusual for sport-related mTBI to result in grossly visible injury, like the macroscopic lesions detected in moderate to severe TBI, in those cases CT and MRI are unrevealing¹⁴¹. In players sustaining a more severe injury, such as those sustaining loss or alteration of consciousness,

emergency neuroimaging is extremely useful to rule out life-threatening injury that may require neurosurgical care. Nonenhanced CT of the head is the mainstay of imaging in emergency case, as it is widely available and can be performed very quickly to evaluate for the presence of primary injuries such as intracranial hemorrhage and skull fracture, edema, mass effect, or vascular injury¹⁴¹. Excellent contrast between bone and brain parenchyma can be achieved with CT, which clearly has the advantage over MRI in demonstrating presence and location of skull fractures, common sequelae of head injury¹⁴⁰. CT angiography also provides methods for examining cerebrovasculature and inflammation in TBI, for rapid and high-resolution assessment of the integrity of the major arteries and veins of the head and neck, e.g., to identify laceration, thrombosis, or dissection, helping in identifying mTBI patients with more permanent sequelae (e.g., SIS) (Figure 9)^{140,141}. Moreover, because CT imaging uses x-ray beam technology, objects with paramagnetic properties including life support and other medical assist devices are not precluded, as occur in MRI, allowing CT to be widely employed for triage and to determine if neurosurgical intervention is needed¹⁴⁰. On the other hand, the increasing widespread use of CT has raised concerns of the risks associated with an increasing radiation exposure to both adult and pediatric population¹⁴². Conventional MRI, including diffusion-weighted imaging (DWI), is useful in evaluating acute injury due to contusion, shear forces, or ischemia. MRI, particularly SWI, is far superior to CT for the detection of microhemorrhage and may be more sensitive than CT to detect subarachnoid blood, when T2-weighted fluid-attenuated inversion recovery imaging is employed¹⁴¹.

However, these findings likely reflect only a minimalist view of the pathology and do not consider all the shear/strain effects which have occurred in the brain. Moreover, even if CT and traditional MRI may be useful in investigating mTBI during the acute to early subacute timeframe²¹, the subtle long-term effects of rmTBI in asymptomatic patients, years after the last mTBI, are not detected¹⁴³.

To best understand mTBI, more advanced neuroimaging methods are necessary to uncover additional neuropathology missed by the traditional “lesion analysis/identification” approach of conventional CT and MRI¹⁴⁰. Furthermore, it is probably a fruitless endeavor to seek the prototypical lesion in mTBI because it likely does not exist. The macroscopic abnormalities identified by CT and traditional MRI, may only indicate “tip-of-the-iceberg” phenomena and are not proportional to the total pathological effects of mTBI at the histological level. This is probably why the presence and location of a day-of-injury CT abnormality does not necessarily predict outcome, because there is more than just the visibly identifiable lesion¹⁴⁰.

Despite concerns about the long-term effects of rmTBI, there are no clear clinical guidelines on when it is safe for an athlete to return to play after a head injury. The current clinical standard only specifies that an injured athlete may return to play following symptom resolution¹⁴⁴ and both CT and traditional MRI are not capable of providing long-term prognostic information¹⁴³.

Further advances in neuroimaging, both in terms of measurement and analysis approaches,

have expanded our ability to see beyond macroscopic injury and elucidate the microstructural changes and associated functional consequences that underlie the pathophysiologic and functional effects of concussion.

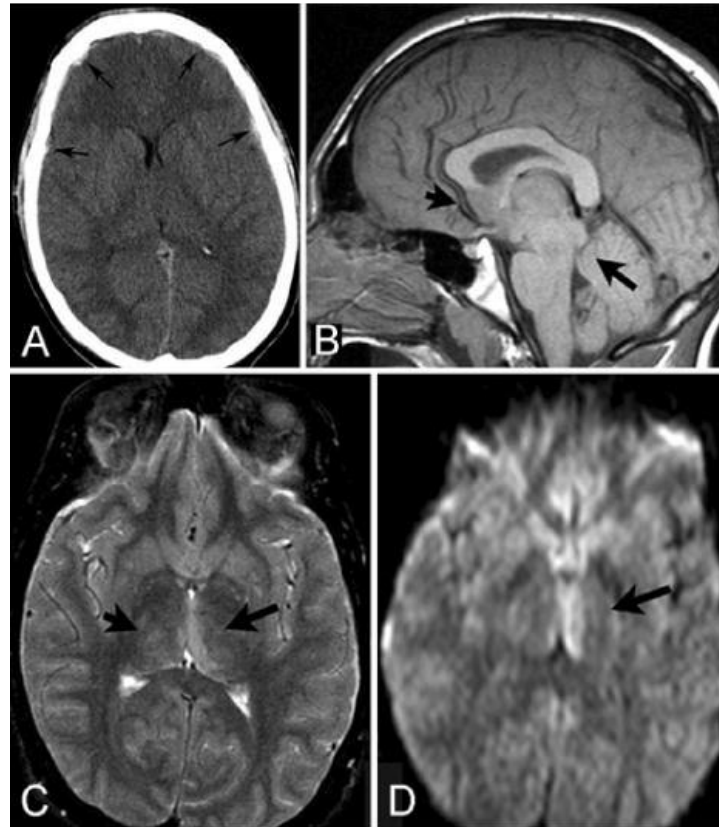


Figure 9 - Typical imaging findings of second-impact syndrome (SIS). A: Head CT obtained after second impact. *Arrows* point to thin bilateral subdural hematomas. B: Sagittal T1-weighted brain MR image. *Arrows* point to downward descent of the midline structures. C: Axial T2-weighted MR image. *Arrows* point to thalamic injury. D: Axial DWI. *Arrow* points to left thalamic injury. Restricted diffusion was proven by calculation of apparent diffusion coefficient (not shown).¹⁴⁵

1.4.2 Advanced magnetic resonance neuroimaging for mild TBI

Thanks to a growing public awareness of the long-term effects of rmTBI, the past decade saw an exponential growth in the number of research articles related to MRI of mTBI as well as the development of novel MR techniques (Figure 10)¹⁴³. Among these, more advanced MRI, including volumetric analysis and DTI, have shown promise in detecting anatomical changes associated with outcome after rmTBI, such as brain atrophy and traumatic axonal injury (TAI)¹⁴⁶. Since the earliest research article reporting DTI applied to TBI was published in 2002¹⁴⁷, there has been an exponential increase in the number of articles published on this topic. Studies indicate that even apparently intact axons with disrupted

physiology may contribute greatly to clinical dysfunction in mTBI¹⁴⁸. Advanced MR neuroimaging modalities are becoming more available and useful as their value in the diagnosis and prognosis of CNS diseases is more fully understood and studied¹⁴⁹. WM abnormalities on advanced neuroimaging studies are evident in many patients in whom CT scans are normal and are strong predictors of long-term consequences¹⁵⁰.

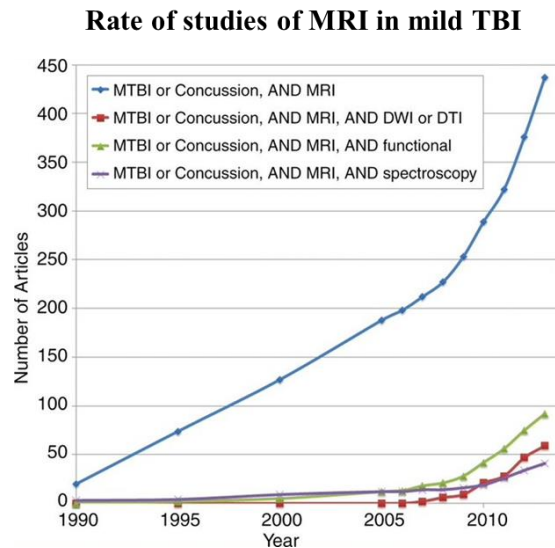


Figure 10 - Graph shows the number of articles found in PubMed from 1990 to the year indicated on the x-axis, with search terms as specified in the legend. An increase in rate of publication is demonstrated with all search parameters after 2005.¹⁴³

1.4.2.1 MRI signal

MRI takes advantage of the atom's magnetic properties. The nucleus of an atom is made up by protons and neutrons and it is characterized by the so-called total angular momentum, otherwise known as nuclear spin. Atoms with even atomic number are unaffected by external magnetic fields, on the contrary, nuclei with half-integer spin (such as 1H , ^{17}O , ^{19}F , ^{23}Na or ^{31}P) have a characteristic magnetic behavior. Due to its natural abundance in biological tissues, the hydrogen atom can be detected by MR techniques. Hydrogen atoms are formed by a single proton and a single electron orbiting the nucleus. Hydrogen nuclei behavior in a magnetic field is similar to the needle of a compass in presence of the external earth's magnetic field. Similarly, hydrogen nuclei are oriented in a random manner and the sum of all their magnetic moments has a zero value, while when immersed in the static magnetic field of the MRI scanner they point along its principal direction. Experiencing both the effect of the MRI and the earth magnetic fields, all protons start precessing (Figure 11C) around the direction of the main MRI magnetic field, yielding to a non-zero net magnetization. The

angular frequency of the precession, called Larmor frequency ω_0 , depends on the strength of the applied magnetic field B_0 , according to the equation:

$$\omega_0 = \gamma * B_0 \quad (1)$$

where γ is a constant called the gyromagnetic ratio, whose value is characteristic for the nucleus of interest.

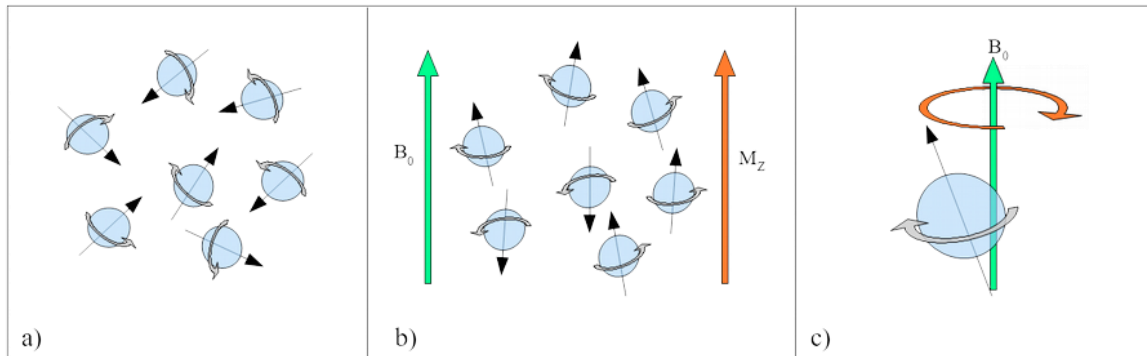


Figure 11 - (a) Spin orientation in absence and (b) in presence of an external magnetic field. M_z is the net magnetization representing the contribution of all spins. (c) Precessional motion of a spin.¹⁵¹

As shown in figure 12, some energy can be introduced when an external electromagnetic wave (B_1) with an orientation of 90° respect to the direction of the main magnetic field and characterized by a frequency equal to the Larmor frequency is applied.

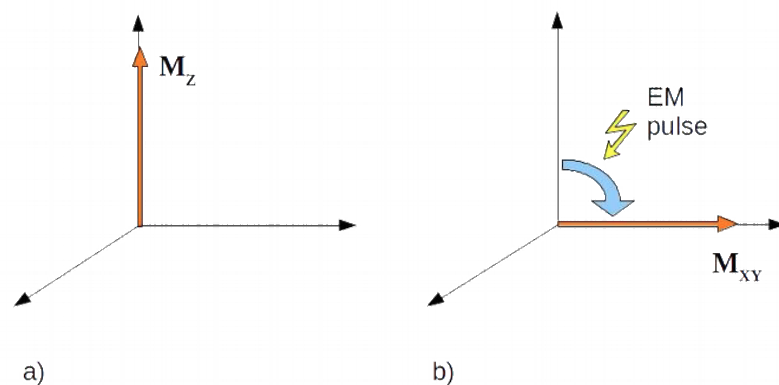


Figure 12 - Net magnetization (a) under normal conditions and (b) after the effect of the external electromagnetic wave.¹⁵¹

All the longitudinal magnetized spins are reversed in the transverse xy-plane, resulting in a net magnetization that is now denoted as M_{xy} rather than M_z . This magnetization rapidly fades out due to two independent processes. Once that the magnetization has been reversed, the spins start precessing with different phases due to the spin-spin interaction (Figure 13)

causing the so-called T2 relaxation of the signal. The T2* decay is also described in medical imaging and it is due to additional field inhomogeneities contributing to the dephasing process. T2 decay is more or less independent of the strength of the external magnetic field (B_0) and it is in the range of 40-300 ms.

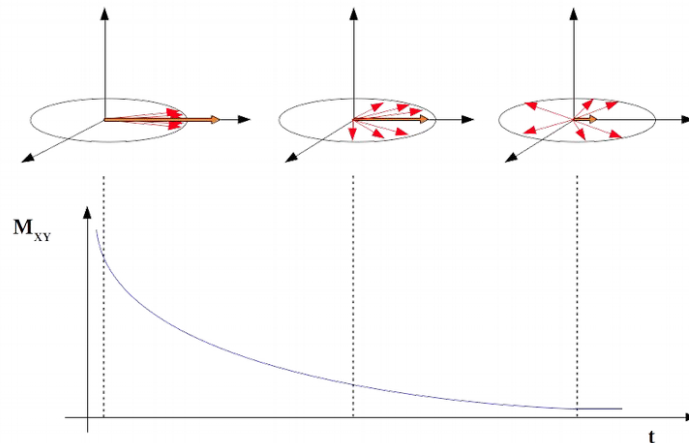


Figure 13 - Relaxation process. Spins reversed in the transverse plane start precessing around the main direction of the magnetic field causing. The sum of these spins (M_{xy}) decrease with a time called T2 relaxation time.¹⁵¹

While the transverse magnetization (M_{xy}) decays, the magnetic moments gradually realign with the z-axis of the main magnetic field (B_0), following the so-called spin-lattice interaction process, that reflects the interaction of nuclei with their molecular surroundings and how quickly the energy can be transferred from the nuclei to the environment. This process is regulated by the T1 relaxation recovery time which is in the range of 0.5-3 sec (Figure 14).

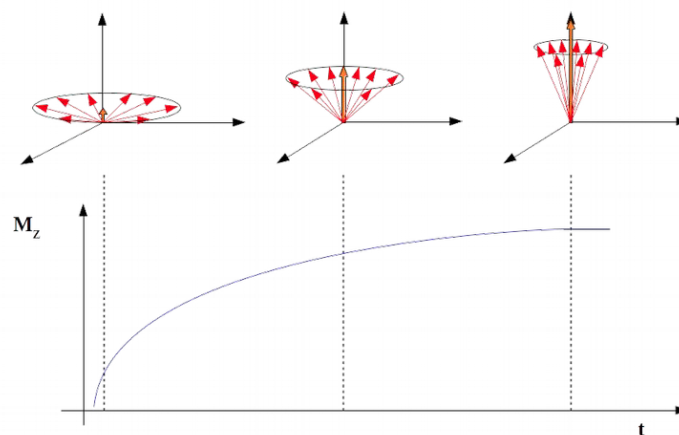


Figure 14 - Relaxation recovery process. Relaxation process. Once the effect of external 90° RF pulse end, spins reversed in the transverse plane start recovering their original magnetization (M_z) with a recovery time called T1.¹⁵¹

Since the oscillating spins are charged particles moving in a magnetic field, currents can be induced in conductor coils making the detection feasible. The detected signal is known as

free induction decay, which is proportional to the number of excited nuclei in the tissue, and it lasts as long as there is a transverse component (M_{xy}) of the net magnetization vector (Figure 15).

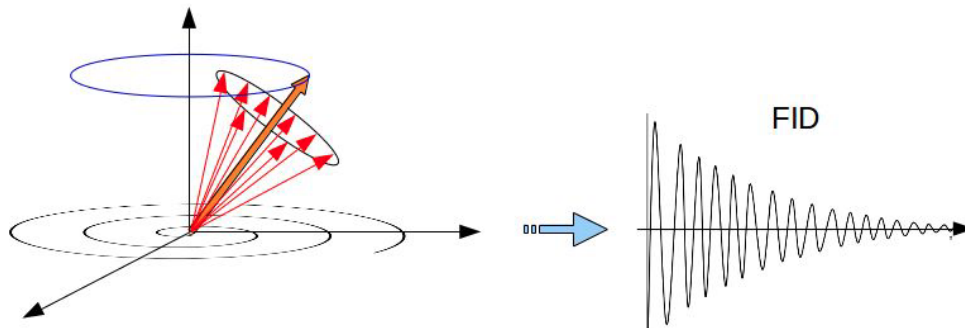


Figure 15 - Left: Temporal evolution of the net magnetization. Right: free induction decay obtained by reading the transverse magnetization.¹⁵¹

While the T1 is few orders of magnitude longer than the T2 relaxation time, the transverse magnetization can be recovered by applying a further 180° electromagnetic pulse (Figure 16). The spins' rotation is reverted obtaining their refocusing in the transverse plane and the recovering of the transverse magnetization.

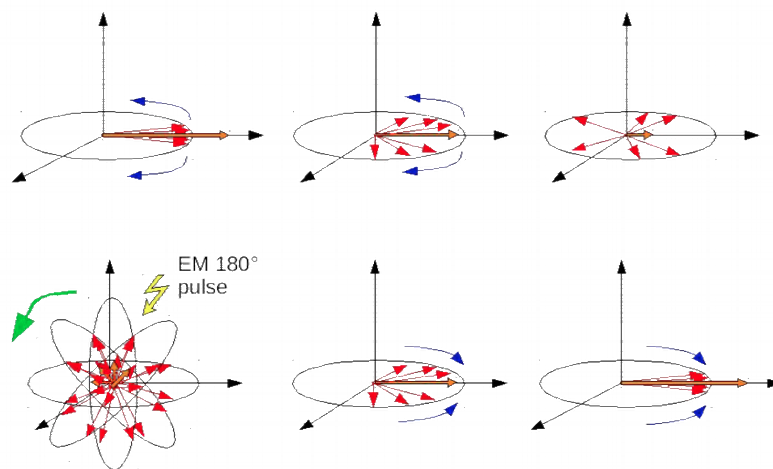


Figure 16 - Spin refocusing with a 180° EM pulse.¹⁵¹

A second class of detectable signal called “echo” is then produced (Figure 17).

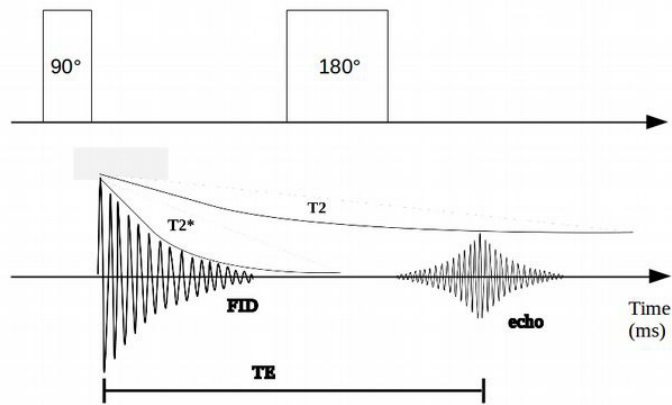


Figure 17 - Spin-echo sequence.¹⁵¹

A series of echoes caused by a train of consecutive 180° radiofrequency (RF) pulses can be obtained and detected. The amplitudes of the echoes diminish with the T2 (Figure 18).

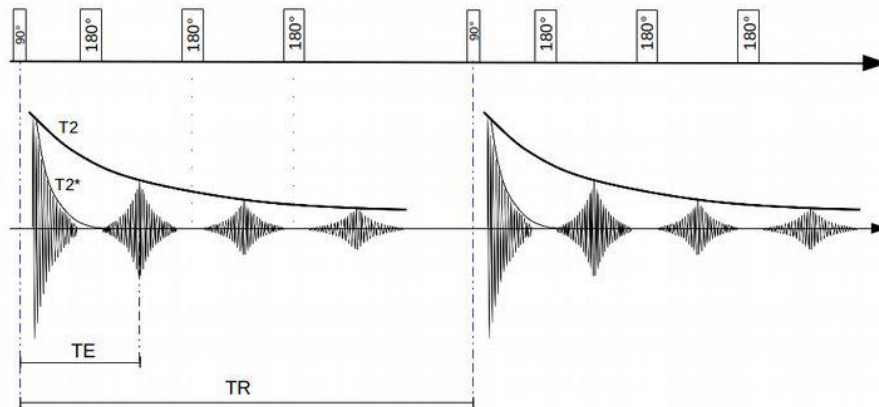


Figure 18 - Generation of a series of echoes using a train of consecutive 180° pulses, following. Repetition time (TR) is the time between 90° pulses.¹⁵¹

1.4.2.2 Structural T2 weighted imaging

When an MRI image is generated, the acquisition parameters repetition time (TR) and echo time (TE) can be chosen in order to emphasize its contrast properties. The signal, S, in a spin-echo sequence could be described by:

$$S \propto \rho * \left[1 - e^{-\frac{TR}{T_1}} \right] * e^{-\frac{TE}{T_2}} \quad (2)$$

Where ρ is the spin density and represents the number of protons per unit volume. The formula indicates that altering the TR and TE acquisition parameters, an effect on the image contrast will be dependent by the T1 or T2 of the tissues (Figure 19). Increasing the TR

period, the T1 information of the image increases resulting in a modulation of the gray/white matter contrast, while cerebrospinal fluid (CSF) remains dark. On the other hand, by shortening the TE the CSF is characterized by a small signal. For intermediate TE the overall contrast is poor but at long TE a large signal, resulting in a bright area, for the CSF can be obtained.

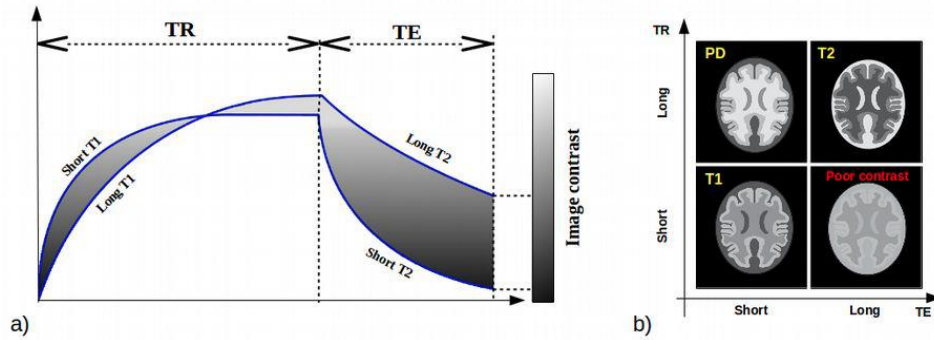


Figure 19 - Simulation that shows how tissues intensities can be modulated varying TR and TE (panel b adapted from 146).¹⁵¹

The so-called T1-weighted or T2-weighted images can be used to evaluate the volume alterations of different brain regions that are typical of mTBI pathology. Moreover, the T1 and T2 tissues times can be measured by acquiring a series of images with respectively fixed TR and varying TE or varying TR and fixed TE. The equations describing the signal evolution can be derived from the equation 2:

$$S \propto \left[e^{-\frac{TE}{T_2}} \right] \quad (3)$$

$$S \propto \left[1 - e^{-\frac{TR}{T_1}} \right] \quad (4)$$

Pathological alteration of the tissue composition can alter T1 and T2 measurements. An accumulation of lipids or iron leads to a reduction of the measured T1 when compared to healthy tissue. An increase of the water (e.g., edema) has the consequence of altering both relaxation times but is more pronounced in T2 sensitive measurements¹⁵².

Based on how each MRI technique manipulates the signal it is possible to describe the principal acquisition parameters.

1.4.2.3 Diffusion tensor imaging

The human brain is comprised of 100 billion neurons that communicate with each other through a complex network. Neuron cell bodies, which form the cerebral cortex, communicate over short distances via a branching network of dendrites and over long

distances via axons. Axons travel in clusters called tracts to remote regions of the brain, and they are wrapped in myelin, which serves to insulate the traveling electrical signal and connect functionally specialized regions of the brain. This extremely complex architecture of the human brain is particularly vulnerable to direct injury from trauma, which causes acceleration, deceleration, shearing forces on the brain, as well as secondary injury from mass effect, neurinflammation, axonal injury¹⁵³. Advanced neuroimaging techniques such as DTI provide quantitative information about potential network-level damage.

DTI has become increasingly utilized in recent years and incorporated by many radiologists into routine clinical practice, as it has been shown to help in improving identification of pathology earlier in its process. DTI does not require contrast and is available on almost all modern MR scanners with relatively quick scan times¹⁴⁹.

The principle underlying DTI imaging is the water molecules diffusion characterized by a diffusion coefficient (D). The particles random movement in a liquid in three-dimensional space, also known as Brownian motion, is governed by particles thermal energy¹⁴⁹. Isotropy is defined as uniformity in all directions and when applied to water molecules, isotropy occurs when the diffusion of water is entirely uninhibited (such as water movement in a glass of water). Anisotropy is when there is a directionality in the diffusion of water, and the movement of water is no longer random (such as water movement along straws placed in a glass). The greater the anisotropy, the more directional and linear the diffusion of water molecules. Water molecules will diffuse differently through space depending on the tissue type, components, structure, architecture, and integrity. DTI measures movement of water along axons, analogous to the straws in a glass of water¹⁴⁹.

As shown in figure 20, water molecules motility can influence the process regulating the magnetization recovery and thus the MRI signal. This influence can be measured by slightly modifying the spin-echo pulse sequence by adding a field gradient module (characterized by the diffusion weighting b factor) just before the 180° pulse. A magnetic field gradient can be described as variation of the magnetic field along one spatial direction. Once that the 90° pulse has been applied protons start dephasing around the main direction of the magnetic field. The amount of this dephasing is proportional to the diffusion distance covered by water molecules during the gradient pulse. The effect of this “dephasing” is a reduction of the MRI signal amplitudes. The equation 2 describing the MRI signal could be then extended as:

$$S \propto \rho * \left[1 - e^{-\frac{TR}{T_1}}\right] * e^{-\frac{TE}{T_2}} * e^{-b*D} \quad (5)$$

Where b is the diffusion weighting factor and D is the diffusion coefficient. In regions with fast water diffusion (e.g., CSF), the signal is reduced more when compared to the signal reduction of areas with slow water diffusion (e.g., WM).

Important parameters when using DTI are the strength of the magnetic field, the number of diffusion-sensitizing gradient magnetic field directions, and the choice of b-values.

Use of greater magnetic field strengths has advantages and disadvantages: greater signal-to-noise ratio, improved spatial resolution, and faster scanning times, at the cost of increased

magnetic field inhomogeneity¹⁵⁴.

In the setting of clinical DTI, most facilities will choose a b-value between 750 and 1000, whereas b-values of up to 3000 are used experimentally¹⁵⁵. Increasing the b-value increases the sensitivity to diffusion, but with a decrease in signal-to-noise ratio.

Spatial resolution is an additional important consideration. Assessments of anisotropy, which are central to studies of TBI, measure the aggregate range of diffusivities across the tissues composing the voxel. Partial volume effects that may spuriously reduce anisotropy will be more likely when larger voxel volumes are examined¹⁵⁶. Voxel sizes vary with an average voxel size of 11.3 mL³ (range, 1.83–31.25 mL³), while average section thickness is 3.08 mm (range, 1.72–6 mm), in articles analysed by Hulkower et al.¹⁵⁶. DTI is a variant of DWI, which utilizes a tissue water diffusion rate for image production. DWI uses volume elements (voxels) as a statistical method for data collection: when a voxel contains scalar values constituting a vector, it is known as a tensor, which is where DTI received its name and explains the additional information provided through DTI¹⁵⁷. DTI MR settings can measure the diffusion of water along an axon in many directions: 6, 9, 33, and 90 are typical parameters used, with 33 directions and above increasing confidence in the accuracy. Encoding the direction of diffusion requires a minimum of 6 diffusion-sensitizing directions: greater resolution can be achieved by introducing additional directions, but this adds time to image acquisition. Ninety directions typically require upwards of 20 additional minutes in the MR scanner; therefore, it may not be suitable for routine clinical practice.

DTI provide an indirect method of assessing neuroanatomy structure on a microscopic level using water molecules' degree of anisotropy and structural orientation within a voxel. Therefore, the principal application for DTI is in the imaging of WM, where the orientation, location, and anisotropy of the tracts can be measured and evaluated. The architecture of the axons in parallel bundles and their myelin sheaths facilitate the diffusion of the water molecules preferentially along their main direction¹⁵⁷.

There are a number of measures calculated using DTI that can provide quantitative power: one of the most widely used DTI measures is fractional anisotropy (FA)¹⁵⁶, mean diffusivity (MD) or apparent diffusion coefficient (ADC), radial (perpendicular) diffusivity (RD), and axial (parallel) diffusivity (AD).

The ADC map is created by acquiring a series of images with fixed TR and TE and b variable.

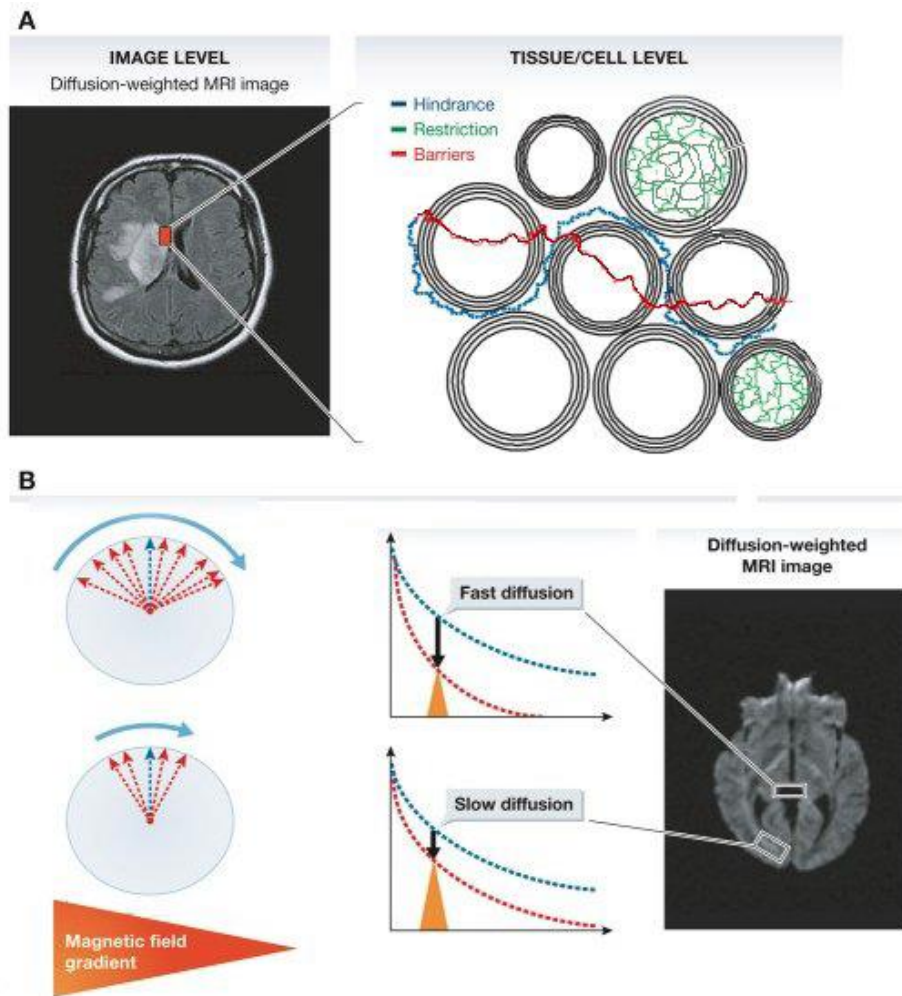


Figure 20 - The origin of DTI contrast. (A) Contrast and signal levels in the DWI of a human brain (left) reflect water diffusion behavior (random walk) (right). Diffusion behavior is modulated by tissue structure at the cellular level: For instance, diffusion can be restricted within cells, water may escape when cell membranes are permeable and might then experience a tortuous pathway in the extracellular space (hindrance). (B) In the presence of a magnetic field gradient, magnetized water molecule hydrogen atoms are dephased. The amount of dephasing is directly related to the diffusion distance covered by water molecules during measurement. The overall effect of this dephasing is an interference, which reduces MRI signal amplitudes. In areas with fast water diffusion (e.g., within ventricles), the signal is deeply reduced, while in areas of slow water diffusion (e.g., WM bundles), the signal is only slightly reduced. This differential effect results in a contrast in the DWI, which is not visible in standard MRI images. Adapted from^{158, 151}

The measured ADC value can vary because the diffusion may not be uniform in all orientations. To overcome this issue different images with fixed b but different gradient orientations can be acquired. In figure 21A is illustrated an ideal phantom that consists of two parts: an upper part that contains ordered structures, shown as arrows, that represent a bundle of axons or well-organized neurons with coherent tissue orientations; a lower part that contains random structures without coherent orientations. In the right panel of figure 21A is shown what happen when ADC is measured along three different orientations: these measurements in the upper part of the phantom show orientation dependence (i.e.,

anisotropic diffusion). Thus, the image intensity, representing ADC values measured in the orange box, change from high to low when the measuring orientation changes from horizontal to vertical. When ADC is measured in the lower part the image intensity does not change due to the random orientation of structures.

A mathematical model¹⁵⁹ can be applied to estimate the components of the effective diffusion tensor that can be visualized as an ellipsoid. The length of this ellipsoid, figure 21B, is proportional to the eigenvalues of the diffusion tensor ($\lambda_1, \lambda_2, \lambda_3$). The size, shape, and orientation of each ellipsoid can be described by combinations of these components corresponding to the diffusion tensor.

Where:

- Mean Diffusivity: $MD = \frac{\lambda_1 + \lambda_2 + \lambda_3}{3}$ (6)

- Axial Diffusivity (often indicated as λ_{\parallel}): $AD = \lambda_1$ (7)

- Radial Diffusivity (often indicated as λ_{\perp}): $RD = \frac{\lambda_1 + \lambda_2}{2}$ (8)

- Fractional Anisotropy: $FA = \sqrt{\frac{(\lambda_1 - \lambda_2)^2 + (\lambda_1 - \lambda_3)^2 + (\lambda_2 - \lambda_3)^2}{2(\lambda_1^2 + \lambda_2^2 + \lambda_3^2)}}$ (9)

DTI uses FA for the summative direction of the diffusion which provides a prominent vector and is highly sensitive to change in microstructure; however, it can be unspecific to the cause of change. FA values are numerical values, based on the anisotropy of water along the axon, which reflects the health of the axon: abnormal FA values indicate axonal damage. MD calculates the rate of molecular diffusion, quantifies cellular and membrane density, and its increase indicates disease processes such as edema or necrosis. RD indicate the rate of diffusion perpendicular to the main vector, quantifies myelin neuropathology and increases with demyelination processes. AD calculates the rate of diffusion parallel to the main vector, quantifies axonal degeneration and increases with brain maturation¹⁴⁹.

As concerns the data analysis methods, DTI can be used to study brain structure either on a regional or a whole-brain level¹⁵⁶. Regional analyses include both those in which an a priori region of interest (ROI) is chosen for study, and tractography, in which an a priori ROI is used to define a WM tract for study¹⁵⁶. In both approaches, average diffusion values such as FA are extracted from voxels within the ROIs or tracts for subsequent analysis. Whole-brain analyses include voxelwise analyses, tract-based spatial statistics, a specialized type of voxelwise analysis, and histogram analyses of all brain or all WM voxels¹⁵⁶. The whole-brain analysis is gaining popularity due to its automation and ability to analyze more tracts. ROI method, where the regions to be analyzed are traced by a technologist and then analyzed by a computer, remains reliable and replicable¹⁶⁰. One of the most common and standardized ROI methods is the segmentation of the CC¹⁶¹. Being the largest axonal tract in the brain, damage to the CC is well described following head trauma and other pathologies¹⁶². FA values can vary depending on which of the above three analyzing methods is used and on other factors such as MR technique and type of post-processing performed¹⁵⁶. Utilizing a standardized technique, FA values are highly reproducible and are not technologist dependent and can be subjectively interpreted by a radiologist as well as roughly compared

to select values in the literature¹⁴⁹. Pediatric normal values are slightly less than those of adults. However, most changes occur by age 5, and 90% of adult FA values are achieved by 11 years of age in the CC¹⁴⁹. After adulthood, FA values tend to decrease with age linearly. Additionally, FA values comparison across different scanners is now possible, even if those scanners are utilizing different techniques¹⁴⁹. This is achieved using ‘human phantom phenomena’ where a single subject is scanned on two different scanners, enabling a comparison between scanners by a scaling factor, or even to normative databases performed on a different scanner¹⁴⁹. Three-dimensional (3D) reconstructions of the tensor tracts are accomplished with computer modeling and can beautifully illustrate the fiber tracts, identify pathology, and aid neurosurgeons¹⁴⁹.

In the anisotropy map in figure 21B, the upper part of the phantom has higher diffusion anisotropy than the lower part. Consequently, when the diffusion anisotropy is high, the long axes of the diffusion tensor often coincide with the underlying structural orientation and can be visualized using a direction-encoded color map (DEC) where regions with structural orientation running horizontally are red and those running vertically are green. Transition areas become yellow, a mixture of red and green.

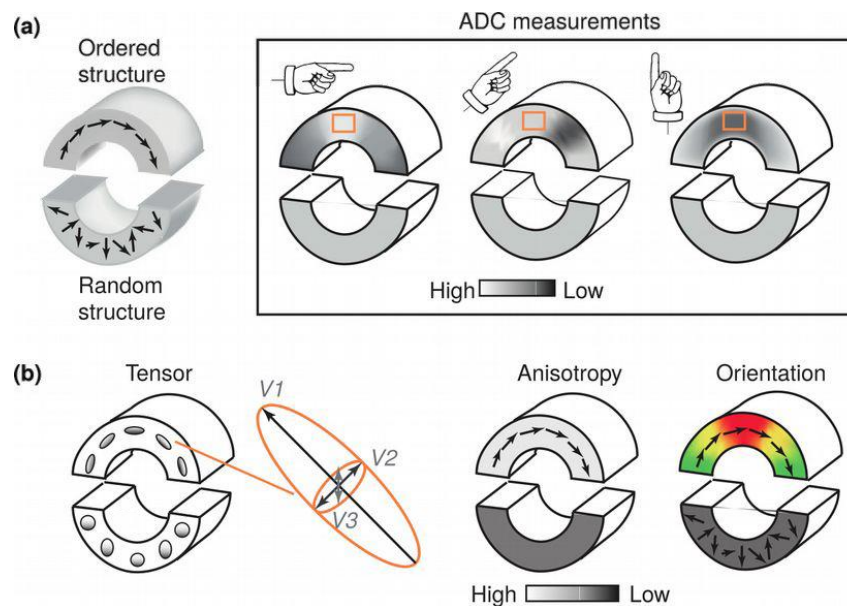


Figure 21 - From diffusion anisotropy to diffusion tensor. (a) An ideal phantom composed by ordered (upper part) and random (lower part) structures. The image intensity is high when the structures have the same orientation as the diffusion gradient applied (represented by the hand). (b) Diffusion tensors visualized as ellipsoids and rendered as anisotropy and orientation-encoded color maps^{163, 151}

The tensor-derived scalar indices are used to generate grayscale images for visualization and quantification. In figure 22 are represented the DTI contrasts of a mouse brain. In the mean diffusivity image, the CSF appears bright while the mouse brain parenchyma appears rather homogeneous. The axial diffusivity and radial diffusivity images show more contrasts between GM and WM structures than the mean diffusivity image. The CC has higher axial diffusivity values and lower radial diffusivity values than the neighboring cortical regions.

In the FA and RA images, major whitematter structures, such as the CC, can be distinguished from GM structures by their high anisotropy values. In the DEC image, the CC appears red because most fibers are arranged along the left–right orientation.

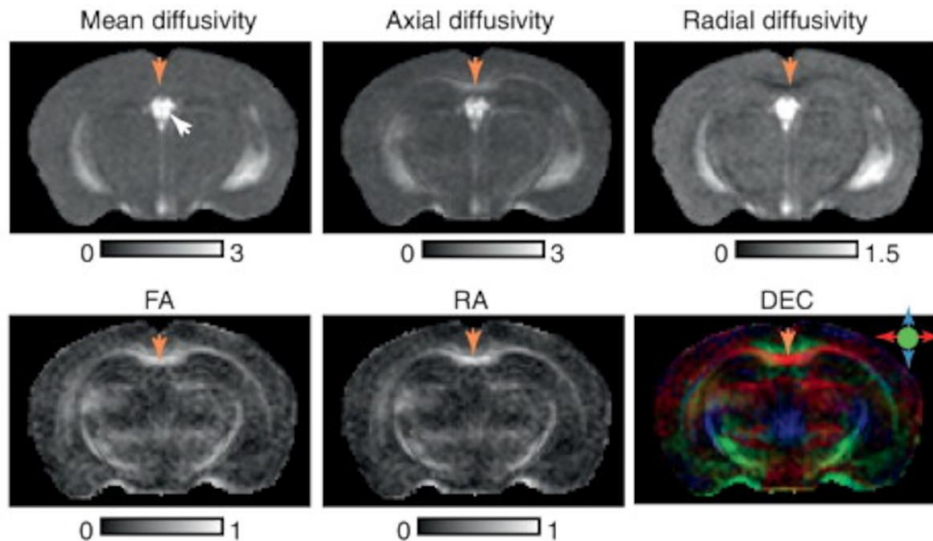


Figure 22 - DTI contrasts in the mouse brain. The CSF in the ventricle is indicated by the white arrow. The CC is indicated by yellow arrows. The unit for mean, axial, and radial diffusivity is $\mu\text{m}^2/\text{ms}$. FA and RA are unitless. In the DEC image, major white-matter tracts characterized by high anisotropy are shown with color-coded orientations. The color scheme is red, left–right; green, rostral–caudal; and blue, superior–inferior^{163,151}

Different models have been proposed to explain how cell infiltration in white-matter regions might influence the diffusion anisotropy and diffusivity measurements (Figure 23). An injury to the axon and to the myelin during early stages will lead to decreases in axial diffusivity and increases in radial diffusivity¹⁶⁴. When axon and myelin debris are removed both axial and radial diffusivity increase¹⁶⁵. The presence of inflammation infiltrating cells will contribute to decrease of axial diffusivity but an increase of radial diffusivity.

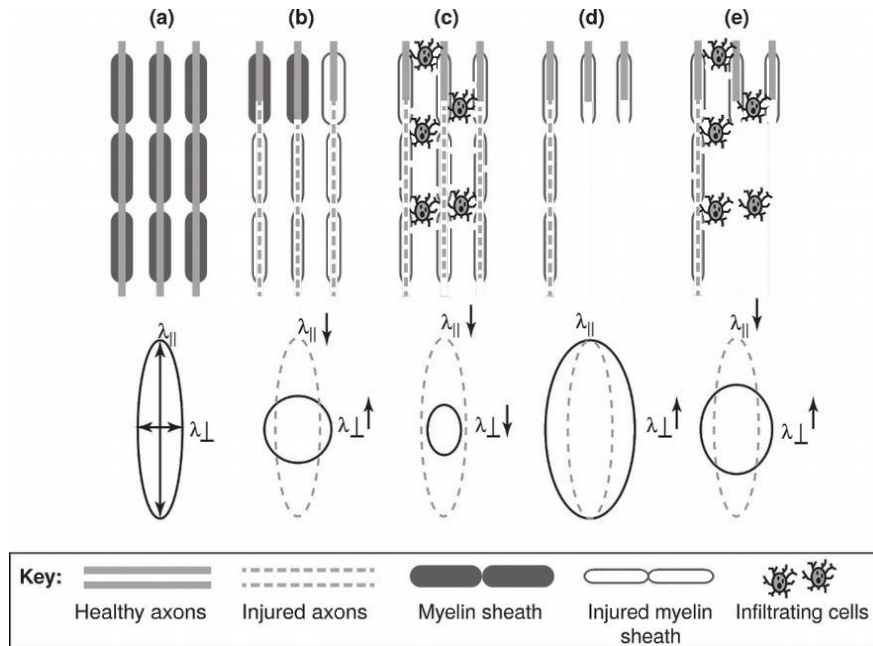


Figure 23 - Schematic diagrams illustrating how complex neuropathology can affect DTI results. (a) Normal myelinated axons and the corresponding diffusion tensor and axial and radial diffusivity ($\lambda_{||}$ and λ_{\perp} , respectively). The diffusion tensor is represented by the ellipsoid here and is shown in subsequent plots as a grey ellipsoid with dashed lines. (b, c) Axon and myelin injury with and without cell infiltration. (d, e) Axon and myelin injury with axonal loss, with and without cell infiltration^{163, 151}

Some issues are associated to DTI. DTI is generally sensitive but has a lower specificity, which, though, can be increased by combining the interpretation of DTI with the clinical history and the other findings on conventional imaging. Another problem regards the generation of artifacts and noise which are seen in all modalities of imaging and have many causes, which can result in misinterpretation of imaging findings if the radiologist is unaware of these artifacts. Fortunately, with a thorough understanding of artifacts associated with DTI, measures can be taken to decrease them. Another limitation of DTI is that it has a low signal to noise ratio (SNR), which may increase scanning times¹⁴⁹. SNR compares the level of background noise to the level of the signal obtained: when the noise is too high in comparison to the signal (low SNR), image quality is poor. Two ways to improve on this signal to noise ratio is to either increase scan times or reduce image resolution¹⁶⁶, although long scan times can result in patient motion artifact which also can cause artifact. Voxels continue to decrease in size, but a current limitation in DTI is that the size of voxels is still too high¹⁴⁹. Low anisotropy shown in a particular voxel may seem to represent unorganized tissue contained within it. However, this may just be apparent and what lie within the particular voxel are multiple anisotropic structures orientated in multiple directions, resulting in isotropy. This means that diffusion anisotropy will only show on DTI when all structures coursing a voxel align on a microscopic (myelin sheath, protein filaments) and macroscopic (axons and dendrites) scale. In the cortex, low FA occurs because of macroscopic disorganization. As image resolution improves, the cortex will likely show higher patterns of anisotropy. Other causes resulting in artifacts can include eddy currents

and motion, but changing data acquisition methods can help decrease these artifacts¹⁶⁷. DTI has now moved beyond research investigation and is becoming incorporated into routine clinical practice. However, some have urged caution in the interpretation of DTI and other advanced imaging sequences at the individual level, including a 9/13/18 Radiological Society of North America guideline statement¹⁶⁸. A minority of studies have not found a relationship between DTI and mTBI, although most of the literature is supportive¹⁶⁵. Given the different techniques in performing DTI, and the wide variety of applications, this caution is well taken. However, if the interpreting radiologist has experience in DTI and has developed a standardized and replicable technique concordant with the literature, and particularly if a trauma database or normative database is available, these valid criticisms become moot, and DTI can be interpreted in individual patients¹⁴⁹. This approach has backing in the literature and studies performed on individual patients demonstrate reproducibility and accuracy in diagnosing them individual patients with TBI¹⁶⁹. Specifically, DTI is most powerful when interpreted in concert with the clinical history and other findings on conventional imaging. The most comprehensive peer review article on TBI and DTI concluded: "Despite significant variability in sample characteristics, technical aspects of imaging, and analysis approaches, the consensus is that DTI effectively differentiates patients with TBI and controls, regardless of the severity and timeframe following injury. Furthermore, many have established a relationship between DTI measures and TBI outcomes."¹⁵⁶

DTI has proven to be highly sensitive to brain injury and a variety of pathological conditions and in many instances is becoming a routine part of clinical practice. Further research will continue to expand the application of DTI in evaluating neurological conditions¹⁵⁶.

1.5 Imaging biomarkers for repetitive mild TBI

A biomarker is an objective measure of a biological or pathological process that can be used to evaluate disease risk or prognosis, to guide clinical diagnosis, and/or to monitor therapeutic interventions²⁰. To date there are no diagnostic tools that can be used to monitor the consequences of a concussion, and return-to-practice guidelines are only based on the evaluation of symptoms. Symptoms caused by rmTBI are highly variable and there are no validated imaging biomarkers to determine whether or not a patient with a normal CT scan of the brain has neuronal damage.

rmTBI, which is highly frequent in contact sports, is a risk factor for a complicated recovery process and for the development of late-life neurodegeneration²⁰. Validated biomarkers for mTBI may help dissecting the cause-and-effect relationships between repetitive head impacts, mTBI, post-concussive syndrome and CTE²⁰.

1.5.1 Microscopic changes: diffuse axonal injury – DTI analysis

Due to its size and viscoelastic nature, the human brain is particularly vulnerable to the mechanical forces imparted during head impacts. The human brain viscoelasticity implies that, on one hand, brain tissue is mechanically compliant under gradual accelerations associated with daily living, being able to endure substantial tissue deformation and to return to its resting shape unharmed², while, on the other hand, brain tissue acts stiffer under very rapid or dynamic deformations which result from rotational accelerations caused by head impacts². In fact, under normal daily mechanical loading conditions, axons can easily stretch to at least twice their resting length and relax back unharmed to their prestretch straight geometry¹⁷⁰, while under dynamic loading with rapid stretch, the axonal cytoskeleton can physically break¹⁷⁰. The WM is at greatest risk of damage, possibly due to its highly organized and highly directional anisotropic structure, which make WM particularly susceptible to rotational acceleration/deceleration forces, causing DAI¹⁷¹. DAI is a microscopic injury that occurs even in the absence of frank tissue disruption and is an important cause of morbidity in patients with TBI. However, there is a lack of a simple and reliable technique to early identify patients with DAI and to prognosticate long-term outcome in this patient group. Although “diffuse” implies that it is widespread throughout the CNS, DAI is better described as lesions in multiple loci throughout the WM tracts, specifically the CC and within the cerebral hemispheres and brainstem¹⁷². Recent human and animal studies using advanced imaging alongside animal histopathology examinations have implicated DAI as a key pathological substrate of concussion¹⁷³. As neuronal circuits and functions depend on WM integrity¹⁴⁰, disruption of the axonal cytoskeleton caused by shear-tensile forces may impair axonal transport, while secondary damage from disruption of transport, proteolysis, and swelling can take place¹⁷². Ionic imbalances, such as intracellular calcium overload, which is caused by neuronal membrane disruption⁷⁹, may further damage axons, progressively affecting structural brain networks, from focal axon alteration to delayed axonal disconnection⁶.

In normal axon bundles, free diffusion of water is radially restricted by these highly organized structures; thus, mTBI, which disrupt axon through DAI, is expected to cause abnormal diffusion metrics in WM¹⁷⁴. In 2002, Arfanakis et al.¹⁴⁷ demonstrated decreased FA, primarily within the CC and internal capsule, in a small cohort of patients with acute mTBI. Kraus et al. corroborated this finding in a chronic mTBI cohort, showing decreased FA in the corticospinal tract, sagittal stratum, and superior longitudinal fasciculus¹³⁵. Numerous articles published since then support the findings of decreased FA and increased MD in various WM tracts after mTBI, some correlating with symptom severity and persistence¹⁵⁶. Alterations in these metrics were strongly correlated with the number of “knockouts” in a study of boxers and mixed martial artists, supporting cumulative effects of multiple episodes of mTBI¹⁷⁵. Animal studies have shown a direct correspondence between even very subtle TAI pathology and decreases in WM anisotropy¹⁴⁸. Bennett et al.¹⁷⁶, in a mouse model of rmTBI, showed reduced AD and MD within WM 7 days post-injury

compared to shams, indicative of axonal degeneration. Animal models suggest that AD correlates with axonal integrity, while RD correlates with myelin integrity and extracellular edema¹⁷⁷. Early increases in AD and RD in the acute phase of mTBI have been attributed to transient edema¹⁷⁸. These findings support the existence of additional pathophysiologic changes that follow axonal injury after mTBI.

Interestingly, a minority of articles report regions of increased FA after mTBI¹⁷⁹. However, Eierud et al.¹⁸⁰ found that such paradoxical findings are significantly more common for studies of acute mTBI (less than 2 weeks), while lower FA values are generally reported for studies of postacute mTBI. These results suggest that anisotropy changes in mTBI are dependent on the time since injury¹⁴³. Transient axonal swelling and loss of extracellular (and thus freely diffusing) water have been proposed as possible reasons behind this early increase in FA¹⁸¹. Compensatory changes related to Wallerian degeneration of other tracts, as well as selective axonal loss within an area of crossing fibers, are other potential explanations for this paradoxical increase¹⁸¹.

There is evidence of correspondence between DTI metrics and clinical symptoms of mTBI. In their meta-analysis, Eierud et al.¹⁸⁰ found that this connection appears to be time dependent, with lower neuropsychological performance correlating with higher anisotropy in the acute phase and lower anisotropy in later phases, while Lipton et al. linked prefrontal WM FA decreases to lower executive function¹⁶⁹. The number of regions with decreased FA has also been negatively correlated with cognitive outcome¹³⁵. In terms of noncognitive symptoms of mTBI, Alhilali et al. demonstrated a correspondence between decreased FA in the cerebellum/fusiform gyri and vestibular symptoms, as well as decreased FA in the right anterior thalamic radiation/geniculate nucleus optic tracts and ocular convergence insufficiency (Figure 24)¹⁸². Fakhran et al. have also demonstrated that sleep/wake disturbances in mTBI patients are correlated with decreased FA in the parahippocampal gyri¹⁸³.

Taken together, these DTI findings suggest that axonal injury is related to cognitive deficits, as well as post-concussive symptoms in mTBI patients¹⁴³.

Although ROI-based, voxel-based, and fiber-tracking analyses of DTI have yielded significant insight into axonal injury and TBI, the presence of crossing axonal fibers in any given voxel poses a significant challenge to the use of FA as an accurate metric of the extent of WM injury. This is because crossing WM fibers in a single voxel may result in a low FA value despite high anisotropy in each of the individual fibers¹⁸⁴. Furthermore, first-order diffusion analysis is still limited by the inherent assumptions of its ellipsoidal, Gaussian modeling of diffusion¹⁷⁴. Cellular structures within each voxel create distinct intracellular and extracellular compartments, leading to non-Gaussian water diffusion¹⁸⁵.

Continued advances in DTI acquisition and postprocessing for tractography attempt to address several of these issues¹⁴³.

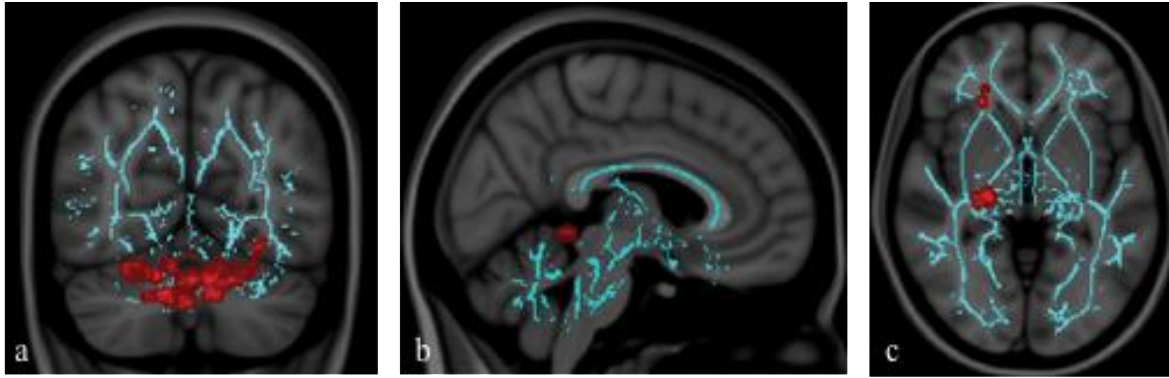


Figure 24 - In 30 mTBI patients, vestibular disturbances correlated with (a) decreased FA in cerebellar regions and (b) increased MD in vermian lobules of the spinocerebellum, while convergence insufficiency in 25 mTBI patients correlated with (c) increased FA in the right anterior thalamic and right geniculate nucleus optic radiations. Images were derived from tract-based spatial statistics (TBSS) results and rendered on T1-weighted images from the Montreal Neurologic Institute in (a) coronal, (b) sagittal, and (c) axial projections. Significant voxels ($P < .05$, corrected for multiple comparisons) were thickened by using TBSS fill function into local tracts (red) and overlaid on WM skeleton (blue).⁷⁷

1.5.2 Macroscopic changes: brain atrophy – Volumetric analysis

In some cases, rmTBI may be associated with long-term brain volume loss, as well as histological changes, including tau-immunoreactive NFTs, the hallmark of CTE⁸⁶, and A β deposition, the hallmark of AD¹²⁸. CTE is a putative tauopathy characterized by global brain atrophy with a thinned CC, enlarged ventricles, and cavum septum pellucidum¹²⁸, which have been found in autopsy studies of a limited number of athletes (including football players) who have suffered from repetitive concussions. Post-concussive symptoms, which include behaviour and personality changes, such as depression, apathy, impulsivity, and aggression, have been associated with generalized and regional brain atrophy in various study populations¹⁸⁶.

Neuronal damage from TBI has been commonly associated with cerebral atrophy in studies of mTBI¹⁹. Blatter et al.¹⁸⁷ studied cerebral atrophy cross-sectionally in 123 TBI patients, concluding that there was a progressive decrease in total brain volume starting 3 weeks after moderate-to-severe TBI, and reaching significance 8–12 months later. Subsequent brain volume loss continued at a rate greater than that seen with normal ageing for up to 3 years after injury¹⁸⁸. A similar finding was reported in patients with mTBI¹⁸⁹. A study including 53 retired Canadian Football League players was aimed at showing that multiple concussions may contribute to measurable brain atrophy independent from normal brain volume loss associated to ageing, and that this atrophy is associated with cognitive deficits and behavioural changes¹⁹⁰. Volumetric analyses revealed greater hippocampal atrophy than expected for age in former athletes with multiple concussions than controls, and that smaller

left hippocampal volume was associated with poorer verbal memory performance in the former athletes. In military service members who sustained mild blast-injury, Tate et al.¹⁹¹ showed subacute-to-chronic cortical thinning in the left superior frontal and temporal gyri, areas that are functionally implicated in audition and language. In a post hoc review, most of their patients were found to have audiology problems¹⁹¹. In a study of professional boxers, caudate volume loss was found to correlate with the number of years of professional fighting after adjusting for age, race, and education, presumably secondary to cumulative effects of multiple concussive episodes⁴⁴.

The use of structural MRI to detect brain changes associated to mTBI is an attractive option due to its widespread clinical use and availability of various techniques. Conventional MRI is the preferred structural brain imaging technique due to its resolution and specificity, allowing to discriminate between white and gray matter, providing useful insight in many neurological conditions where white or gray matter are affected, and detecting brain atrophy. When the brain atrophies, the ventricles increase in size. These two observations are seen in postmortem CTE and they can be easily discovered using conventional MRI. A study conducted by Wilde et al., performed structural MRI scans on a group of 10 boxers and nine controls¹⁹². The group of boxers had significantly larger ventricles than that of the group of noncombat sports controls, suggesting boxing-related cerebral atrophy. However, since cerebral atrophy is a hallmark of AD, ventricles enlargement detection would only determine atrophy, not the pathological cause⁹⁹. Moreover, ventricular enlargement is only seen in 53% of CTE verified cases⁸⁶, reducing the clinical specificity of its measurement. A longitudinal MRI study¹⁹³ that followed collegiate females soccer players over the course of 4 years found several significant alterations including an increase in the width of the sulci in the frontal and occipital cortices, subtle hemorrhagic changes, and in some players, a decrease in overall brain volume during what is generally a developmental phase of growth for young adults. Despite documented physical brain alterations, none of the athletes demonstrated long-term clinical deficits^{99,193}. A recent study by Churchill et al.¹⁹⁴ explored the long-term effects of sport-related concussions by performing comprehensive MRI techniques by comparing 21 athletes with a history of concussions with 22 concussive free athletes of both contact and non-contact sports. To characterize brain abnormalities associated with concussions, Churchill and colleagues measured structural changes, cerebral blood flow, and gray matter abnormalities. They found significant volumetric differences in the right hippocampus, left caudate, and cuneus, and, correlated with the number of concussions, they observed a decrease in perfusion in the temporal and frontal lobes^{99,194}. A longitudinal case study performed by Raji et al.¹⁹⁵ followed an ex-high school football player with history of concussions. They performed two MRI brain scans over the course of four years and found a 14% decrease in total gray matter, particularly in the midbrain, ventral diencephalon, and frontal lobes^{99,195}.

In a longitudinal study of civilian individuals after a single episode of mTBI, Zhou et al.¹⁹⁶ found global volume loss greater than what was seen in age-matched healthy control subjects between the subacute phase of injury (average 1 month) and 1-year follow-up (Figure 25).

There was significant WM volume loss in the anterior cingulum and the cingulate gyrus isthmus, as well as precuneal cortex¹⁹⁶. In addition, these structural findings correlated with neuropsychiatric testing performance. Over time, left rostral anterior cingulate volume loss correlated with a decrease in verbal learning scores, right rostral anterior cingulate volume loss correlated with decreases in scores of sustained attention, concentration, working memory, and information processing, and lower left cingulate gyrus isthmus WM volumes correlated with higher scores on anxiety and PCS clinical symptoms¹⁹⁶. Even decades after injury, middle-aged adults who sustained remote mTBI were found to have lower hippocampal volume when compared with age-matched control subjects¹⁹⁷. Overall, the presence of macroscopic morphologic changes supports the presence of long-term brain injury after mTBI in at least a subgroup of patients, despite the lack of evidence for direct injury at conventional imaging¹⁴³.

A study from Ding et al. found a relationship between acute DAI and cerebral atrophy months later in 20 patients who suffered non-penetrating TBI¹⁸⁸. Although the pathophysiology of the post-TBI cerebral atrophy remains unknown, axonal injury and subsequent Wallerian degeneration may be a possible mechanism. Their hypothesis, based on animal data¹⁹⁸, is that at the acute stage (hours to days after non-penetrating brain injury), the axons swell due to the local ionic homeostatic disruption, increased permeability of the axolemma, with immediate mechanical damage to the axonal cytoskeleton (primary axotomy) seen in severe cases. Days to months after the injury, pathological changes of DAI are believed to consist of progressive disorganization of the axonal cytoskeleton and progressive protein accumulation, leading to disconnection of axons (secondary axotomy). The primary and secondary axotomy also triggers the local or even global metabolic changes which would lead to further cell death and Wallerian degeneration¹⁹⁸. This pathologic process may lead to cerebral atrophy in the chronic phase after TBI¹⁸⁸.

Although MRI is an attractive option, limitations exist. MRI can provide information on the extent of diffuse injuries, but its widespread application is restricted by cost, the limited availability of MRI in many centers, and the difficulty of performing it in physiologically unstable patients.

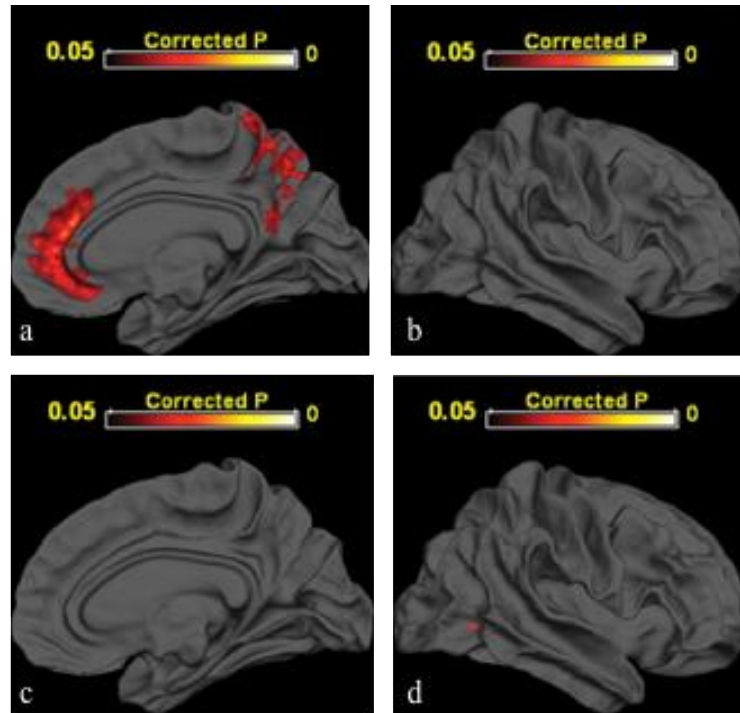


Figure 25 - Areas of significant volume loss are demonstrated by projecting coregistered data from (a) medial and (b) lateral projections in 28 mTBI patients and (c) medial and (d) lateral projections in 22 control subjects onto right cerebral hemisphere templates after 1 year (Bonferroni-corrected $P < 0.05$).¹⁹⁶

Chapter 2

Aim

The aims of the study are:

- 1) to provide an in dept characterization of acute and chronic neurological dysfunction emerging after repetitive mild traumatic brain injury in mice¹¹⁸.
- 2) to understand wheter in vivo MRI may allow to detect micro and macro structural changes before the emergence of neurological impairments in mice.

Chapter 3

Materials and methods

3.1 Ethics statement

The IRCCS Istituto di Ricerche Farmacologiche Mario Negri (IRFMN) adheres to the principles set out in the following laws, regulations, and policies governing the care and use of laboratory animals: Italian Governing Law (D.lgs 26/2014; Authorization no. 19/2008-A issued March 6, 2008 by the Ministry of Health), IRFMN Institutional Regulations and Policies providing internal authorization for persons conducting animal experiments (quality management system certificate: UNI EN ISO 9001:2008, Registration no. 8576-A), and the EU directives and guidelines (European Economic Community Council Directive 2010/63/UE). They were reviewed and approved by the IRFMN Animal Care and Use Committee, which includes ad hoc members for ethical issues, and by the Italian Ministry of Health (Decree nos D/07/2013-B and 301/2017-PR; authorization no. 317/2018-PR). Animal facilities meet international standards and are regularly checked by a certified veterinarian who is responsible for health monitoring, animal welfare supervision, experimental protocols, and review of procedures.

3.2 Animals

A total of 46 mice were randomly assigned to 1 of 4 groups: repetitive sham (n=8 male, n=8 female), repetitive injury (n=9 male, n=9 female), single sham (n=10, male), single injury (n=12, male). Male and female C57BL/6J mice (9 weeks of age) from Envigo (Horst, Netherlands) were housed in a specific pathogen free vivarium at a constant temperature (21 ± 1 °C) and relative humidity (60 ± 5 %) with a 12 h light/dark cycle and free access to pellet food and water. All animal experiments were designed in accordance with the ARRIVE guidelines, with a commitment to refinement, reduction, and replacement, minimizing the numbers of mice, and using biostatistics to optimize mouse numbers (as in our previous work with the mouse TBI model¹⁹⁹). Thus, for statistical validity, we used 12 to 18 mice for the behavioral tests, and 7 to 8 mice for histology. The mice were assigned to the different experimental groups using randomization lists (www.randomizer.org). Behavioral, imaging, circulating biomarker and histological assessments were done by researchers blinded to the experimental groups.

3.3 Injury Protocol

Mice were anesthetized with isoflurane inhalation (induction 3%; maintenance 1.5%) in an N₂O/O₂ (70%/30%) mixture and placed in a stereotaxic frame. The animals were placed on a heating pad to maintain their body temperature at 37 °C. MTBI was induced using a 5 mm diameter rigid impactor driven by an electromagnetic controlled impact device (impactOne, Leica), rigidly mounted at an angle of 20° to the vertical plane and applied to the intact scalp, between bregma and lambda, over the left parieto-temporal cortex (antero-posteriority: -2.5 mm, laterality: -2.5 mm), at impactor velocity 5 m/s and deformation depth 1 mm, resulting in a mTBI (Figure 26). The criteria for a mTBI were: (1) a short period of post-traumatic apnea <30 seconds (recognized as an animal analog to human LOC); (2) a short period of righting reflex (<6 minutes); (3) no sign of skull fractures at the time of euthanasia, and (4) no history of major hemorrhages¹²³. At the end of the procedure, each animal was removed from the stereotaxic table, was allowed to recover and upon becoming ambulatory, was returned to its home cage. RmTBI mice received a total of five hits, with a 48 h interinjury interval; smTBI mice received a single hit; repetitive sham animals were subjected to the same procedures and were exposed to anesthesia for the same length of time as the rmTBI animals, but did not receive a hit, to control for the effects of anesthesia; single sham animals were subjected to the same procedures and were exposed to anesthesia for the same length of time as the smTBI animals, but did not receive the hit, to control for the effects of anesthesia. A total of 5 injuries was used to mimic the impacts incurred during contact sports where the brain receives multiple injuries within days or weeks prior to full recovery of the previous injury¹²³. The choice of a 48-hour interval between injuries derives from the work of Longhi et al.¹²⁶, which showed a window of vulnerability of 72 hours in the mouse after injury.

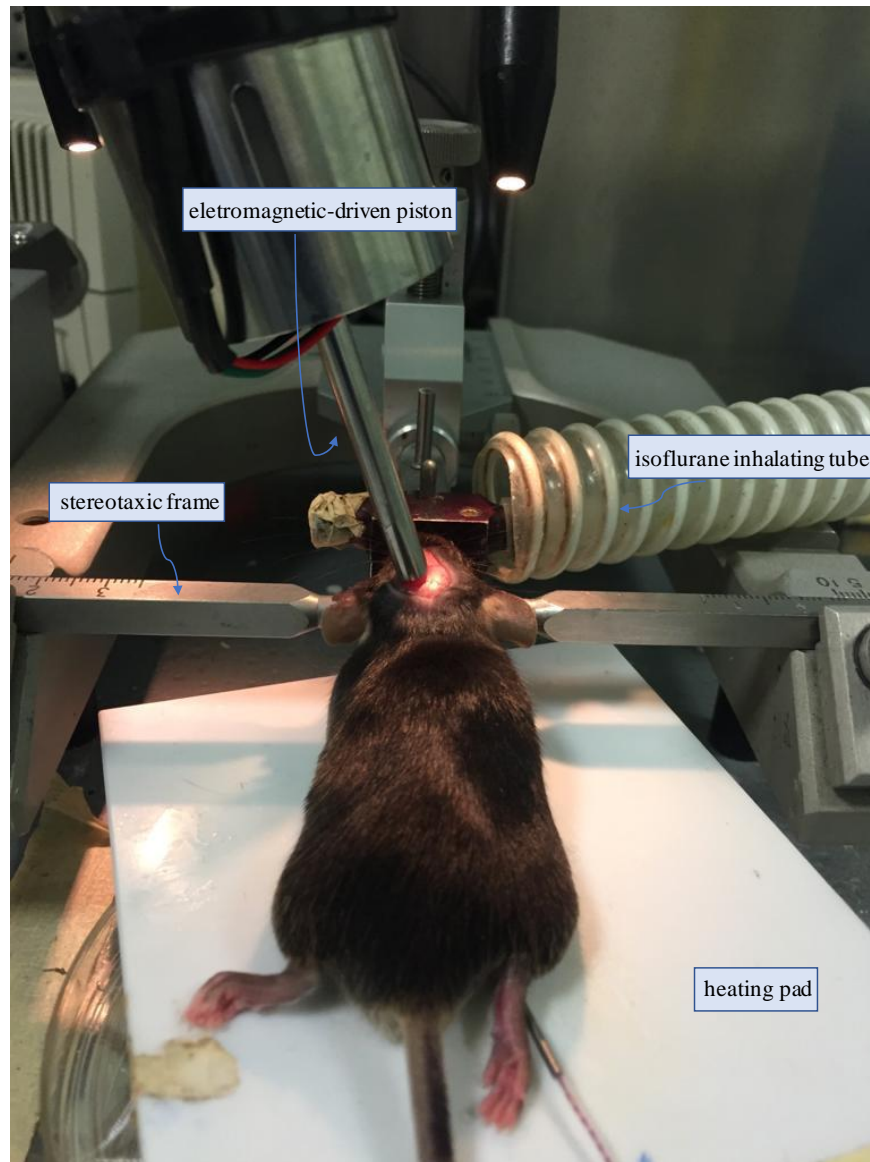


Figure 26 - Mice were anesthetized with isoflurane inhalation (induction 3%; maintenance 1.5%) in an N₂O/O₂ (70%/30%) mixture and placed in a stereotaxic frame on a heating pad to maintain their body temperature at 37 °C. MTBI was induced using a 5 mm diameter rigid impactor driven by an electromagnetic controlled impact device (impactOne, Leica), rigidly mounted at an angle of 20° to the vertical plane and applied to the intact scalp, between bregma and lambda, over the left parieto-temporal cortex (antero-posteriority: -2.5 mm, laterality: -2.5 mm), at impactor velocity 5 m/s and deformation depth 1 mm.

3.4 Experimental Design

Repetitive sham (male n=8, female n=8), rmTBI (n=18), single sham (male n=10) and smTBI (male n=12) were longitudinally analysed following the experimental plan shown (Figure 27). Sensorimotor deficits were evaluated by SNAP and Neuroscore tests (1 and 5 weeks, 3, 6 and 12 months) by the same operator for the entire duration of the study. Imaging studies were done as T2 weighted (T2w) MRI (6 and 12 months) and DTI MRI (6 and 12 months). Body weight at all time points was recorded in all mice. Blood samples were taken at 1 and 5 weeks post injury, and at 3, 6 and 12 months post injury. All mice were sacrificed at 12 months for histopathological analysis.

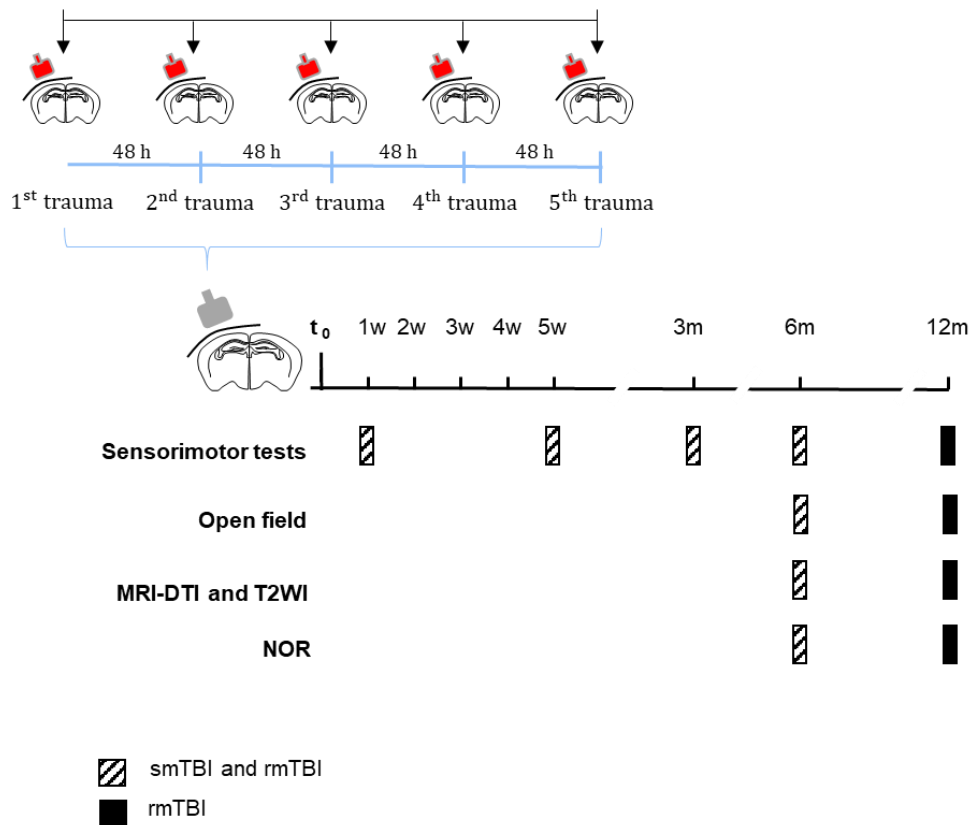


Figure 27 - Schematic representation of the experimental design. mTBI was induced by electromagnetic controlled impact device on the left parietal bone in anesthetised mice. Mice subjected to repeated mTBI (rmTBI) received 5 injuries 2 days apart, over a period of 8 days. Mice subjected to a single head impact (smTBI) received one injury the 8th day. w, week; m, month; MRI, magnetic resonance imaging; DTI, diffusion tensor imaging; T2WI, T2-weighted imaging; SNAP, Simple Neuroassessment of Asymmetric Impairment; NOR, novel object recognition.

3.5 Assessment of consciousness

The state of consciousness was assessed immediately after each mTBI or sham procedure by examining two indicators for LOC: apnea and righting reflex. Apnea was examined immediately after removing the animal from the stereotaxic frame, and any latency for breathing to resume was recorded. The righting reflex is an acute neurological evaluation which was assessed by placing the subject on their side, after removing the animal from the stereotaxic frame, and measuring the time the animal took to return to an upright position. The presence or absence of LOC is a useful tool in grading TBI severity in animal models. Additionally, when utilizing the repeat mTBI paradigm, it is important to maintain a record of mouse weights before each trauma, and for the duration of the study. This is to ensure consistent monitoring for stress and general animal welfare throughout the entire time course of the mTBI procedures. Normal grooming, eating and drinking should be observed within the first hour post procedure¹²⁵.

Body weight at all time points was recorded in all mice before receiving any stress or mTBI manipulations in that particular day. Baseline body weights were measured before the 1st trauma for all groups. The percentage change in body weight was then calculated relative to each animal's baseline.

3.6 Behavioural tests

3.6.1 Simple Neuroassessment of Asymmetric Impairment

Simple Neuroassessment of Asymmetric Impairment (SNAP) is a battery of neurological tests developed to assess neurological deficits induced in mouse models of TBI. Mice were evaluated using eight tests to assess neurological parameters including vision, proprioception, motor strength and posture. Each test could be rated from 0 to 4. The results from each of the eight tests were summed to derive the overall SNAP score (Figure 28). A neurologically intact animal would be expected to have a SNAP score of "0". SNAP scores were high when asymmetric deficits were apparent.

SCORE:	0	1	2	3	4	5
A. Interactions	Avoids being handled	Responds quickly only after briefly touched	Freezes before escaping	Responds after multiple nudges	Only moves head	Comatose
B. Cage Grasp	Both paws release simultaneously	CL paw first to release <50% of grasps. Struggles or an otherwise active, alert mouse that does not grasp.	CL paw first to release >50% but <100% of grasps	CL paw always first to release	CL paw does not grasp	Does not grasp with either paw
C. Visual Placing	Once aware of ledge, arches back & reaches out with both forepaws	May reach with both paws but IL leads. Twists body. Taps CL paw	Occasionally does not reach with CL paw	Does not reach with CL paw at all	Head not raised and neither paw reaches	Comatose
D. Pacing or Circling	Random directions	Freezing, but able to guide into either direction	Turns in one direction predominantly	Pacing, obstinate progression in same direction	Tight circling	Rolling
E. Gait and Posture	Normal gait & posture	Occasionally notice CL limb abduction, but inconsistent or also observed IL	CL limb abducts when walking or stays caudal to body when mouse stops	CL limbs knuckle or too weak to support weight of mouse	Drags CL limbs	Recumbent
F. Head tilt	No tilt	Ambiguous head tilt	Occasional head tilt noticed	Obvious head tilt	Torticollis	Recumbent
G. Visual Field	Responds to visual stimulus bilaterally	No response but an otherwise active, alert mouse and/or has other indications of normal vision	<50 % CL responses and >50% IL responses	Consistent positive IL response, consistent lack of CL response	No response on either side and other indications of visual loss	Comatose
H. Baton	Normal	An otherwise alert, active mouse that struggles or does not grasp. Tosses applicator. Loose CL grasp	Occasionally does not grasp with CL paws	Frequently does not use CL paws	Does not use CL paws at all	Unable to grasp swab

Figure 28 - Description of score system assigned to the SNAP test.

The first test, interaction with the handler, not only assesses the level of alertness, but also requires integration of vision to escape the evaluator's hand. Interaction was tested upon removal of the mouse from the home cage (Figure 29A). An alert and active mouse that avoided handling was assigned a score of "0" for that test.

The second test, cage grasp, was used to evaluate grip strength, and was performed immediately after removal of the mouse from its home cage. The mouse was held suspended by the tail over the cage lid (metal bars, 1.5 mm in diameter, spaced 6 mm apart) and was allowed to grasp a bar with both forepaws (Figure 29B). The mouse was slowly pulled away from the cage, noting which paw released first. An injured mouse was expected to have contralateral grip weakness; therefore, if the contralateral forepaw was the first to release greater than 50% but less than 100% of the time, the score would be "2".

For the third test, visual placing (Figure 29C), the mouse was held suspended by the tail and slowly advanced toward a countertop or a ledge level with its torso. The uninjured mouse extended its upper torso to simultaneously reach out toward the edge of the countertop with both forepaws. Visual placing evaluated vision, torso strength, forelimb coordination, proprioception, and tactile input. Ambiguous responses (score of "1"), seen in a number of injured mice, included twisting of the body, or "tapping" of the ledge with the contralateral paw, perhaps due to decreased contralateral vision, decreased proprioception and/or tactile input from the contralateral paw.

The fourth test, pacing/circling, was an observation of the ambulation direction in a test chamber (18 cm deep and 40 cm on each side). An uninjured mouse would ambulate in a random fashion, turning to either the right or the left when facing a corner. Brain-injured mice were expected to consistently turn toward one direction and to not be readily coaxed in the opposite direction (Figure 29D).

The fifth test was an observation of gait and limb posture. Uninjured mice kept all limbs tucked beneath the body when standing still or ambulating. Weakness, dragging or abduction of contralateral limbs was expected in brain-injured mice (Figure 29E).

In the sixth test, varying degrees of head tilt were present if the head was rotated within the coronal plane (Figure 29F).

The seventh test examined each visual field by waving a fiber-tipped applicator (2 mm diameter) on either side of the head, allowing enough distance to avoid contact with the vibrissae (Figure 29G). If the mouse consistently turned its head toward the source of the movement on both sides, the score for the visual field test would be “0”.

The eighth and final test, “baton”, evaluated coordination and proprioception. The mouse was held suspended by the tail and allowed to grasp a fiber-tipped applicator with all four paws. The applicator was released while the mouse remained suspended. An uninjured mouse would grasp the applicator tightly with all four paws and often would attempt to “climb” it (Figure 29H)²⁰⁰.

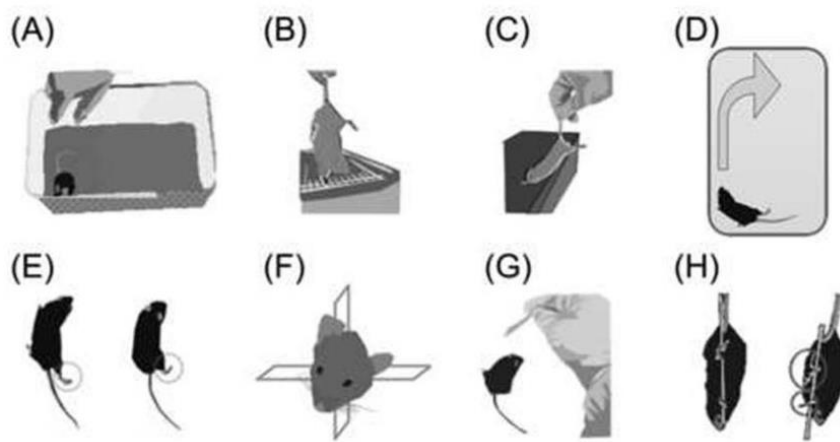


Figure 29 - Graphical representation of the test to perform on the animal.

3.6.2 Neuroscore

Neuroscore is a short neurological assessment which detects deficits in mice reflexes. Animals are scored from 4 (normal) to 0 (severely impaired) for each of the following indices: 1) forelimb function during walking on the grid; 2) flexion function response during suspension by the tail; 3) hindlimb function during walking on the grid and extension function during suspension by the tail; and 4) resistance to lateral right and left pulsion. The maximum score per animal is 12.

1. Grid walk: animals are allowed to walk on an open wire grid for 1 minute during which a qualitative assessment of the foot-faults of both forelimb and hindlimb is performed to establish whether an observable motor deficit is present. The deficit is measured by the inability of the animal to immediately retract its paw after falling through the grid. This evaluation (deficit/no deficit) has been shown to sensitively detect both forelimb and hindlimb motor dysfunction. If the animal has forelimb or hindlimb deficits, a point of 1 should be subtracted from evaluation.

2. Forelimb function: the animals are suspended over the cage grid from the tail. The following deficits should be evaluated: a) the hyperactivity (rapid movements of the right vs left forelimb while suspended over the grid), b) the strength (right versus left forelimb when grasping the grid), c) the use of the fingers (affected forelimb usually is not able to grasp the grid with all fingers) and d) if the animals grasp the same grid bar with both forelimbs.

Based on number of deficits, we assigned the following score:

- 4 = no deficits;
- 3 = at least 2 deficits;
- 2 = at least 3 deficits;
- 1 = more than 3 deficits or none movement of forelimb when touches the grid;
- 0 = the forelimb remains flexed against the body.

To the final score, we subtracted 1 point if the animal had the forelimb deficit while walking on the grid (*).

3. Hindlimb function: the animals are suspended from the tail over the cage (near the grid edge, animals should not grasp the grid). Animals are observed for 30 seconds, evaluating the pattern of toes spread and hindlimb extension.

We assigned the following score:

- 4 = hindlimb extension > 75% of the time and hindlimb finger extension (22-30/30 sec);
- 3 = hindlimb extension < 75% of the time (15-22/30 sec) or >75% of time but lacked hindlimb toes extension.
- 2 = hindlimb extension < 50% of the time (8-15/30 sec);
- 1 = hindlimb extension < 25% of the time (1-8/30 sec);
- 0 = hindlimb flexed without extension.

To the final score, remember to subtract 1 point if the animal had the hindlimb deficit while walking on the grid (*).

4. Resistance to lateral right and left pulsion. Finally, the animals are tested for both right and left resistance to the lateral push into 1 meter alternated from left to right and from right to left. Animals are pushed over tissue papers, to allow them grabbing on it. The earlier the mouse is knocked over, the lower is the score received.

The score is assigned based on this scale:

- 4 = mouse is not knocked over;
- 3 = mouse is knocked over at 3/4 of the push;
- 2 = mouse is knocked over 1/2 of the push;
- 1 = mouse is knocked over 1/4 on the push;
- 0 = mouse is knocked over immediately.

3.6.3 Open Field

The open field test (OFT) measures locomotor activity and anxiety-like behavior in mice, exploiting the natural aversion of rodents to exposed fields. The OFT is a fast and relatively easy test which utilizes: 1) a generally square arena with surrounding walls that prevent escape, made from white or black plastic contrasted to the color of the mouse; 2) a video camera placed above the arena to record the movements of the mouse; 3) a video tracking software that tracks and analyzes the behavior, movement, and activity of the animal, supplied by Noldus (Ethovision; Wageningen, The Netherlands). The most common outcome of interest are: distance moved, time spent moving, rearing, and change in activity over time, time spent in center, time spent in borders, velocity. Animals are placed in the arena by the investigator and thus forced to interact with a novel environment for 5 minutes, while they are tracked by the camera placed above the arena. This short length of time emphasizes exploratory behavior and response to novelty, rather than baseline activity. In TBI mice we expect them to spend the majority of their time in close proximity to the walls, a phenomenon referred to as thigmotaxis, and to walk a greater distance respect to sham mice²⁰¹.

We performed the OF test as follows:

- 1) We set all the trial parameters in Ethovision software (contrast, recording time etc.). At least one day before starting the experiment we put one animal inside the arena to adjust the contrast and make sure that the center-point, nose-point and tail-base detection were optimal.
- 2) We transported mice to the testing room at least 1 hour prior to testing to allow mice to acclimate to the experimental room. This time period should be extended if the transfer involves excessive changes in the ambient environment or other potential stressors.
- 3) We turned on video camera. Note that it is good practice to record each session to allow one to reassess the results of a session at a later time if necessary.
- 4) It's important to clean the arena prior to each trial, even if it is not dirty, to avoid any residual smell which could distract the animal.
- 5) We placed the mouse in the center of the arena and immediately after the positioning we started the timer in EthoVision.
- 6) The tester was positioned away from the arena and field of view of the mouse and remained still and quiet throughout each trial.
- 7) At completion of trial, after 5 minutes, we removed the mouse from the arena and placed in a new cage, to avoid the contact with the other animals which were not yet subjected to the trial.
- 8) Cleaned the OF with disinfectant.
- 9) Waited until disinfectant has fully dried prior to placing next mouse in the OF.

3.6.4 Novel Object Recognition

Novel Object Recognition (NOR) test is an assay for the investigation of learning and memory in mice. It is a relatively fast test which utilizes: 1) an open-square grey arena (40 × 40 cm), 30 cm high as described previously²⁰², with surrounding walls that prevent escape, made from white or black plastic contrasted to the color of the mouse; 2) a video camera placed above the arena to record the movements of the mouse; 3) a video tracking software that tracks and analyzes the behavior, movement, and activity of the animal, supplied by Noldus (Ethovision XT 5.0, Wageningen, The Netherlands); 4) different objects used to evaluate memory in mice. The test is completed over 3 steps: habituation, training, and testing step (Figure 30). The first is for habituation of the mouse in the new environment during which mice were placed in the empty arena for 5 min and their movements were recorded (Ethovision XT 5.0, Noldus). The next day, the training phase simply involves visual exploration of two identical objects, placed in the same arena, while during testing one of the previously explored objects is replaced with a novel object. As rodents have an innate preference for novelty, a rodent that remembers the familiar object will spend more time exploring the novel object, while an animal with impaired memory will explore both objects in the same way. Exploration was recorded in a 10 minutes trial by an investigator blinded to the experimental group. Sniffing, touching and stretching the head toward the object at a distance of no more than 2 cm were scored as object investigation. The time between training and testing, known as the retention interval, can be altered to assess short- and long-term memory. At a retention interval of 24 h, most mice, even those without memory impairment, will not be able to discriminate between the familiar and novel object: to probe for memory deficits an optimal retention interval would be between 20 min to 4 h²⁰³. In our experiment, we choose a retention interval of 24 hours. In the test phase mice were placed in the arena containing two objects: one identical to one of the objects presented during the familiarization phase (familiar object), and a new, different one (novel object), and the time spent exploring the two objects was recorded for 10 min (Ethovision XT 5.0, Noldus). Memory was expressed as a discrimination index (DI), i.e. (seconds on novel – seconds on familiar)/(total time on objects).

We performed the NOR test as follows:

- *Step 1: Habituation.*

- 1) We set all the trial parameters in Ethovision software (contrast, recording time etc.). At least one day before starting the experiment we put one animal inside the arena to adjust the contrast and make sure that the center-point, nose-point and tail-base detection were optimal.
- 2) We transported mice to the testing room at least 1 hour prior to testing to allow mice to acclimate to the experimental room. This time period should be extended if the transfer involves excessive changes in the ambient environment or other potential stressors.
- 3) We turned on the video camera. Note that it is good practice to record each session to

allow one to reassess the results of a session at a later time if necessary.

- 4) It is important to clean the arena prior to each trial, even if it is not dirty, to avoid any residual smell which could distract the animal.
- 5) For the habituation day, we placed the mouse in the center of the arena and immediately after the positioning we started the timer in EthoVision.
- 6) The tester was positioned away from the arena and field of view of the mouse and remained still and quiet throughout each trial.
- 7) At completion of trial, after 5 minutes, we removed the mouse from the arena and placed in a new cage, to avoid the contact with the other animals which were not yet subjected to the trial.
- 8) Cleaned the arena with disinfectant.
- 9) Waited until disinfectant has fully dried prior to placing next mouse in the arena.

○ *Step 2: Training.*

- 1) We opened the trial file performed during habituation to continue the experiment in Ethovision.
- 2) It is important to handle mice well prior to training in order reduce any stress or anxiety that may interfere with their desire to explore the arena and the objects.
- 3) We transported mice to the testing room at least 1 hour prior to testing to allow mice to acclimate to the experimental room. This time period should be extended if the transfer involves excessive changes in the ambient environment or other potential stressors.
- 4) We turned on video camera. Note that it is good practice to record each session to allow one to reassess the results of a session at a later time if necessary.
- 5) It is important to clean the arena prior to each trial, even if it is not dirty, to avoid any residual smell which could distract the animal.
- 6) We placed 2 identical objects on the diagonal (i.e., one in the NW corner and one in the SE corner). Objects must be mouse-sized or only slightly larger to encourage exploration; to reduce induced preference, mice should be able to climb on both objects or neither object (time spent just sitting on an object is not counted towards exploration time); if objects are too light and can be moved by the mouse, they should be fasten to the floor.
- 7) 24 hours after the habituation step, we placed the mouse in the center of the arena, equidistant from the 2 identical objects, and immediately after the positioning we started the timer in EthoVision.
- 8) The tester was positioned away from the arena and field of view of the mouse and remained still and quiet throughout each trial.
- 9) At completion of trial, after 10 minutes, we removed the mouse from the arena and placed in a new cage, to avoid the contact with the other animals which were not yet subjected to the trial.
- 10) We cleaned the arena with disinfectant.
- 11) We waited until disinfectant has fully dried prior to placing next mouse in the arena.

○ *Step 3: Testing.*

- 1) We opened the trial file performed during training to continue the experiment in Ethovision.
- 2) It is important to handle mice well prior to training in order reduce any stress or anxiety that may interfere with their desire to explore the arena and the objects.
- 3) We transported mice to the testing room at least 1 hour prior to testing to allow mice to acclimate to the experimental room. This time period should be extended if the transfer involves excessive changes in the ambient environment or other potential stressors.
- 4) We turned on video camera. Note that it is good practice to record each session to allow one to reassess the results of a session at a later time if necessary.
- 5) It is important to clean the arena prior to each trial, even if it is not dirty, to avoid any residual smell which could distract the animal.
- 6) We placed one object used during training (i.e., the familiar object) and one novel object in opposite quadrants of the arena, using the same locations as used during training for each mouse.
- 7) 4 hours after the training step, we placed the mouse in the center of the arena, equidistant from the 2 objects, and immediately after the positioning we started the timer in EthoVision.
- 8) The tester was positioned away from the arena and field of view of the mouse and remained still and quiet throughout each trial.
- 9) At completion of trial, after 10 minutes, we removed the mouse from the arena and placed in a new cage, to avoid the contact with the other animals which were not yet subjected to the trial.
- 10) We cleaned the arena with disinfectant.
- 11) We waited until disinfectant has fully dried prior to placing next mouse in the arena.

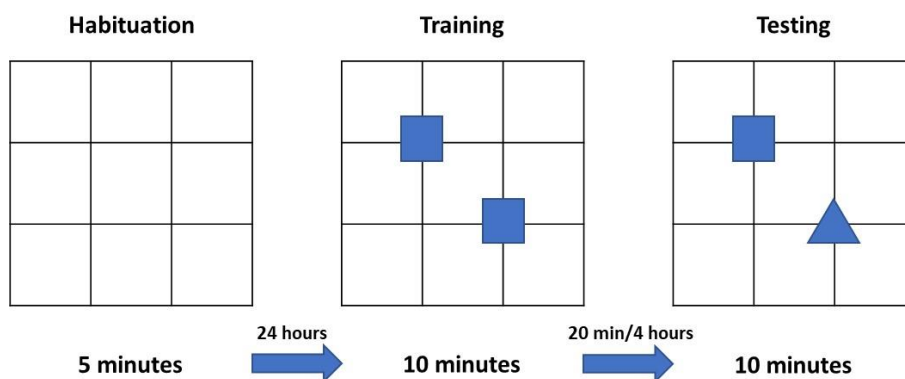


Figure 30 - Graphical representation of the position of the objects inside the arena.

3.7 MRI acquisition and analysis

3.7.1 Acquisition

Mice were anesthetised with isoflurane (induction 3 vol %, maintenance 1.5 vol %) in a mixture of N₂O/O₂ (70%/30%). The head was fixed using a stereotaxic frame and positioned in the magnet. Respiratory frequency was monitored throughout the experiment and body temperature was maintained at 37°C with a heating pad. Brain imaging was done on a 7T small-bore animal scanner (BioSpec®; Bruker, Ettlingen, Germany) running ParaVision 6.01 and equipped with a quadrature 1H CryoProbe™ (Bruker, Ettlingen, Germany) surface coil as transmitter and receiver. DTI, and 3D T2-weighted imaging (T2WI) were obtained to quantify, WM damage and brain volumes/cortical thickness, respectively.

DTI: echo-planar imaging sequences were acquired (TR/TE=7000/32 ms, resolution 125 × 125 μm²; FOV 1.5 × 1.5 cm²; acquisition matrix 120 × 120, slice thickness 0.3 mm). Diffusion encoding b factors of 800 mm²/s were applied along 19 isotropic directions and two B₀ unweighted images for each repetition.

Anatomical images: T2 weighted imaging (T2WI) were obtained with a 3D fast low-angle shot MRI (FLASH) sequence (TR/TE 250/3 ms; Flip angle 15°; image resolution 100 × 100 × 100 μm³; FOV 3 × 0.8 × 1.1 cm²; acquisition matrix 300 × 80 × 110).

3.7.2 Analysis

DTI analysis. To investigate the white matter integrity, a tract based spatial statistics (TBSS) method was adopted²⁰⁴. The diffusion tensor was computed using FSL software²⁰⁵. A group mean full tensor template was first created using a population-based DTI atlas construction algorithm that adopts a tensor-based registration procedure embedded in the DTI-TK software library. The average template was then resampled to an in-plane resolution of 100 × 100 μm² and slice thickness 0.2 mm, and skeletonized. Fractional anisotropy (FA) images of all subjects were normalized to the mean template with a diffeomorphic transformation and the transformations were applied to all the DTI metrics (MD, RD, AD) which were warped to the mean FA skeleton enabling a voxel wise statistical comparison of the DTI metrics. The skeleton of the FA map generated from the population-based DTI template was binarized and manually subdivided into 4 white matter regions of interest (ROI, Figure 35B) allowing the computation of the mean value of each DTI metric for each mouse.

Brain volumes analysis. We applied multi-atlas approach for automatic brain segmentation without the need of manual tracing^{206–208}. After the creation of an in-house set of mouse brain atlases (Figure 31) all the anatomical brain images acquired in the study were preprocessed by correcting the non-uniform bias field and parcellated following the steps

(Figure 32): each subject was warped to the full template and the template mask was backprojected to the subject space obtaining the subject mask and therefore the brain extraction. Multi-atlas segmentation approach, using the `antsJointLabelFusion.sh` script²⁰⁹ embedded in the ANTs software²¹⁰ have been used to warp the ten brains templates to the subject brain. The reference atlases were backprojected to the subject space and fused together to create the anatomical parcellation. *Cortical thickness analysis*. All cortical labels of the Dorr MRI atlas of the mouse brain²¹¹ were combined (enthorinal cortex, frontal, occipital and parieto-temporal lobe) into one single label. Voxelwise computational approach was based on the `KellyKapowsky` command within ANTs toolkit²¹² a gradient step size for the optimization of 0,1. The final result of this process is a cortical voxelwise map with a nominal thickness value in each voxel, reflecting the deformation field that voxel has been subjected to²¹³.

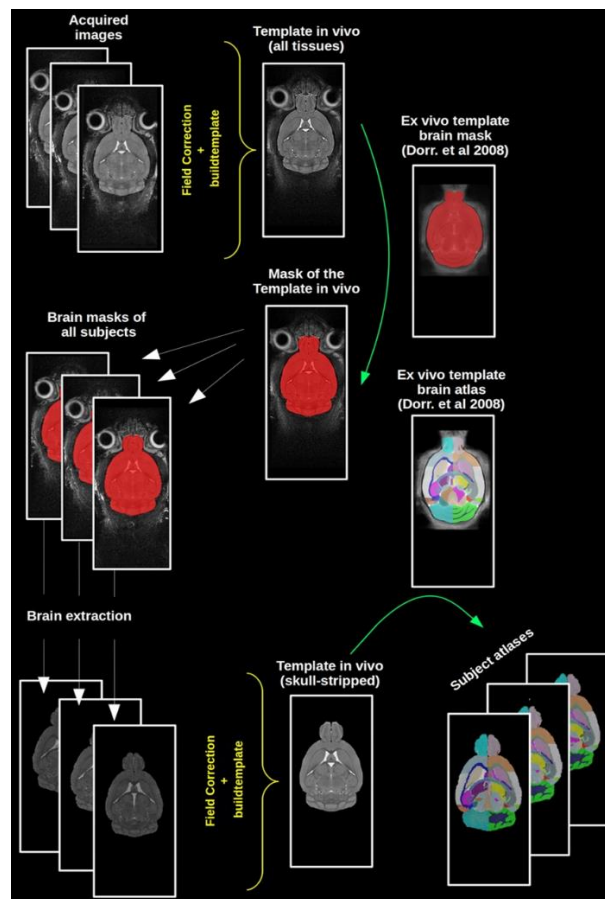


Figure 31 - Workflow followed to create the in-house atlases. Acquired images are corrected and averaged to create an in-house Template. This is normalized over an ex vivo template and masked. The template mask is projected to the reference images that are subsequently masked and averaged to create an in-house skull stripped template. This brain template is again normalized over the ex-vivo template and reference atlases obtained back-projecting the ex-vivo atlas.¹⁵¹

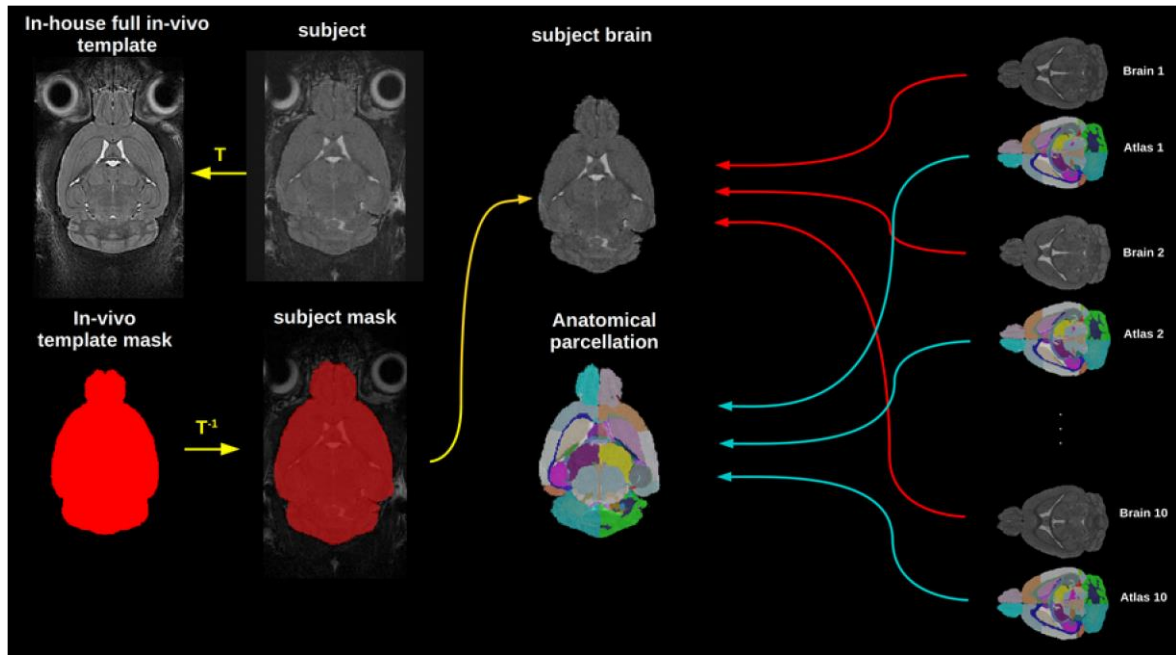


Figure 32 - Automatic parcellation procedure. Firstly, the brain extraction is performed (yellow arrows). Subsequently the normalization of the reference images to the subject brain (red arrows) allowed the projection and the fusion of all the reference atlases to the subject space (blue arrows).¹⁵¹

3.8 Statistics

Differences between male and female mice, unless specified in the text, never reach statistically significant differences and for this reason considered as a whole group.

Statistical analysis was done with GraphPad Prism 8 (GraphPad Software, USA), using absolute values. The choice between parametric or non-parametric tests was based on passing the Shapiro–Wilk normality test, and data distribution was inspected by QQ plot. For each experiment, the figure legend reports the statistical analysis of data. Outliers were identified using the ROUT method and excluded from analysis. Differences between groups were reported as statistically significant for $p < 0.05$.

Voxel-Based Analysis (VBA) on the entire skeletonized WM and cortical thickness were performed using SPM12. Second level analysis was done using a full factorial model with trauma and time as variables. Statistical maps were thresholded with a significance level of $p < 0.05$ and corrected for family wise error.

Chapter 4

Results

Single sham (n=10, male) and single mild TBI (smTBI) (n=12, male) animals were evaluated at a different period compared to repetitive sham (n=8 male, n=8 female) and repetitive mild TBI (rmTBI) (n=9 male, n=9 female). Sensorimotor performances, diffusion tensor imaging (DTI) analysis and structural magnetic resonance imaging (MRI) analysis were taken at 1w, 5w, 3m, 6m for the single sham and smTBI groups. A 12 months' time point was added for the repetitive sham and rmTBI groups.

4.1 Assessment of consciousness following repetitive mild TBI

Immediately after each mild TBI (mTBI) or sham procedure two indicators of loss of consciousness (LOC) (apnea and righting reflex) were assessed. Mice weight before each trauma and after 1w, 5w, 3m, 6m, 12m for the rmTBI group was recorded, as well as for the smTBI group, the mouse weight was recorded before the single trauma and after the same time points as the rmTBI group except the 12m time point.

As expected, subjects in the sham group did not show signs of LOC for any indicator.

The righting reflex in the first day of trauma (rmTBI) and in the day of single trauma (smTBI), was higher compared to sham subjects (mean rmTBI: 3,5 min; mean smTBI: 3,1 min; mean sham: 0,28 min) (Figure 33A). Importantly no difference was present between smTBI and rmTBI, meaning that there was not any difference between the baseline procedure imparted to the single and the repetitive group.

The righting reflex duration slightly decreased with each mTBI, although this was not significant, indicating a sort of habituation to the trauma from mice (Figure 33B). Similar to righting reflex, there were no significant differences among impact apneas across injury group, although the time of apnea did decrease with each mTBI in the rmTBI group (Figure 33C).

To avoid bias due to differences in baseline body weight values, we measured the percentage change in body weight relative to each animal baseline. There were no significant differences in the percentage of weight change between sham group and rmTBI group at all time points (Figure 33D).

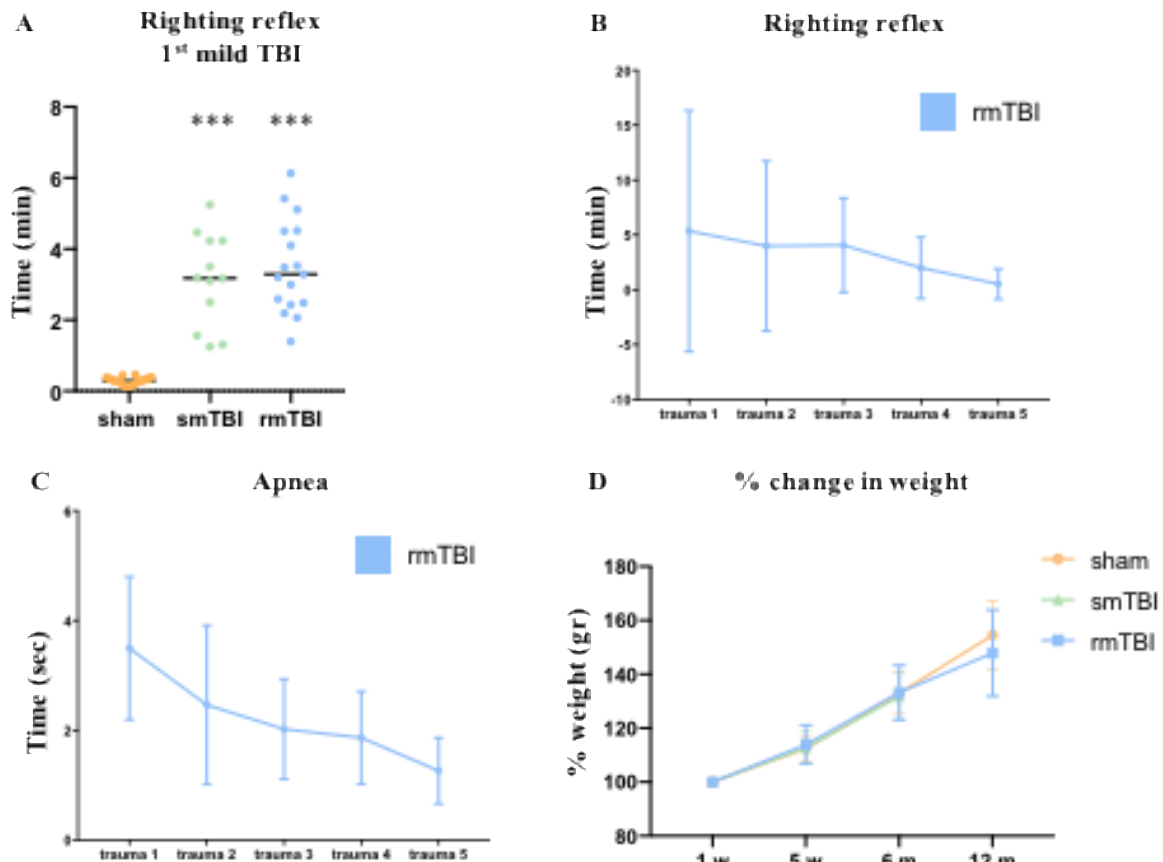


Figure 33 - Effect of rmTBI on apnea, righting reflex and percentage of weight change on sham, smTBI and rmTBI groups. (A) Righting reflex in smTBI (n=12), rmTBI (n=17), and sham (n=22) group. (B) Righting reflex in rmTBI mice (n=17). (C) Apnea duration in rmTBI mice (n=17). (D) Percentage of weight change between sham group (n=26) and rmTBI group (n=18) at all time points. Note: the 12m time point for the smTBI group was not recorded for any of the parameters. Data are presented as mean \pm standard deviation. ** $P < 0.01$; *** $P < 0.001$ versus sham by a 2-way ANOVA followed by Tukey's multiple comparison test.

4.2 Effects of repetitive mild TBI on behavioural outcome

Sensorimotor function examined by SNAP and neuroscore tests (Figure 34A/B) showed an acute transient impairment in rmTBI (SNAP sham: 2.4, rmTBI: 4.2; $p < 0.01$ vs sham at 1 week; and neuroscore sham: 10.1, rmTBI: 8.1; $p < 0.001$ vs sham at 1 week). From 5 weeks till 6 months after rmTBI, no differences were found between rmTBI and sham mice ($p > 0.05$) in both tests. Interestingly 12 months post injury sensorimotor deficits evaluated by SNAP emerged again in rmTBI mice (sham: 2.1, rmTBI: 3.8; $p < 0.01$ vs sham at 12 months) (Figure 34B). No differences were ever detected between sham and smTBI ($p > 0.05$).

Locomotor activity was examined by OF test at 6 (smTBI and rmTBI) and 12 (rmTBI) months (Figure 34 C/D).

Hyperactivity was detected in rmTBI mice at both 6 (sham: 1385 cm, rmTBI: 1858 cm; $p < 0.05$) and 12 months (sham: 2304 cm, rmTBI: 2850 cm; $p < 0.05$). No differences were found between smTBI and sham mice. Novel object recognition (NOR) test showed the emergence of a mnemonic impairment at 12 months in rmTBI. No difference in the memory performance was found between single sham and smTBI at 6 months ($p > 0.05$) (Figure 35D) that was not present at 6 months.

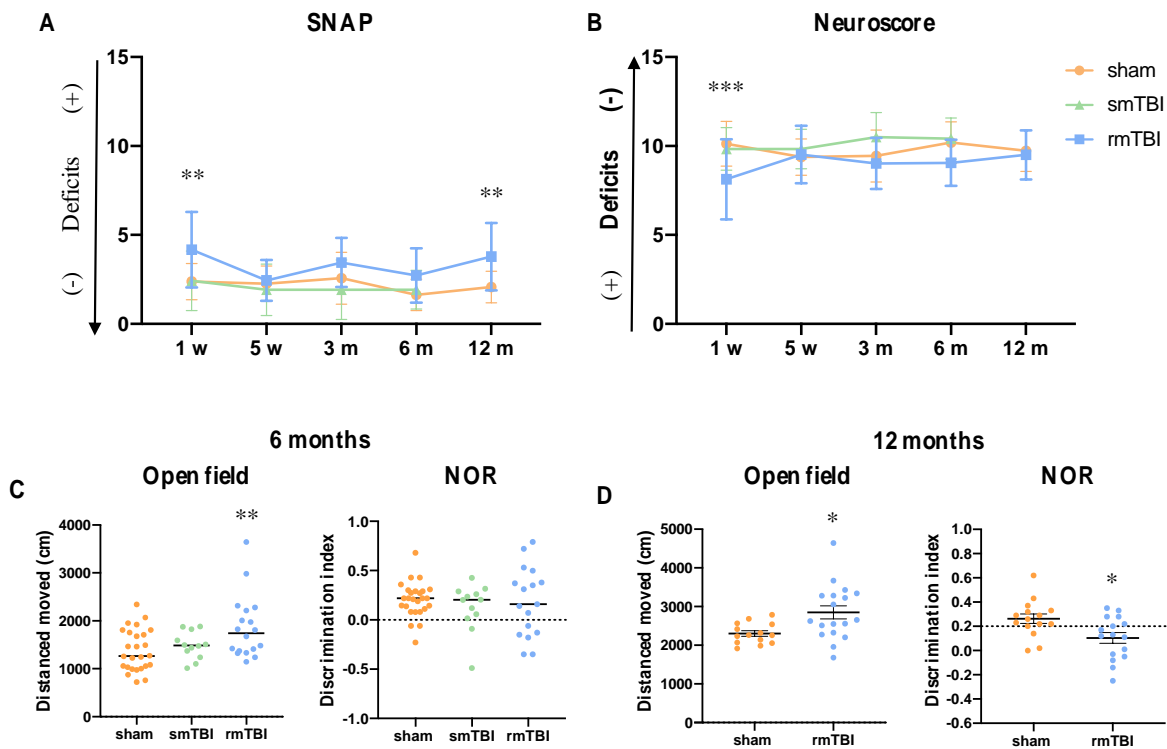


Figure 34 - Behavioural deficits. Sensorimotor deficits were longitudinally rated at 1 and 5 weeks, 3 and 6 months after the last smTBI, and 1 and 5 weeks, 3, 6 and 12 months after the last rmTBI (n=18) or sham (n=26) by Simple Neuroassessment of Asymmetric Impairment (SNAP) (A) and Neuroscore (B). RmTBI had a significantly worse SNAP score and Neuroscore at 1 week that emerged again with SNAP test at 12 months. No differences were found between smTBI (n=12) and sham mice at all time points in both tests. Data are presented as mean \pm standard deviation. ** $P < 0.01$; *** $P < 0.001$ versus sham by a mixed-effect model followed by Sidak's post hoc multicomparison test.

Open Field (OF) test for measuring locomotor activity and Novel Object Recognition (NOR) test for the investigation of learning and memory were performed at 6 months for smTBI (n=12), rmTBI (n=18) and sham (n=26) (C) and at 12 months (D) after the last repetitive mTBI (rmTBI, n=18) or sham (n=14). The OF test revealed that the rmTBI moved significantly more compared to shams both at 6 and 12 months. The NOR test showed no differences between sham and rmTBI at 6 months, while a significant difference emerged at 12 months. Data are presented as mean \pm standard error of the mean deviation. * $P < 0.05$ versus sham by unpaired t-test.

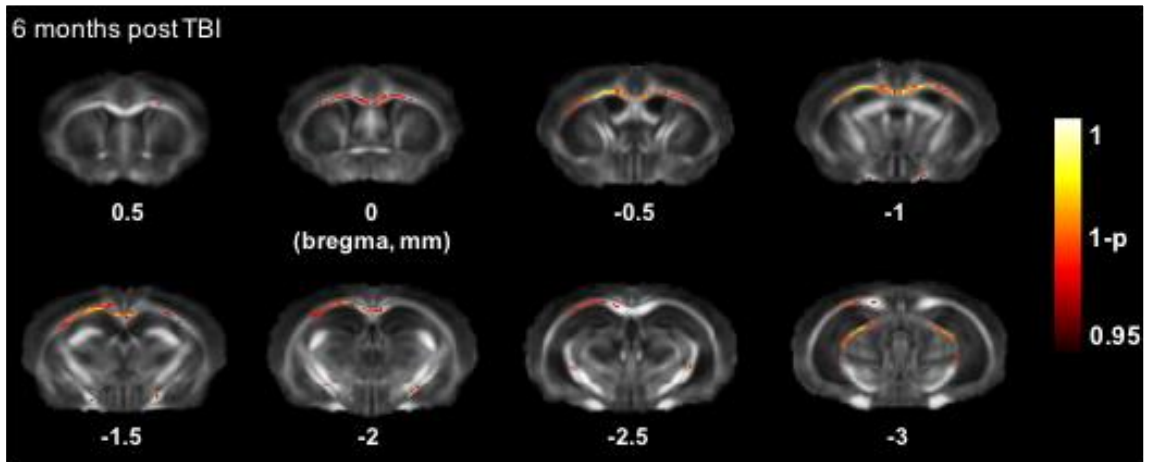
4.3 White matter damage assessed by DTI

DTI analysis performed at 6 and 12 months post injury showed a reduction in FA values in several WM tracts. Voxel based analysis (VBA) at 6 months show voxels with reduced FA values in correspondence to the corpus callosum (CC), external capsule (EC) and fimbria and the ipsilateral hemisphere was more affected than the contralateral ($p < 0.05$) (Figure 35A). ROI based analysis confirmed the VBA findings by showing that rmTBI mice have lower mean FA values in the ipsilateral and controlateral EC ($p < 0.001$) and the three subregions of the CC in rmTBI mice: genu (GCC) ($p < 0.001$), body (BCC) ($p < 0.001$) and splenium (SCC) ($p < 0.001$) (Figure 36A-D).

Axial diffusivity (AD) radial diffusivity (RD) and mean diffusivity (MD) were also affected by rmTBI. AD was reduced at both time points compared to sham values in the il-EC ($p < 0.001$), il-SCC ($p < 0.001$) and il-BCC at 12m ($P < 0.001$) and cl-EC ($p < 0.05$), cl-SCC ($p < 0.01$) and cl-BCC at 12m ($P < 0.01$) (Figure 37A-D). RD was increased at both time points compared to sham values in the il-EC ($p < 0.001$), il-SCC ($p < 0.01$), il-BCC ($P < 0.001$), il-GCC at 6m ($P < 0.001$) and cl-EC ($p < 0.05$), cl-SCC ($p < 0.01$), cl-BCC ($P < 0.01$), cl-GCC at 6m ($p < 0.5$) (Figure 37E-H). MD was increased only in the il-GCC at 6 m ($P < 0.05$) and BCC at 12 m ($p < 0.01$) (Figure 37I-M).

When comparing smTBI with sham mice at 6 months no differences were found in the WM FA by VBA (Figure 38A) while ROI based analysis in smTBI showed a significant FA reduction in the il-EC ($p < 0.05$) (Figure 38B-E). No differences were found in the other DTI metrics between smTBI and sham (Table 3).

A



B

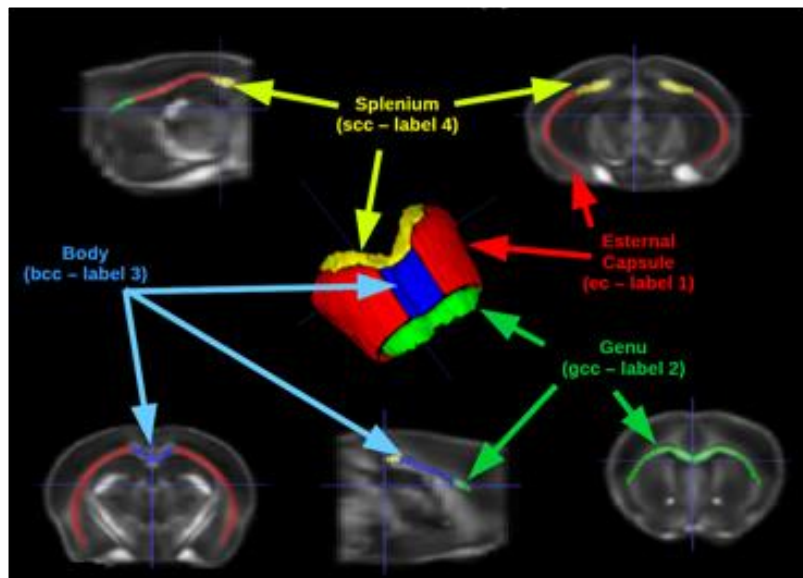


Figure 35 - DTI analysis of WM. (A) Voxel-based analysis evaluated at 6 months post rmTBI with red-yellow voxels showing a significant FA reduction ($p < 0.05$ by unpaired t-test) in rmTBI ($n=18$) compared to sham ($n=14-16$) mice. (B) Schematic representation of the ROI of WM tracts.

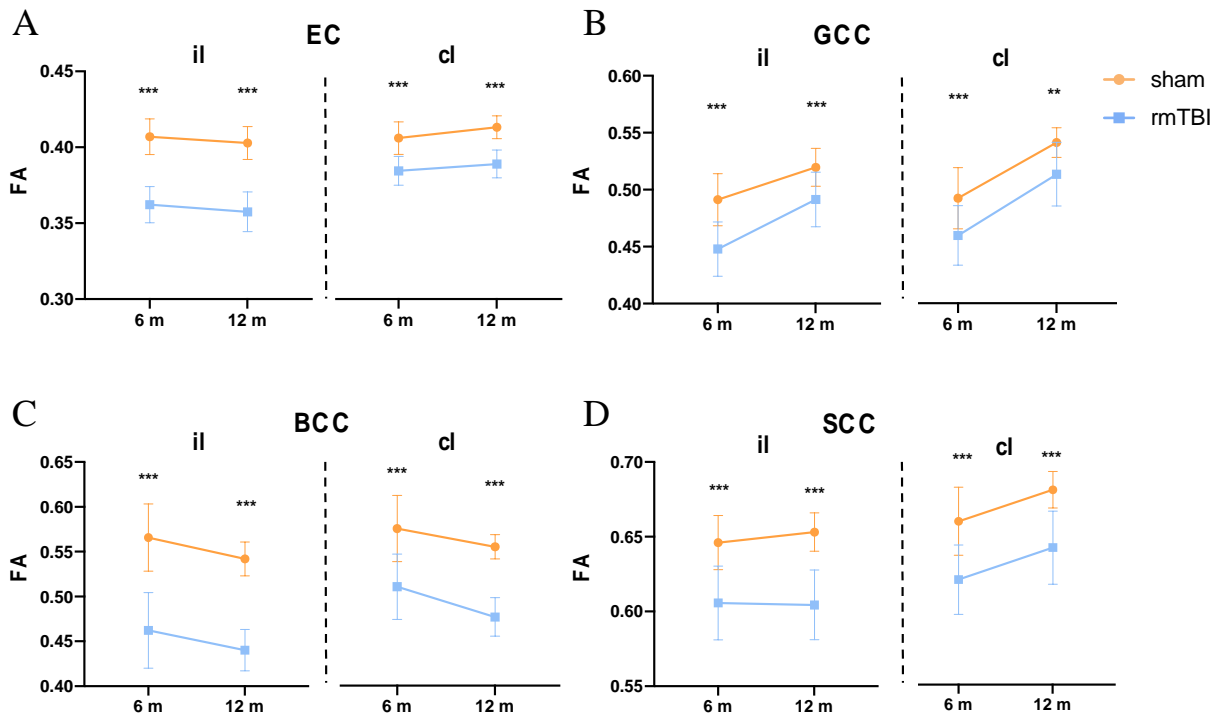


Figure 36 - ROI based analysis of ipsilateral (il) and contralateral (cl) WM showing mean FA values longitudinally assessed at 6 and 12 months post rmTBI. Data are presented as mean \pm standard deviation. ** $P < 0.01$, *** $P < 0.001$ rmTBI vs sham by a mixed-effect model followed by Sidak's post hoc multicomparison test.

EC: external capsule, BCC: body of the corpus callosum, GCC: genu of the corpus callosum; SCC: splenium of the corpus callosum

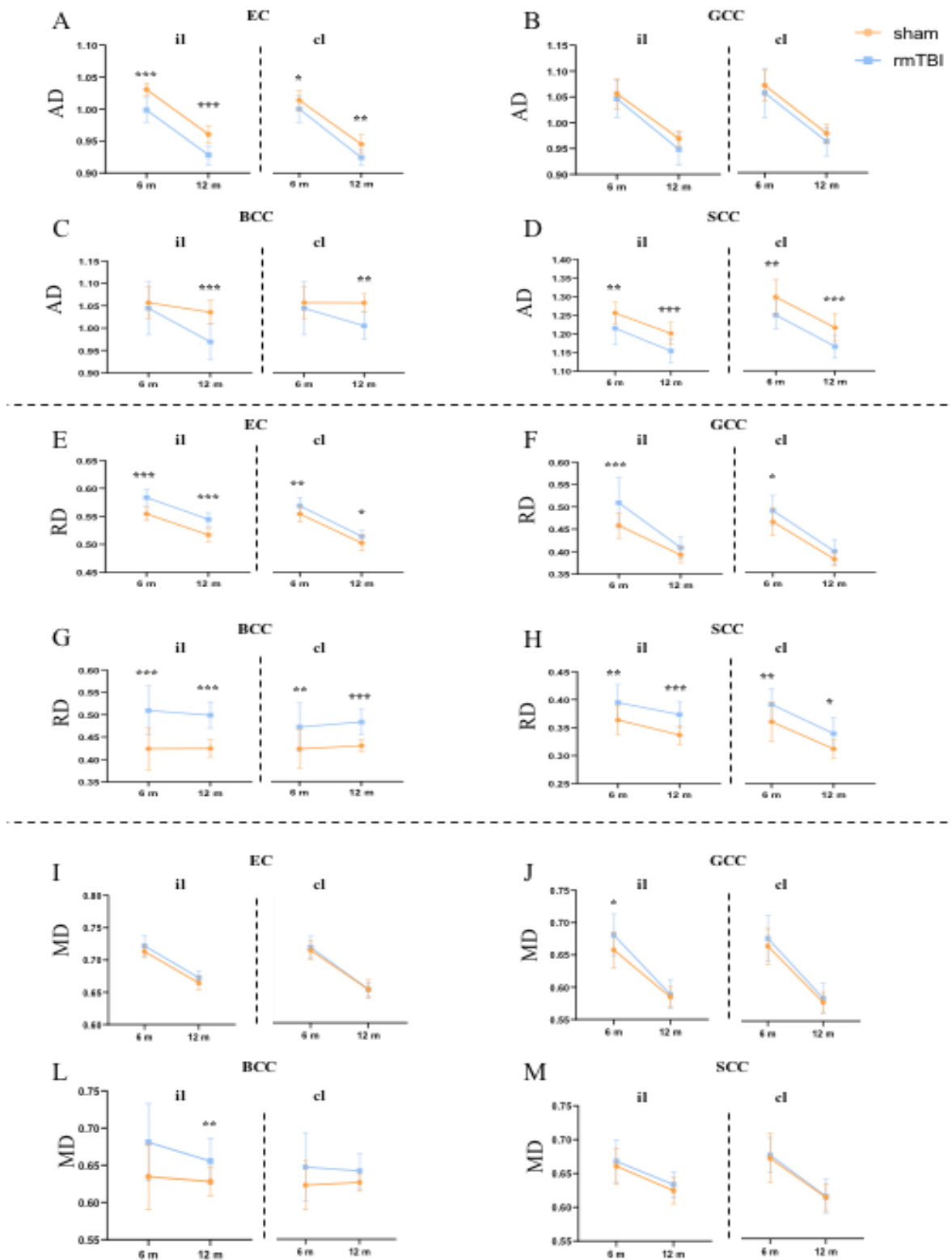


Figure 37 - ROI based analysis of ipsilateral (il) and contralateral (cl) WM showing mean AD, RD, MD values longitudinally assessed at 6 and 12 months post rmTBI. (A-D) AD was reduced at both time points compared to sham values in the il-EC ($p < 0.001$), il-SCC ($p < 0.001$) and il-BCC at 12m ($P < 0.001$) and cl-EC ($p < 0.05$), cl-SCC ($p < 0.01$) and cl-BCC at 12m ($p < 0.01$). (E-H) RD was increased at both time points compared to sham values in the il-EC ($p < 0.001$), il-

SCC ($p < 0.01$), il-BCC ($P < 0.001$), il-GCC at 6m ($P < 0.001$) and cl-EC ($p < 0.05$), cl-SCC ($p < 0.01$), cl-BCC ($P < 0.01$), cl-GCC at 6m ($p < 0.5$). (I-M) MD was increased only in the il-GCC at 6m ($P < 0.05$) and il-BCC at 12m ($p < 0.01$). Data are presented as mean \pm standard deviation. ** $P < 0.01$, *** $P < 0.001$ rmTBI vs sham by a mixed-effect model followed by Sidak's post hoc multicomparison test.

EC: external capsule, BCC: body of the corpus callosum, GCC: genu of the corpus callosum; SCC: splenium of the corpus callosum.

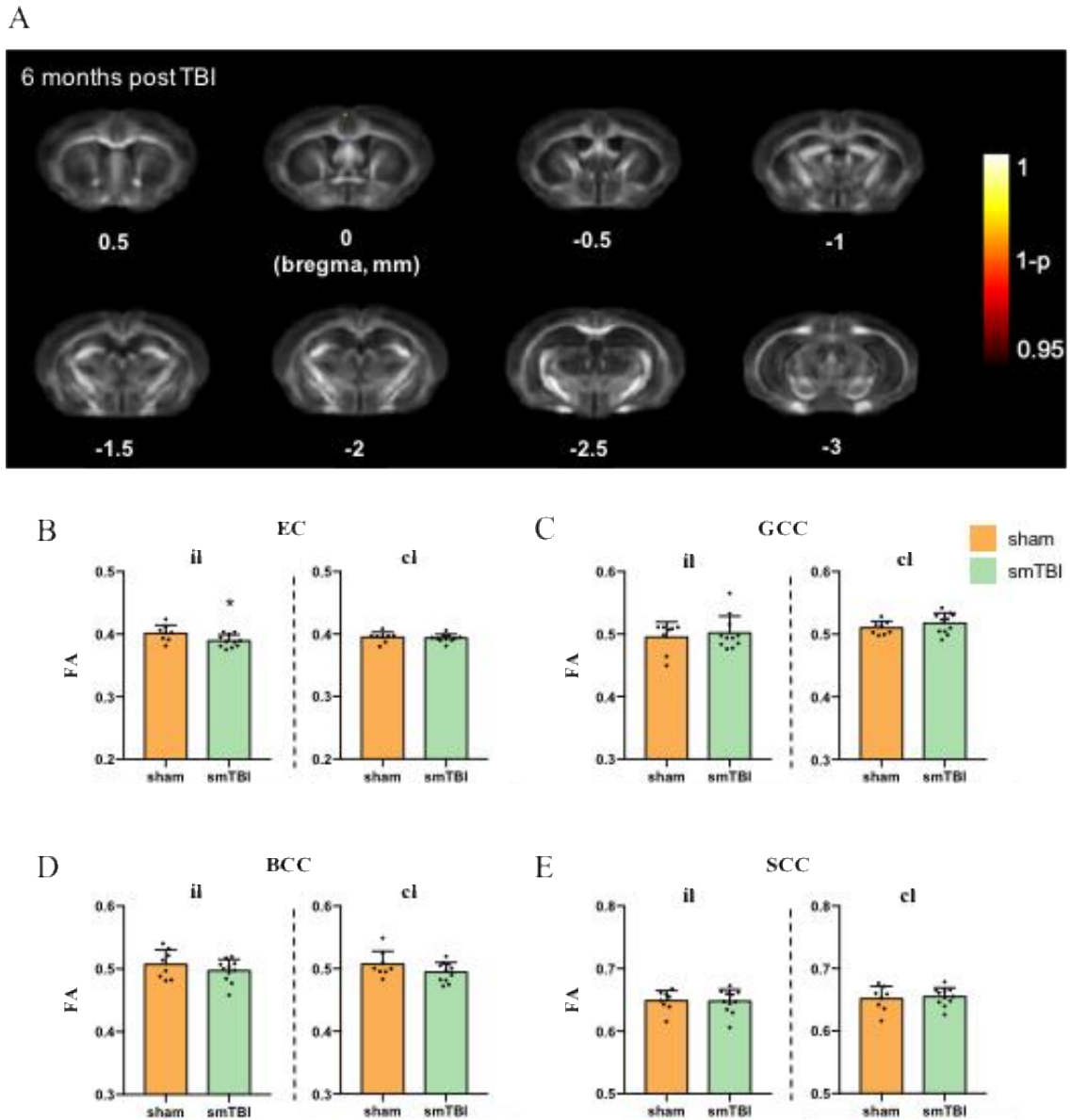


Figure 38 - ROI based analysis in smTBI (n=9) and sham (n=9) mice. Data are presented as mean \pm SEM. * $P < 0.05$ versus sham by unpaired t-test. EC: external capsule, BCC: body of the corpus callosum, GCC: genu of the corpus callosum; SCC: splenium of the corpus callosum

Table 3 - ROI based analysis at 6 months revealed no differences were found in AD, RD, MD between smTBI and sham.
*P<0.05 versus sham by unpaired t-test.

	group	il-EC (mean ± SD)	il-GCC (mean ± SD)	il-BCC (mean ± SD)	il-SCC (mean ± SD)	cl-EC (mean ± SD)	cl-GCC (mean ± SD)	cl-BCC (mean ± SD)	cl-SCC (mean ± SD)
AD	smTBI:	0.95±0.02	0.93±0.03	0.99±0.02	1.25±0.03	0.95±0.02	0.96±0.03	1.06±0.03	1.24±0.02
	sham:	0.96±0.02	0.95±0.02	1.01±0.02	1.25±0.04	0.97±0.02	0.96±0.03	1.07±0.02	1.24±0.03
RD	smTBI:	0.53±0.01	0.39±0.02	0.46±0.01	0.33±0.02	0.52±0.01	0.39±0.02	0.49±0.01	0.33±0.01
	sham:	0.52±0.02	0.40±0.02	0.46±0.03	0.33±0.02	0.52±0.01	0.40±0.01	0.49±0.03	0.34±0.02
MD	smTBI:	0.67±0.01	0.57±0.02	0.64±0.01	0.63±0.02	0.66±0.01	0.58±0.02	0.68±0.02	0.63±0.01
	sham:	0.66±0.02	0.58±0.01	0.64±0.02	0.64±0.02	0.67±0.01	0.58±0.02	0.68±0.02	0.64±0.02

4.4 Brain atrophy assessed by structural MRI

Structural MRI analysis was performed at 6 and 12 months post injury. The evaluation of the cortical thickness at 6 months showed a thinning of the ipsilateral cortex below the site of injury (Figure 39A). VBA showed that cortical thinning was more prominent in the ipsilateral hemisphere, with only small portion of the contralateral cortex thinned compared to sham mice ($p<0.05$, Figure 39B). The quantification of brain volumes revealed that at 6 months il-frontal ($p<0.01$), il-occipital ($p<0.01$), il-parietotemporal ($p<0.001$) and il-entorhinal ($p<0.05$) cortex were reduced compared to sham mice and that the reduction persisted up to 12 months (Figure 40). Cortical atrophy was present also in the cl-cortex and was more pronounce in the parietotemporal cortex (6m: $p<0.001$; 12m: $p<0.01$). cl-frontal and occipital cortex were greatly reduced at 6 months ($p<0.001$) than at 12 months ($p<0.05$). No difference was found in the cl-entorhinal cortex at both time points (Figure 41A-D). Not only cortical but also subcortical volumes including the hippocampus and the corpus callosum were reduced in rmTBI compared to sham mice (Figure 40D/E). In particular hippocampal atrophy was detected at 6 ($p<0.01$) but not 12 months ($p>0.05$) in the contralateral hemisphere while a marked reduction ($p<0.001$) of both cl- and il- CC was shown at 6 and 12 months post injury. When comparing smTBI with sham mice at 6 months the quantification of brain volumes no difference in brain volumes between smTBI and sham mice (Figure 41).

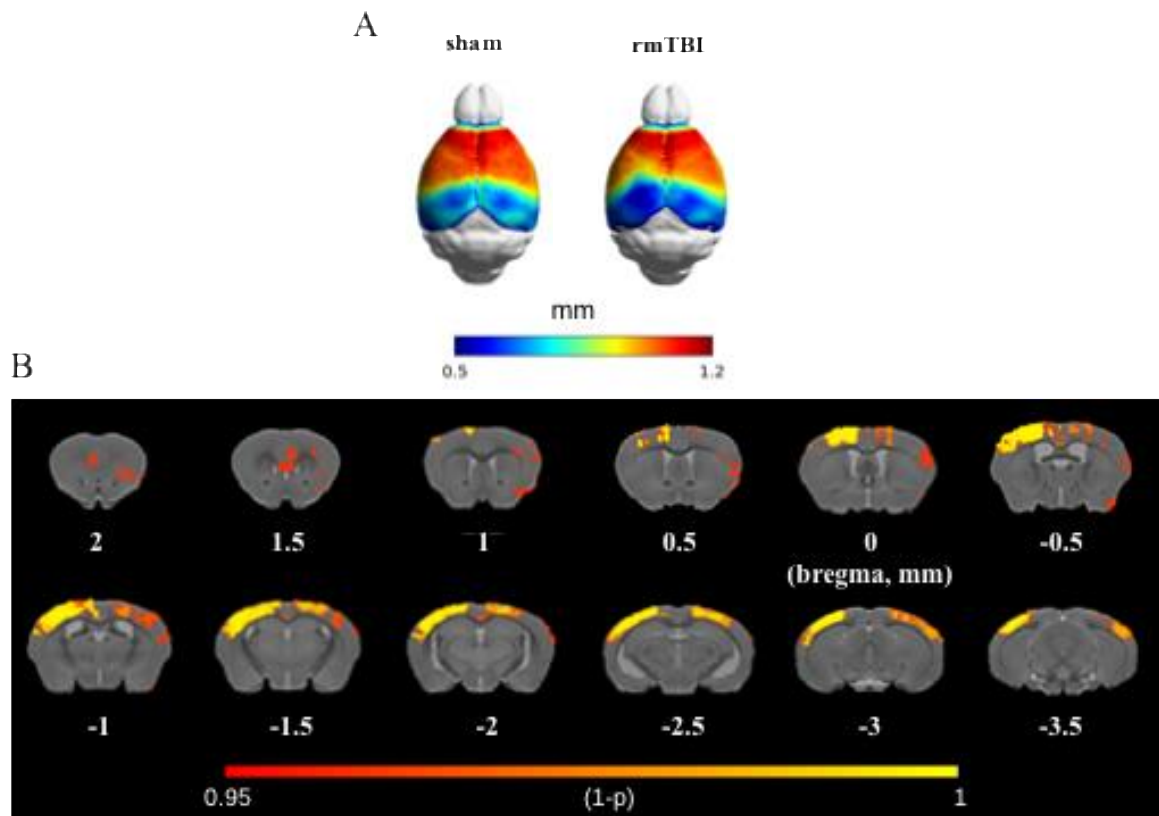


Figure 39 - Structural MRI analysis. (A) Representative image showing cortical thickness in sham and rmTBI mice. (B) Voxel-based analysis of the cortical thickness showing red-yellow voxels in which the thickness was reduced in rmTBI (n=18) compared to sham (n=15-16) mice ($p < 0.05$ by unpaired t-test).

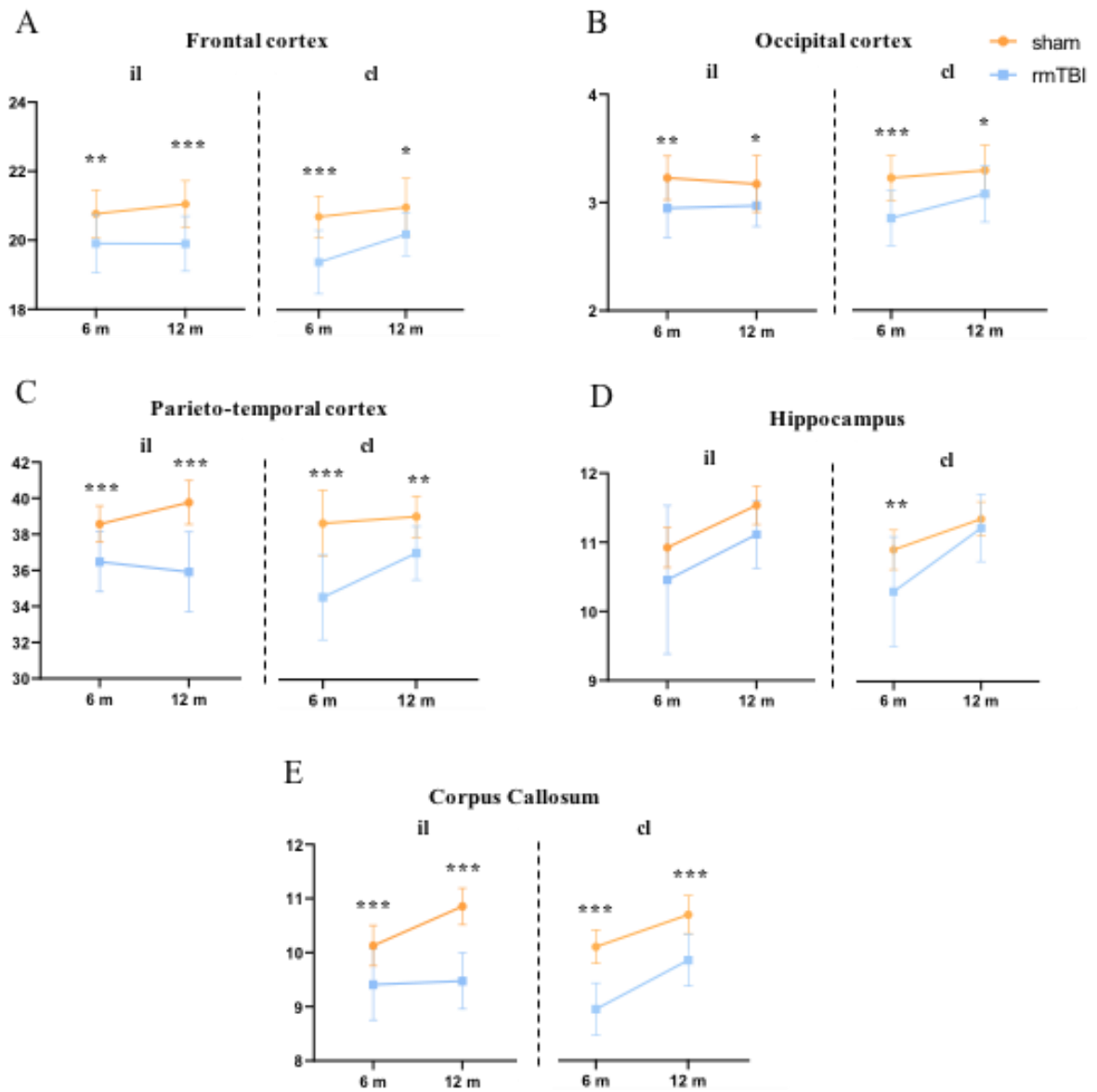


Figure 40 - Semi-automatic quantification of ipsilateral (il) and contralateral (cl) volumes of the frontal-cortex (A), occipital cortex (B), parietotemporal cortex (C), hippocampus (D) and corpus callosum (E) longitudinally assessed at 6 and 12 months post rmTBI. * $P < 0.05$, ** $P < 0.01$, *** $P < 0.001$ rmTBI vs sham by a mixed-effect model followed by Sidak's post hoc multicomparison test.

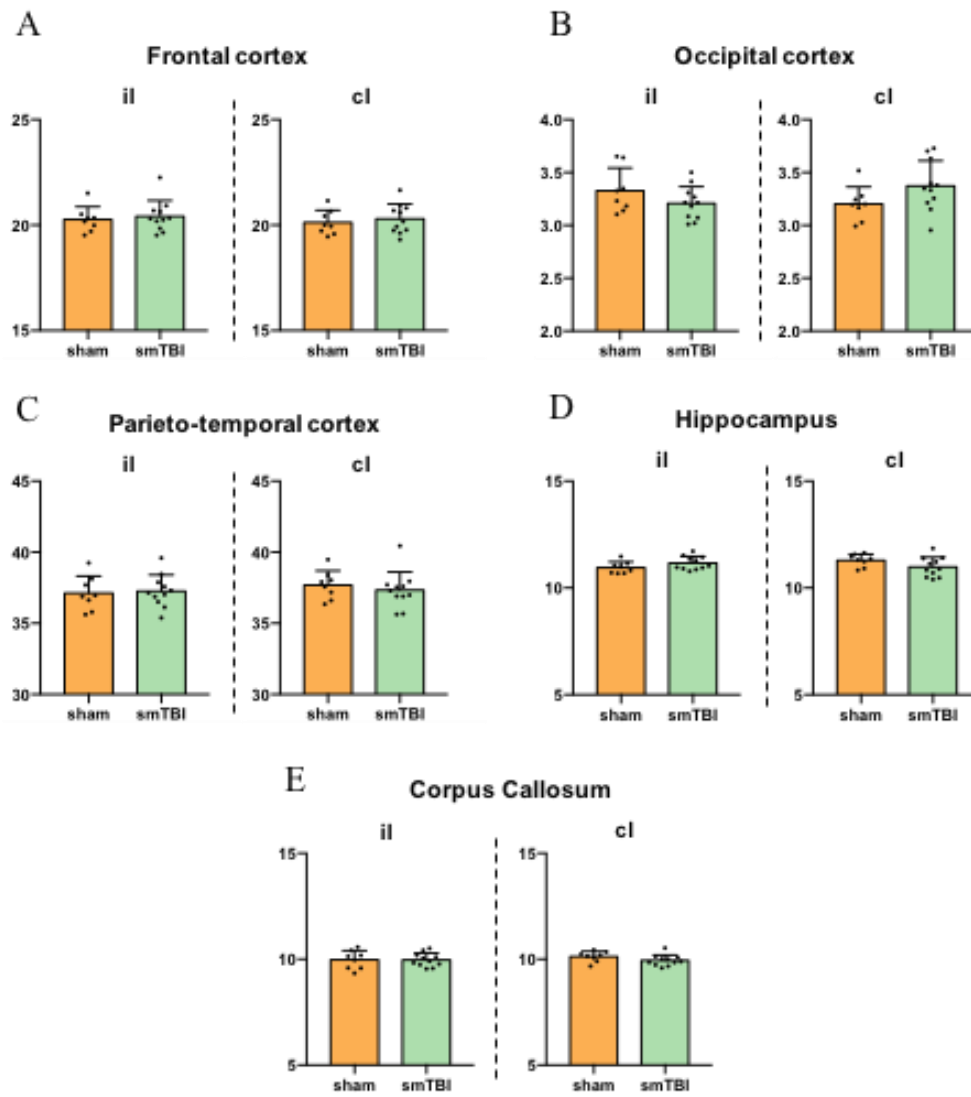


Figure 41 - Comparing smTBI with sham mice at 6 months the quantification of brain volumes in (A) frontal, (B) occipital, (C) parieto-temporal cortex, (D) hippocampus and (E) corpus callosum. Data are presented as mean \pm SEM. Unpaired t-test.

Chapter 5

Discussion and conclusions

Our study provides an in dept characterization of acute and chronic neurological dysfunction after rmTBI in mice, documenting the emergence of functional deficits 6 months post-injury. Furthermore, here we show that in vivo MRI may allow to detect micro and macro structural changes before the emergence of neurological impairments in mice.

Our model uses an electromagnetic rigid impactor device to deliver a total of 5 lateral impacts above the closed skull, over the left parietal bone, at a 48-hour inter-injury interval. Hence, the impact is made under precise velocity and deformation parameters, creating a reliable and reproducible model to examine the consequences of rmTBI.

We opted for lateral impact site that, in addition to linear acceleration, can also induce rotational acceleration of the brain, which is a key feature of concussion. In our model we use the same location for multiple impacts, in order to improve the reproducibility of results, although this may limit the translational potential of the model given that repeated head impacts during sports typically vary in impact location on the head¹⁰⁹. Another important issue in the design of animal TBI models is the choice of head immobilization technique. In our model mouse's head is completely immobilized in a stereotaxic frame with ear bars. The reason for this choice is that full head immobilization enables precise impact localization and reproducibility. However, a great number of rmTBI studies use models where the mouse's head is not fixed but only supported by a foam pad or similar material, allowing the head to move after impact. These models take into account the important mechanical forces (linear and rotational acceleration) that act on the head and brain after impact, which contribute to diffuse injury associated with mTBI, but, at the same time, cause a decrease of reproducibility¹⁰⁹. To this regard it should be noted that the level of experimental variability among mTBI models is substantial, especially regarding CHI models due to the many factors that affect the mechanical response of the head^{109,214}. For this reason, we used a fixed head model that allow highly reproducible head trauma thus increasing the reproducibility of results.

The rationale for using multiple injuries is to mimic the human situation during contact sports in which the brain receives multiple injuries within days or weeks prior to full recovery of the previous injury¹²³. Inter-injury interval in animal models of rmTBI should be scaled to clinically relevant inter-injury intervals¹⁰⁶, considering that contact sport athletes are often exposed to multiple head impacts per training or competitive event, sustained prior to full recovery from the previous injury¹¹⁸. The choice of a 48-hour inter-injury interval derives from the work of Longhi et al.¹²⁶ which showed a window of brain vulnerability of 72 hours in the mouse after injury.

In particular, they showed that mice subjected to a second concussion within 3 or 5 days exhibited significantly impaired cognitive function and significantly greater TAI compared

with either sham-injured animals or mice receiving a smTBI, while when extending the inter-injury interval to 7 days mice showed no cognitive deficits¹²⁶.

In our study we sought to investigate both single impact and repetitive impact paradigms, in order to understand how multiple concussions contribute to neurological impairment later in life. The single hit model recapitulates the hallmark characteristics of mTBI in humans, while the repetitive model allows for the examination of how these cumulative mild injuries contribute to chronic and persistent degeneration over time¹²⁵.

Even though cognitive impairments in human subjects that receive a smTBI seems to return to their normal status within a week^{132,133}, retired players with at least 3 concussions during their career had an increased risk to develop mild cognitive impairment and memory problems¹²³.

When evaluating functional outcomes in between smTBI, rmTBI and sham we found increased sensorimotor deficits only in the rmTBI group, that were present at 1 week and 12 months after injury. Importantly, at acute time points, where rmTBI mice showed sensorimotor deficits, no differences were present between smTBI and sham mice, thus indicating that multiple injuries are needed to cause functional impairment after mTBI. Our results showed that mice subjected to smTBI, rmTBI and sham injury had a similar evolution up to 1-year post injury thus reflecting the “mild” injury even in the rmTBI mice.

Interestingly, the decrease in memory performance in the rmTBI group followed a similar pattern of that of Mouzon and colleagues²¹⁵, where no impairment was present at 6 months while memory deficits emerged only in the rmTBI group 12 months after injury, thus reflecting a worsening of functional and cognitive impairment in the repetitive injured mice. The finding that cognitive impairment was present only after 12 months in rmTBI but not at early time points is in line with the results obtained by Mouzon and colleagues using a similar mouse model²¹⁵.

Cognitive impairment often occurs as a consequence of rmTBI in athletes, with a distinct clinical and neuropathological profile that becomes symptomatic usually 8–10 years after experiencing rmTBI. Manifestations include symptoms of irritability, impulsivity, aggression, depression, short-term memory loss and heightened suicidality. With advancing disease, more severe neurological changes develop, such as dementia, gait and speech abnormalities and parkinsonism¹⁸.

To date there are no diagnostic tools that can be used to monitor the long-term consequences of multiple concussions, and return-to-practice guidelines are only based on the evaluation of symptoms. Validated imaging biomarkers to determine whether or not a patient with a normal CT scan of the brain has neuronal damage are needed³³.

In our study we performed MRI analysis at 6 and 12 months after the last head injury. At different time point since the last injury, from acute to chronic stages, we performed sensorimotor tests to assess the presence of neurological deficits, locomotor activity changes, anxiety-like behavior, learning and memory impairments in mice. The ultimate goal was to identify WM damage and brain atrophy early before delayed functional impairments

appeared up in mice. Translating this situation in athletes, the aim would be to find macrostructural and, importantly, microstructural brain damage with the use of advanced structural MRI sequences in order to act therapeutically before changes in cognition, mood and motor control appear. This would be extremely helpful as, up to now, these changes can be diagnosed only post-mortem, and finding early biomarkers with the use of routine neuroimaging would lighten the huge burden of the long-term effects of rmTBI on healthcare systems, but, mainly, on athlete which experience dramatic physical, psychiatric, emotional, and cognitive disabilities.

Structural MRI may offer important insights after TBI, in particular in sports-related brain injuries. Whilst CT is the most used imaging modality in the acute phase of all TBIs, and it is particularly useful in the detection of lesions that require neurosurgical intervention, it is poor at detection of TAI. This lack of sensitivity for microstructural injury may explain, at least in part, why CT is not predictive of outcomes after rmTBI. The distribution and extent of such lesions, detected using structural MRI with conventional sequences (including T1-weighted and T2-weighted), have been shown to improve prediction of outcome in mTBI³⁸, detecting key prognosis-defining lesions⁴⁷.

DTI is one of the most commonly used advanced structural MRI sequences in TBI. This technique characterizes the diffusion of water molecules in tissue environments, which are influenced by the microstructural organization of tissues and their constituent cells and can provide unique insights into pathophysiology of mTBI. DTI may identify lesions not detectable on CT or more conventional MRI sequences in mTBI¹⁰¹. Dynamic structural changes after TBI can also be detected using DTI and have been found to correlate with changes in behaviour¹⁰¹. Knowledge of such changes is important to provide insights into late pathophysiology and provide a framework that allows MRI to be used as an imaging biomarker for therapy response.

Our results show that diffusion and structural MRI performed at 6 months detect white and grey matter changes that anticipate one-year functional impairments of rmTBI. Callosal atrophy was evident at 6 and 12 months by structural MRI.

In agreement with previous data using the same experimental procedure we found that rmBI but not smTBI induced persistent neuropathology at the level of commissural fibers such as the CC and the cortex^{118,123,124}. We found that WM damages and cortical and sub-cortical atrophy can be detect by in-vivo MRI before the development of functional impairment. FA, one of the DTI metrics, has been shown to reveal WM pathology after TBI in patients^{135,216} and in experimental models of rmTBI¹⁴⁸. DTI analysis showed that already at 6 months post injury FA values in the CC and EC were reduced and this was associated to an increased AD and reduced RD reflecting axonal injuries and demyelination²¹⁷. Interesting CC volumes evaluated by structural MRI at 6 months in rmTBI mice correlated with RD values in the splenium of the CC, thus suggesting that callosal atrophy can be related to demyelination.

In conclusion, our data show that structural MRI and DTI are able to identify macrostructural and microstructural changes following rmTBI early before the emergence of delayed functional impairments. This is an important finding since imaging biomarkers can be used

to monitor disease-modifying strategies and at decreasing/avoiding neurological impairment and neurodegeneration. MRI can be easily performed in humans, thus our findings support the use of DTI and structural MRI to monitor long-term consequences of mild TBI in contact sports and suggest longitudinal MRI imaging as a tool to identify the best timing to act therapeutically before the onset of symptoms.

Acronyms

TBI	Traumatic brain injury
mTBI	Mild traumatic brain injury
rmTBI	Repetitive mild traumatic brain injury
smTBI	Single mild traumatic brain injury
CT	Computed tomography
MRI	Magnetic resonance imaging
MR	Magnetic resonance
DWI	Diffusion-weighted imaging
SWI	Susceptibility-weighted imaging
DTI	Diffusion tensor imaging
DAI	Diffuse Axonal Injury
WM	White matter
TAI	Traumatic axonal injury
SIS	Second impact syndrome
CHI	Closed head injury
GCS	Glasgow Coma Scale
ACRM	American College of Rehabilitation Medicine
LOC	Loss of consciousness
PTA	Post-traumatic amnesia
CDC	Centers for Disease Control and Prevention
WHO	World Health Organization
CVA	Cerebrovascular accident
AMI	Acute myocardial infarction
NFTs	Neurofibrillary tangles
A β	Amiloid- β
CNS	Central nervous system
p-tau	Hyperphosphorylated tau
CC	Corpus callosum
CSF	Cerebrospinal fluid
RF	Radiofrequency
ROI	Region of interest
3D	Three-dimensional
DEC	Direction-encoded color map
CTE	Chronic traumatic encephalopathy

AD	Alzheimer's disease
CSTE	Centre for the Study of Traumatic Encephalopathy
CCI	Controlled cortical impact
FPI	Fluid percussion injury
FA	Fractional anisotropy
ADC	Apparent diffusion coefficient
AD	Axial diffusivity
MN	Mean diffusivity
RD	Radial diffusivity
TR	Repetition time
TE	Echo time
CCI	Controlled cortical impact
SNAP	Simple Neuroassessment of Asymmetric impairment
OFT	Open field test
SEM	Standard error of the mean
ANOVA	Analysis of variance
TBSS	Tract based spatial statistics

Bibliography

1. Menon DK, Schwab K, Wright DW, Maas AI. Position Statement: Definition of Traumatic Brain Injury. *Arch Phys Med Rehabil.* 2010;91(11):1637-1640. doi:10.1016/j.apmr.2010.05.017
2. Risling M, Smith D, Stein TD, et al. Modelling human pathology of traumatic brain injury in animal models. *J Intern Med.* 2019;285(6):594-607. doi:10.1111/joim.12909
3. Wojnarowicz MW, Fisher AM, Minaeva O, Goldstein LE. Considerations for Experimental Animal Models of Concussion, Traumatic Brain Injury, and Chronic Traumatic Encephalopathy—These Matters Matter. *Front Neurol.* 2017;8:240. doi:10.3389/fneur.2017.00240
4. Fleminger S, Ponsford J. Long term outcome after traumatic brain injury. *BMJ.* 2005;331(7530):1419. doi:10.1136/bmj.331.7530.1419
5. Rosenfeld JV, Maas AI, Bragge P, Morganti-Kossmann MC, Manley GT, Gruen RL. Early management of severe traumatic brain injury. *The Lancet.* 2012;380(9847):1088-1098. doi:10.1016/S0140-6736(12)60864-2
6. Stocchetti N, Zanier ER. Chronic impact of traumatic brain injury on outcome and quality of life: a narrative review. *Crit Care.* 2016;20(1):148. doi:10.1186/s13054-016-1318-1
7. Hyder AA, Wunderlich CA, Puvanachandra P, Gururaj G, Kobusingye OC. The impact of traumatic brain injuries: a global perspective. *NeuroRehabilitation.* 2007;22(5):341-353.
8. Coronado VG, McGuire LC, Sarmiento K, et al. Trends in Traumatic Brain Injury in the U.S. and the public health response: 1995–2009. *J Safety Res.* 2012;43(4):299-307. doi:10.1016/j.jsr.2012.08.011
9. Rowson S, Duma SM, Greenwald RM, et al. Can helmet design reduce the risk of concussion in football?: Technical note. *J Neurosurg.* 2014;120(4):919-922. doi:10.3171/2014.1.JNS13916
10. Maas AIR, Menon DK, Adelson PD, et al. Traumatic brain injury: integrated approaches to improve prevention, clinical care, and research. *Lancet Neurol.* 2017;16(12):987-1048. doi:10.1016/S1474-4422(17)30371-X
11. World Health Organization. Neurological disorders : public health challenges. Published online 2006:218.
12. Fleminger S. Head injury as a risk factor for Alzheimer’s disease: the evidence 10 years on; a partial replication. *J Neurol Neurosurg Psychiatry.* 2003;74(7):857-862. doi:10.1136/jnnp.74.7.857

13. Li W, Risacher SL, McAllister TW, Saykin AJ. Traumatic brain injury and age at onset of cognitive impairment in older adults. *J Neurol.* 2016;263(7):1280-1285. doi:10.1007/s00415-016-8093-4
14. Burke JF, Stulc JL, Skolarus LE, Sears ED, Zahuranec DB, Morgenstern LB. Traumatic brain injury may be an independent risk factor for stroke. *Neurology.* 2013;81(1):33-39. doi:10.1212/WNL.0b013e318297eecf
15. Liao C-C, Chou Y-C, Yeh C-C, Hu C-J, Chiu W-T, Chen T-L. Stroke Risk and Outcomes in Patients With Traumatic Brain Injury: 2 Nationwide Studies. *Mayo Clin Proc.* 2014;89(2):163-172. doi:10.1016/j.mayocp.2013.09.019
16. Jafari S, Etminan M, Aminzadeh F, Samii A. Head injury and risk of Parkinson disease: A systematic review and meta-analysis: Head Injury and Risk of Parkinson Disease. *Mov Disord.* 2013;28(9):1222-1229. doi:10.1002/mds.25458
17. Crane PK, Gibbons LE, Dams-O'Connor K, et al. Association of Traumatic Brain Injury With Late-Life Neurodegenerative Conditions and Neuropathologic Findings. *JAMA Neurol.* 2016;73(9):1062. doi:10.1001/jamaneurol.2016.1948
18. Walsh S, Donnan J, Fortin Y, et al. A systematic review of the risks factors associated with the onset and natural progression of epilepsy. *NeuroToxicology.* 2017;61:64-77. doi:10.1016/j.neuro.2016.03.011
19. Shenton ME, Hamoda HM, Schneiderman JS, et al. A review of magnetic resonance imaging and diffusion tensor imaging findings in mild traumatic brain injury. *Brain Imaging Behav.* 2012;6(2):137-192. doi:10.1007/s11682-012-9156-5
20. Zetterberg H, Winblad B, Bernick C, et al. Head trauma in sports – clinical characteristics, epidemiology and biomarkers. *J Intern Med.* 2019;285(6):624-634. doi:10.1111/joim.12863
21. Yuh EL, Mukherjee P, Lingsma HF, et al. Magnetic resonance imaging improves 3-month outcome prediction in mild traumatic brain injury: MRI in MTBI. *Ann Neurol.* 2013;73(2):224-235. doi:10.1002/ana.23783
22. Pervez M, Kitagawa RS, Chang TR. Definition of Traumatic Brain Injury, Neurosurgery, Trauma Orthopedics, Neuroimaging, Psychology, and Psychiatry in Mild Traumatic Brain Injury. *Neuroimaging Clin N Am.* 2018;28(1):1-13. doi:10.1016/j.nic.2017.09.010
23. Carroll L, Cassidy JD, Peloso P, et al. Prognosis for mild traumatic brain injury: results of the who collaborating centre task force on mild traumatic brain injury. *J Rehabil Med.* 2004;36(0):84-105. doi:10.1080/16501960410023859
24. Joseph B, Pandit V, Aziz H, et al. Mild traumatic brain injury defined by Glasgow Coma Scale: Is it really mild? *Brain Inj.* 2015;29(1):11-16. doi:10.3109/02699052.2014.945959

25. Sternbach GL. The Glasgow Coma Scale. *J Emerg Med.* 2000;19(1):67-71. doi:10.1016/S0736-4679(00)00182-7
26. Ruff R. Two Decades of Advances in Understanding of Mild Traumatic Brain Injury: *J Head Trauma Rehabil.* 2005;20(1):5-18. doi:10.1097/00001199-200501000-00003
27. Povlishock J, Coburn T. *Morphological Changes Associated with Mild Head Injury.*; 1989.
28. American Congress of Rehabilitation Medicine. Definition of mild traumatic brain injury. *J Head Trauma Rehabil.* Published online 1993;8:86-87.
29. National Center for Injury Prevention Control. Report to Congress on Mild Traumatic Brain Injury in the United States: Steps to Prevent A Serious Public Health Problem. Atlanta, GA: Centers for Disease Control and Prevention. Published online 2003.
30. Carroll L, Cassidy JD, Holm L, Kraus J, Coronado V. Methodological issues and research recommendations for mild traumatic brain injury: the who collaborating centre task force on mild traumatic brain injury. *J Rehabil Med.* 2004;36(0):113-125. doi:10.1080/16501960410023877
31. Kristman VL, Borg J, Godbolt AK, et al. Methodological Issues and Research Recommendations for Prognosis After Mild Traumatic Brain Injury: Results of the International Collaboration on Mild Traumatic Brain Injury Prognosis. *Arch Phys Med Rehabil.* 2014;95(3):S265-S277. doi:10.1016/j.apmr.2013.04.026
32. Practice Parameter [RETIRED]: The management of concussion in sports (summary statement). *Neurology.* 1997;48(3):581-585. doi:10.1212/WNL.48.3.581
33. McCrory P, Meeuwisse W, Johnston K, et al. Consensus Statement on Concussion in Sport 3rd International Conference on Concussion in Sport Held in Zurich, November 2008. *Clin J Sport Med.* 2009;19(3):185-200. doi:10.1097/JSM.0b013e3181a501db
34. Okie S. Traumatic brain injury in the war zone. *N Engl J Med.* 2005;352(20):2043-2047. doi:10.1056/NEJMp058102
35. Montenigro PH, Bernick C, Cantu RC. Clinical Features of Repetitive Traumatic Brain Injury and Chronic Traumatic Encephalopathy: Chronic traumatic encephalopathy in boxers vs. football players. *Brain Pathol.* 2015;25(3):304-317. doi:10.1111/bpa.12250
36. Rigg JL, Mooney SR. Concussions and the Military: Issues Specific to Service Members. *PM&R.* 2011;3:S380-S386. doi:10.1016/j.pmrj.2011.08.005
37. Langlois JA, Rutland-Brown W, Wald MM. The Epidemiology and Impact of Traumatic Brain Injury: A Brief Overview. *J Head Trauma Rehabil.* 2006;21(5):375-378. doi:10.1097/00001199-200609000-00001
38. Daneshvar DH, Nowinski CJ, McKee AC, Cantu RC. The Epidemiology of Sport-Related Concussion. *Clin Sports Med.* 2011;30(1):1-17. doi:10.1016/j.csm.2010.08.006

39. Guskiewicz KM, Marshall SW, Bailes J, et al. Association between recurrent concussion and late-life cognitive impairment in retired professional football players. *Neurosurgery*. 2005;57(4):719-726; discussion 719-726. doi:10.1093/neurosurgery/57.4.719
40. Pellman EJ, Viano DC, Casson IR, et al. Concussion in Professional Football: Repeat Injuries—Part 4. *Neurosurgery*. 2004;55(4):860-876. doi:10.1227/01.NEU.0000137657.00146.7D
41. Giza CC, Griesbach GS, Hovda DA. Experience-dependent behavioral plasticity is disturbed following traumatic injury to the immature brain. *Behav Brain Res*. 2005;157(1):11-22. doi:10.1016/j.bbr.2004.06.003
42. Guskiewicz KM, McCrea M, Marshall SW, et al. Cumulative Effects Associated With Recurrent Concussion in Collegiate Football Players: The NCAA Concussion Study. *JAMA*. 2003;290(19):2549. doi:10.1001/jama.290.19.2549
43. Bernick C, Banks S. What boxing tells us about repetitive head trauma and the brain. *Alzheimers Res Ther*. 2013;5(3):23. doi:10.1186/alzrt177
44. Bernick C, Banks S, Phillips M, et al. Professional Fighters Brain Health Study: Rationale and Methods. *Am J Epidemiol*. 2013;178(2):280-286. doi:10.1093/aje/kws456
45. Robbins C, Daneshvar D, Picano J, et al. Self-reported concussion history: impact of providing a definition of concussion. *Open Access J Sports Med*. Published online May 2014:99. doi:10.2147/OAJSM.S58005
46. Corrigan JD, Bogner J. Initial reliability and validity of the Ohio State University TBI Identification Method. *J Head Trauma Rehabil*. 2007;22(6):318-329. doi:10.1097/01.HTR.0000300227.67748.77
47. Kerr ZY, Marshall SW, Guskiewicz KM. Reliability of Concussion History in Former Professional Football Players. *Med Sci Sports Exerc*. 2012;44(3):377-382. doi:10.1249/MSS.0b013e31823240f2
48. Cantu RC, Herring SA, Putukian M, American College of Sports Medicine. Concussion. *N Engl J Med*. 2007;356(17):1787; author reply 1789. doi:10.1056/NEJMc070289
49. Cantu RC, Guskiewicz K, Register-Mihalik JK. A retrospective clinical analysis of moderate to severe athletic concussions. *PM R*. 2010;2(12):1088-1093. doi:10.1016/j.pmrj.2010.07.483
50. Makdissi M, Darby D, Maruff P, Ugoni A, Brukner P, McCrory PR. Natural history of concussion in sport: markers of severity and implications for management. *Am J Sports Med*. 2010;38(3):464-471. doi:10.1177/0363546509349491
51. Karr JE, Areshenkoff CN, Garcia-Barrera MA. The neuropsychological outcomes of concussion: a systematic review of meta-analyses on the cognitive sequelae of mild traumatic brain injury. *Neuropsychology*. 2014;28(3):321-336. doi:10.1037/neu0000037

52. Stern RA, Daneshvar DH, Baugh CM, et al. Clinical presentation of chronic traumatic encephalopathy. *Neurology*. 2013;81(13):1122-1129. doi:10.1212/WNL.0b013e3182a55f7f
53. Smith DH, Johnson VE, Trojanowski JQ, Stewart W. Chronic traumatic encephalopathy — confusion and controversies. *Nat Rev Neurol*. 2019;15(3):179-183. doi:10.1038/s41582-018-0114-8
54. Martland HS. PUNCH DRUNK. *J Am Med Assoc*. 1928;91(15):1103. doi:10.1001/jama.1928.02700150029009
55. Saigal R, Berger MS. The Long-term Effects of Repetitive Mild Head Injuries in Sports: *Neurosurgery*. 2014;75:S149-S155. doi:10.1227/NEU.0000000000000497
56. Corsellis JAN, Bruton CJ, Freeman-Browne D. The aftermath of boxing. *Psychol Med*. 1973;3(3):270-303. doi:10.1017/S0033291700049588
57. DeKosky ST, Blennow K, Ikonovic MD, Gandy S. Acute and chronic traumatic encephalopathies: pathogenesis and biomarkers. *Nat Rev Neurol*. 2013;9(4):192-200. doi:10.1038/nrneurol.2013.36
58. Roberts GW, Allsop D, Bruton C. The occult aftermath of boxing. *J Neurol Neurosurg Psychiatry*. 1990;53(5):373-378. doi:10.1136/jnnp.53.5.373
59. Omalu BI, DeKosky ST, Minster RL, Kamboh MI, Hamilton RL, Wecht CH. Chronic Traumatic Encephalopathy in a National Football League Player. *Neurosurgery*. 2005;57(1):128-134. doi:10.1227/01.NEU.0000163407.92769.ED
60. Kokaia Z, Lindvall O. Neurogenesis after ischaemic brain insults. *Curr Opin Neurobiol*. 2003;13(1):127-132. doi:10.1016/s0959-4388(03)00017-5
61. Zhao C, Deng W, Gage FH. Mechanisms and functional implications of adult neurogenesis. *Cell*. 2008;132(4):645-660. doi:10.1016/j.cell.2008.01.033
62. Bye N, Carron S, Han X, et al. Neurogenesis and glial proliferation are stimulated following diffuse traumatic brain injury in adult rats. *J Neurosci Res*. 2011;89(7):986-1000. doi:10.1002/jnr.22635
63. Chen X-H, Iwata A, Nonaka M, Browne KD, Smith DH. Neurogenesis and glial proliferation persist for at least one year in the subventricular zone following brain trauma in rats. *J Neurotrauma*. 2003;20(7):623-631. doi:10.1089/089771503322144545
64. Ozen LJ, Fernandes MA. Slowing down after a mild traumatic brain injury: a strategy to improve cognitive task performance? *Arch Clin Neuropsychol Off J Natl Acad Neuropsychol*. 2012;27(1):85-100. doi:10.1093/arclin/acr087
65. Proctor MR, Cantu RC. HEAD AND NECK INJURIES IN YOUNG ATHLETES. *Clin Sports Med*. 2000;19(4):693-715. doi:10.1016/S0278-5919(05)70233-7

66. Hovda DA, Yoshino A, Kawamata T, Katayama Y, Becker DP. Diffuse prolonged depression of cerebral oxidative metabolism following concussive brain injury in the rat: a cytochrome oxidase histochemistry study. *Brain Res.* 1991;567(1):1-10. doi:10.1016/0006-8993(91)91429-5
67. Yoshino A, Hovda DA, Kawamata T, Katayama Y, Becker DP. Dynamic changes in local cerebral glucose utilization following cerebral concussion in rats: evidence of a hyper- and subsequent hypometabolic state. *Brain Res.* 1991;561(1):106-119. doi:10.1016/0006-8993(91)90755-K
68. Bailes JE, Petraglia AL, Omalu BI, Nauman E, Talavage T. Role of subconcussion in repetitive mild traumatic brain injury. *J Neurosurg.* 2013;119(5):1235-1245. doi:10.3171/2013.7.JNS121822
69. ATLS Subcommittee, American College of Surgeons' Committee on Trauma, International ATLS working group. Advanced trauma life support (ATLS®): the ninth edition. *J Trauma Acute Care Surg.* 2013;74(5):1363-1366. doi:10.1097/TA.0b013e31828b82f5
70. Loane DJ, Faden AI. Neuroprotection for traumatic brain injury: translational challenges and emerging therapeutic strategies. *Trends Pharmacol Sci.* 2010;31(12):596-604. doi:10.1016/j.tips.2010.09.005
71. Fehily B, Fitzgerald M. Repeated Mild Traumatic Brain Injury: Potential Mechanisms of Damage. *Cell Transplant.* 2017;26(7):1131-1155. doi:10.1177/0963689717714092
72. Giza CC, Hovda DA. The new neurometabolic cascade of concussion. *Neurosurgery.* 2014;75 Suppl 4:S24-33. doi:10.1227/NEU.0000000000000505
73. McKee AC, Daneshvar DH, Alvarez VE, Stein TD. The neuropathology of sport. *Acta Neuropathol (Berl).* 2014;127(1):29-51. doi:10.1007/s00401-013-1230-6
74. Cherry JD, Tripodis Y, Alvarez VE, et al. Microglial neuroinflammation contributes to tau accumulation in chronic traumatic encephalopathy. *Acta Neuropathol Commun.* 2016;4(1):112. doi:10.1186/s40478-016-0382-8
75. Ghosh S, Wu MD, Shaftel SS, et al. Sustained interleukin-1 β overexpression exacerbates tau pathology despite reduced amyloid burden in an Alzheimer's mouse model. *J Neurosci Off J Soc Neurosci.* 2013;33(11):5053-5064. doi:10.1523/JNEUROSCI.4361-12.2013
76. Maphis N, Xu G, Kokiko-Cochran ON, et al. Reactive microglia drive tau pathology and contribute to the spreading of pathological tau in the brain. *Brain J Neurol.* 2015;138(Pt 6):1738-1755. doi:10.1093/brain/awv081
77. Gennarelli TA. Mechanisms of brain injury. *J Emerg Med.* 1993;11 Suppl 1:5-11.
78. Jenkins LW, Moszynski K, Lyeth BG, et al. Increased vulnerability of the mildly traumatized rat brain to cerebral ischemia: the use of controlled secondary ischemia as a research tool to identify common or different mechanisms contributing to mechanical

- and ischemic brain injury. *Brain Res.* 1989;477(1-2):211-224. doi:10.1016/0006-8993(89)91409-1
79. Greco T, Ferguson L, Giza C, Prins ML. Mechanisms underlying vulnerabilities after repeat mild traumatic brain injuries. *Exp Neurol.* 2019;317:206-213. doi:10.1016/j.expneurol.2019.01.012
80. Huang L, Coats JS, Mohd-Yusof A, et al. Tissue vulnerability is increased following repetitive mild traumatic brain injury in the rat. *Brain Res.* 2013;1499:109-120. doi:10.1016/j.brainres.2012.12.038
81. Cantu RC. SECOND-IMPACT SYNDROME. *Clin Sports Med.* 1998;17(1):37-44. doi:10.1016/S0278-5919(05)70059-4
82. Boden BP, Tacchetti RL, Cantu RC, Knowles SB, Mueller FO. Catastrophic Head Injuries in High School and College Football Players. *Am J Sports Med.* 2007;35(7):1075-1081. doi:10.1177/0363546507299239
83. Cantu RC, Gean AD. Second-Impact Syndrome and a Small Subdural Hematoma: An Uncommon Catastrophic Result of Repetitive Head Injury with a Characteristic Imaging Appearance. *J Neurotrauma.* 2010;27(9):1557-1564. doi:10.1089/neu.2010.1334
84. McKee AC, Stein TD, Nowinski CJ, et al. The spectrum of disease in chronic traumatic encephalopathy. *Brain.* 2013;136(1):43-64. doi:10.1093/brain/aws307
85. Stein TD, Alvarez VE, McKee AC. Chronic traumatic encephalopathy: a spectrum of neuropathological changes following repetitive brain trauma in athletes and military personnel. *Alzheimers Res Ther.* 2014;6(1):4. doi:10.1186/alzrt234
86. McKee AC, Cantu RC, Nowinski CJ, et al. Chronic Traumatic Encephalopathy in Athletes: Progressive Tauopathy After Repetitive Head Injury. *J Neuropathol Exp Neurol.* 2009;68(7):709-735. doi:10.1097/NEN.0b013e3181a9d503
87. Gavett BE, Stern RA, Cantu RC, Nowinski CJ, McKee AC. Mild traumatic brain injury: a risk factor for neurodegeneration. *Alzheimers Res Ther.* 2010;2(3):18. doi:10.1186/alzrt42
88. Lewis J, Dickson DW. Propagation of tau pathology: hypotheses, discoveries, and yet unresolved questions from experimental and human brain studies. *Acta Neuropathol (Berl).* 2016;131(1):27-48. doi:10.1007/s00401-015-1507-z
89. Goedert M, Eisenberg DS, Crowther RA. Propagation of Tau Aggregates and Neurodegeneration. *Annu Rev Neurosci.* 2017;40(1):189-210. doi:10.1146/annurev-neuro-072116-031153
90. Prusiner SB. Cell biology. A unifying role for prions in neurodegenerative diseases. *Science.* 2012;336(6088):1511-1513. doi:10.1126/science.1222951

91. Zanier ER, Bertani I, Sammali E, et al. Induction of a transmissible tau pathology by traumatic brain injury. *Brain J Neurol.* 2018;141(9):2685-2699. doi:10.1093/brain/awy193
92. Pischiutta F, Micotti E, Hay JR, et al. Single severe traumatic brain injury produces progressive pathology with ongoing contralateral white matter damage one year after injury. *Exp Neurol.* 2018;300:167-178. doi:10.1016/j.expneurol.2017.11.003
93. Cloots RJH, Gervaise HMT, van Dommelen J a. W, Geers MGD. Biomechanics of traumatic brain injury: influences of the morphologic heterogeneities of the cerebral cortex. *Ann Biomed Eng.* 2008;36(7):1203-1215. doi:10.1007/s10439-008-9510-3
94. Ghajari M, Hellyer PJ, Sharp DJ. Computational modelling of traumatic brain injury predicts the location of chronic traumatic encephalopathy pathology. *Brain.* 2017;140(2):333-343. doi:10.1093/brain/aww317
95. Braak H, Thal DR, Ghebremedhin E, Del Tredici K. Stages of the pathologic process in Alzheimer disease: age categories from 1 to 100 years. *J Neuropathol Exp Neurol.* 2011;70(11):960-969. doi:10.1097/NEN.0b013e318232a379
96. Adams JW, Alvarez VE, Mez J, et al. Lewy Body Pathology and Chronic Traumatic Encephalopathy Associated With Contact Sports. *J Neuropathol Exp Neurol.* 2018;77(9):757-768. doi:10.1093/jnen/nly065
97. McKee AC, Cairns NJ, Dickson DW, et al. The first NINDS/NIBIB consensus meeting to define neuropathological criteria for the diagnosis of chronic traumatic encephalopathy. *Acta Neuropathol (Berl).* 2016;131(1):75-86. doi:10.1007/s00401-015-1515-z
98. Mez J, Daneshvar DH, Kiernan PT, et al. Clinicopathological Evaluation of Chronic Traumatic Encephalopathy in Players of American Football. *JAMA.* 2017;318(4):360-370. doi:10.1001/jama.2017.8334
99. Dallmeier JD, Meysami S, Merrill DA, Raji CA. Emerging advances of in vivo detection of chronic traumatic encephalopathy and traumatic brain injury. *Br J Radiol.* 2019;92(1101):20180925. doi:10.1259/bjr.20180925
100. Viano DC, Casson IR, Pellman EJ, et al. Concussion in professional football: comparison with boxing head impacts--part 10. *Neurosurgery.* 2005;57(6):1154-1172; discussion 1154-1172. doi:10.1227/01.neu.0000187541.87937.d9
101. Jordan BD, Relkin NR, Ravdin LD, Jacobs AR, Bennett A, Gandy S. Apolipoprotein E epsilon4 associated with chronic traumatic brain injury in boxing. *JAMA.* 1997;278(2):136-140.
102. Johnson VE, Stewart W, Graham DI, Stewart JE, Praestgaard AH, Smith DH. A Nepriylsin Polymorphism and Amyloid- β Plaques after Traumatic Brain Injury. *J Neurotrauma.* 2009;26(8):1197-1202. doi:10.1089/neu.2008.0843

103. Cao J, Gaamouch FE, Meabon JS, et al. ApoE4-associated phospholipid dysregulation contributes to development of Tau hyper-phosphorylation after traumatic brain injury. *Sci Rep*. 2017;7(1):11372. doi:10.1038/s41598-017-11654-7
104. Cherry JD, Mez J, Crary JF, et al. Variation in TMEM106B in chronic traumatic encephalopathy. *Acta Neuropathol Commun*. 2018;6(1):115. doi:10.1186/s40478-018-0619-9
105. Savica R, Parisi JE, Wold LE, Josephs KA, Ahlskog JE. High School Football and Risk of Neurodegeneration: A Community-Based Study. *Mayo Clin Proc*. 2012;87(4):335-340. doi:10.1016/j.mayocp.2011.12.016
106. Shultz SR, McDonald SJ, Vonder Haar C, et al. The potential for animal models to provide insight into mild traumatic brain injury: Translational challenges and strategies. *Neurosci Biobehav Rev*. 2017;76(Pt B):396-414. doi:10.1016/j.neubiorev.2016.09.014
107. Stern RA, Riley DO, Daneshvar DH, Nowinski CJ, Cantu RC, McKee AC. Long-term Consequences of Repetitive Brain Trauma: Chronic Traumatic Encephalopathy. *PM&R*. 2011;3:S460-S467. doi:10.1016/j.pmrj.2011.08.008
108. Mouse Genome Sequencing Consortium. Initial sequencing and comparative analysis of the mouse genome. *Nature*. 2002;420(6915):520-562. doi:10.1038/nature01262
109. Hoogenboom WS, Branch CA, Lipton ML. Animal models of closed-skull, repetitive mild traumatic brain injury. *Pharmacol Ther*. 2019;198:109-122. doi:10.1016/j.pharmthera.2019.02.016
110. Smith DH, Johnson VE, Stewart W. Chronic neuropathologies of single and repetitive TBI: substrates of dementia? *Nat Rev Neurol*. 2013;9(4):211-221. doi:10.1038/nrneurol.2013.29
111. Ojo JO, Mouzon BC, Crawford F. Repetitive head trauma, chronic traumatic encephalopathy and tau: Challenges in translating from mice to men. *Exp Neurol*. 2016;275 Pt 3:389-404. doi:10.1016/j.expneurol.2015.06.003
112. Bodnar CN, Roberts KN, Higgins EK, Bachstetter AD. A Systematic Review of Closed Head Injury Models of Mild Traumatic Brain Injury in Mice and Rats. *J Neurotrauma*. 2019;36(11):1683-1706. doi:10.1089/neu.2018.6127
113. Albert-Weissenberger C, Sirén A-L. Experimental traumatic brain injury. *Exp Transl Stroke Med*. 2010;2(1):16. doi:10.1186/2040-7378-2-16
114. Shah EJ, Gurdziel K, Ruden DM. Mammalian Models of Traumatic Brain Injury and a Place for Drosophila in TBI Research. *Front Neurosci*. 2019;13:409. doi:10.3389/fnins.2019.00409
115. Bolouri H, Zetterberg H. Animal Models for Concussion: Molecular and Cognitive Assessments—Relevance to Sport and Military Concussions. In: Kobeissy FH, ed. *Brain Neurotrauma: Molecular, Neuropsychological, and Rehabilitation Aspects*. Frontiers in

Neuroengineering. CRC Press/Taylor & Francis; 2015. Accessed September 9, 2021. <http://www.ncbi.nlm.nih.gov/books/NBK299196/>

116. Adams FS, Schwarting RK, Huston JP. Behavioral and neurochemical asymmetries following unilateral trephination of the rat skull: is this control operation always appropriate? *Physiol Behav.* 1994;55(5):947-952. doi:10.1016/0031-9384(94)90084-1
117. Cole JT, Yarnell A, Kean WS, et al. Craniotomy: true sham for traumatic brain injury, or a sham of a sham? *J Neurotrauma.* 2011;28(3):359-369. doi:10.1089/neu.2010.1427
118. Mouzon B, Chaytow H, Crynen G, et al. Repetitive mild traumatic brain injury in a mouse model produces learning and memory deficits accompanied by histological changes. *J Neurotrauma.* 2012;29(18):2761-2773. doi:10.1089/neu.2012.2498
119. Vink R, Mullins PG, Temple MD, Bao W, Faden AI. Small shifts in craniotomy position in the lateral fluid percussion injury model are associated with differential lesion development. *J Neurotrauma.* 2001;18(8):839-847. doi:10.1089/089771501316919201
120. Floyd CL, Golden KM, Black RT, Hamm RJ, Lyeth BG. Craniectomy position affects morris water maze performance and hippocampal cell loss after parasagittal fluid percussion. *J Neurotrauma.* 2002;19(3):303-316. doi:10.1089/089771502753594873
121. Flierl MA, Stahel PF, Beauchamp KM, Morgan SJ, Smith WR, Shohami E. Mouse closed head injury model induced by a weight-drop device. *Nat Protoc.* 2009;4(9):1328-1337. doi:10.1038/nprot.2009.148
122. Levin HS, Robertson CS. Mild traumatic brain injury in translation. *J Neurotrauma.* 2013;30(8):610-617. doi:10.1089/neu.2012.2394
123. Mouzon BC, Bachmeier C, Ferro A, et al. Chronic neuropathological and neurobehavioral changes in a repetitive mild traumatic brain injury model. *Ann Neurol.* 2014;75(2):241-254. doi:10.1002/ana.24064
124. Dewitt DS, Perez-Polo R, Hulsebosch CE, Dash PK, Robertson CS. Challenges in the development of rodent models of mild traumatic brain injury. *J Neurotrauma.* 2013;30(9):688-701. doi:10.1089/neu.2012.2349
125. Main BS, Sloley SS, Villapol S, Zapple DN, Burns MP. A Mouse Model of Single and Repetitive Mild Traumatic Brain Injury. *J Vis Exp.* 2017;(124):55713. doi:10.3791/55713
126. Longhi L, Saatman KE, Fujimoto S, et al. Temporal Window of Vulnerability to Repetitive Experimental Concussive Brain Injury. *Neurosurgery.* 2005;56(2):364-374. doi:10.1227/01.NEU.0000149008.73513.44
127. Laurer HL, Bareyre FM, Lee VM, et al. Mild head injury increasing the brain's vulnerability to a second concussive impact. *J Neurosurg.* 2001;95(5):859-870. doi:10.3171/jns.2001.95.5.0859

128. Uryu K, Laurer H, McIntosh T, et al. Repetitive mild brain trauma accelerates Abeta deposition, lipid peroxidation, and cognitive impairment in a transgenic mouse model of Alzheimer amyloidosis. *J Neurosci Off J Soc Neurosci.* 2002;22(2):446-454.
129. Shitaka Y, Tran HT, Bennett RE, et al. Repetitive closed-skull traumatic brain injury in mice causes persistent multifocal axonal injury and microglial reactivity. *J Neuropathol Exp Neurol.* 2011;70(7):551-567. doi:10.1097/NEN.0b013e31821f891f
130. Mannix R, Meehan WP, Mandeville J, et al. Clinical correlates in an experimental model of repetitive mild brain injury. *Ann Neurol.* 2013;74(1):65-75. doi:10.1002/ana.23858
131. Meehan WP, Zhang J, Mannix R, Whalen MJ. Increasing recovery time between injuries improves cognitive outcome after repetitive mild concussive brain injuries in mice. *Neurosurgery.* 2012;71(4):885-891. doi:10.1227/NEU.0b013e318265a439
132. Lovell MR, Collins MW, Iverson GL, et al. Recovery from mild concussion in high school athletes. *J Neurosurg.* 2003;98(2):296-301. doi:10.3171/jns.2003.98.2.0296
133. McCrea M, Guskiewicz K, Randolph C, et al. Incidence, clinical course, and predictors of prolonged recovery time following sport-related concussion in high school and college athletes. *J Int Neuropsychol Soc JINS.* 2013;19(1):22-33. doi:10.1017/S1355617712000872
134. Brooks J, Fos LA, Greve KW, Hammond JS. Assessment of executive function in patients with mild traumatic brain injury. *J Trauma.* 1999;46(1):159-163. doi:10.1097/00005373-199901000-00027
135. Kraus MF, Susmaras T, Caughlin BP, Walker CJ, Sweeney JA, Little DM. White matter integrity and cognition in chronic traumatic brain injury: a diffusion tensor imaging study. *Brain J Neurol.* 2007;130(Pt 10):2508-2519. doi:10.1093/brain/awm216
136. Sterr A, Herron KA, Hayward C, Montaldi D. Are mild head injuries as mild as we think? Neurobehavioral concomitants of chronic post-concussion syndrome. *BMC Neurol.* 2006;6:7. doi:10.1186/1471-2377-6-7
137. Perry VH, Nicoll JAR, Holmes C. Microglia in neurodegenerative disease. *Nat Rev Neurol.* 2010;6(4):193-201. doi:10.1038/nrneurol.2010.17
138. Tsitsopoulos PP, Marklund N. Amyloid- β Peptides and Tau Protein as Biomarkers in Cerebrospinal and Interstitial Fluid Following Traumatic Brain Injury: A Review of Experimental and Clinical Studies. *Front Neurol.* 2013;4:79. doi:10.3389/fneur.2013.00079
139. Haacke EM, Duhaime AC, Gean AD, et al. Common data elements in radiologic imaging of traumatic brain injury. *J Magn Reson Imaging JMRI.* 2010;32(3):516-543. doi:10.1002/jmri.22259
140. Bigler ED. Neuropathology of Mild Traumatic Brain Injury: Correlation to Neurocognitive and Neurobehavioral Findings. In: Kobeissy FH, ed. *Brain*

Neurotrauma: Molecular, Neuropsychological, and Rehabilitation Aspects. Frontiers in Neuroengineering. CRC Press/Taylor & Francis; 2015. Accessed September 9, 2021. <http://www.ncbi.nlm.nih.gov/books/NBK299214/>

141. Suri AK, Lipton ML. Neuroimaging of brain trauma in sports. *Handb Clin Neurol*. 2018;158:205-216. doi:10.1016/B978-0-444-63954-7.00021-5
142. Brenner DJ, Hall EJ. Computed tomography--an increasing source of radiation exposure. *N Engl J Med*. 2007;357(22):2277-2284. doi:10.1056/NEJMra072149
143. Wu X, Kirov II, Gonen O, Ge Y, Grossman RI, Lui YW. MR Imaging Applications in Mild Traumatic Brain Injury: An Imaging Update. *Radiology*. 2016;279(3):693-707. doi:10.1148/radiol.16142535
144. Kim HJ, Tsao JW, Stanfill AG. The current state of biomarkers of mild traumatic brain injury. *JCI Insight*. 2018;3(1):97105. doi:10.1172/jci.insight.97105
145. Weinstein E, Turner M, Kuzma BB, Feuer H. Second impact syndrome in football: new imaging and insights into a rare and devastating condition. *J Neurosurg Pediatr*. 2013;11(3):331-334. doi:10.3171/2012.11.PEDS12343
146. Karlsen RH, Einarsen C, Moe HK, et al. Diffusion kurtosis imaging in mild traumatic brain injury and postconcussional syndrome. *J Neurosci Res*. 2019;97(5):568-581. doi:10.1002/jnr.24383
147. Arfanakis K, Haughton VM, Carew JD, Rogers BP, Dempsey RJ, Meyerand ME. Diffusion tensor MR imaging in diffuse axonal injury. *AJNR Am J Neuroradiol*. 2002;23(5):794-802.
148. Mac Donald CL, Dikranian K, Bayly P, Holtzman D, Brody D. Diffusion tensor imaging reliably detects experimental traumatic axonal injury and indicates approximate time of injury. *J Neurosci Off J Soc Neurosci*. 2007;27(44):11869-11876. doi:10.1523/JNEUROSCI.3647-07.2007
149. Ranzenberger LR, Snyder T. Diffusion Tensor Imaging. In: *StatPearls*. StatPearls Publishing; 2021. Accessed September 9, 2021. <http://www.ncbi.nlm.nih.gov/books/NBK537361/>
150. Miles L, Grossman RI, Johnson G, Babb JS, Diller L, Inglese M. Short-term DTI predictors of cognitive dysfunction in mild traumatic brain injury. *Brain Inj*. 2008;22(2):115-122. doi:10.1080/02699050801888816
151. Tolomeo D. Development of a multimodal MRI study to characterize morpho-functional features in rodent models of Alzheimer's Disease, Istituto di Ricerche Farmacologiche Mario Negri IRCCS, 2018.
152. Puntmann VO, Peker E, Chandrashekar Y, Nagel E. T1 Mapping in Characterizing Myocardial Disease: A Comprehensive Review. *Circ Res*. 2016;119(2):277-299. doi:10.1161/CIRCRESAHA.116.307974

153. Douglas DB, Ro T, Toffoli T, et al. Neuroimaging of Traumatic Brain Injury. *Med Sci*. 2018;7(1):2. doi:10.3390/medsci7010002
154. Jolly RD, Thompson KG, Winchester BG. Bovine mannosidosis--a model lysosomal storage disease. *Birth Defects Orig Artic Ser*. 1975;11(6):273-278.
155. Dudink J, Larkman DJ, Kapellou O, et al. High b-value diffusion tensor imaging of the neonatal brain at 3T. *AJNR Am J Neuroradiol*. 2008;29(10):1966-1972. doi:10.3174/ajnr.A1241
156. Hulkower MB, Poliak DB, Rosenbaum SB, Zimmerman ME, Lipton ML. A decade of DTI in traumatic brain injury: 10 years and 100 articles later. *AJNR Am J Neuroradiol*. 2013;34(11):2064-2074. doi:10.3174/ajnr.A3395
157. Thaler HT, Ferber PW, Rottenberg DA. A statistical method for determining the proportions of gray matter, white matter, and CSF using computed tomography. *Neuroradiology*. 1978;16:133-135. doi:10.1007/BF00395227
158. Le Bihan D. Diffusion MRI: what water tells us about the brain. *EMBO Mol Med*. 2014;6(5):569-573. doi:10.1002/emmm.201404055
159. Basser PJ, Mattiello J, LeBihan D. Estimation of the effective self-diffusion tensor from the NMR spin echo. *J Magn Reson B*. 1994;103(3):247-254. doi:10.1006/jmrb.1994.1037
160. Rutgers DR, Fillard P, Paradot G, Tadié M, Lasjaunias P, Ducreux D. Diffusion tensor imaging characteristics of the corpus callosum in mild, moderate, and severe traumatic brain injury. *AJNR Am J Neuroradiol*. 2008;29(9):1730-1735. doi:10.3174/ajnr.A1213
161. Lövdén M, Bodammer NC, Kühn S, et al. Experience-dependent plasticity of white-matter microstructure extends into old age. *Neuropsychologia*. 2010;48(13):3878-3883. doi:10.1016/j.neuropsychologia.2010.08.026
162. Parizel PM, Ozsarlak null, Van Goethem JW, et al. Imaging findings in diffuse axonal injury after closed head trauma. *Eur Radiol*. 1998;8(6):960-965. doi:10.1007/s003300050496
163. Zhang J, Aggarwal M, Mori S. Structural insights into the rodent CNS via diffusion tensor imaging. *Trends Neurosci*. 2012;35(7):412-421. doi:10.1016/j.tins.2012.04.010
164. Sun S-W, Liang H-F, Cross AH, Song S-K. Evolving Wallerian degeneration after transient retinal ischemia in mice characterized by diffusion tensor imaging. *NeuroImage*. 2008;40(1):1-10. doi:10.1016/j.neuroimage.2007.11.049
165. Macdonald C, Dikranian K, Song S, Bayly P, Holtzman D, Brody D. Detection of traumatic axonal injury with diffusion tensor imaging in a mouse model of traumatic brain injury. *Exp Neurol*. 2007;205(1):116-131. doi:10.1016/j.expneurol.2007.01.035

166. Farrell JAD, Landman BA, Jones CK, et al. Effects of signal-to-noise ratio on the accuracy and reproducibility of diffusion tensor imaging-derived fractional anisotropy, mean diffusivity, and principal eigenvector measurements at 1.5 T. *J Magn Reson Imaging JMRI*. 2007;26(3):756-767. doi:10.1002/jmri.21053
167. Rohde GK, Barnett AS, Basser PJ, Marengo S, Pierpaoli C. Comprehensive approach for correction of motion and distortion in diffusion-weighted MRI. *Magn Reson Med*. 2004;51(1):103-114. doi:10.1002/mrm.10677
168. Wintermark M, Sanelli PC, Anzai Y, Tsiouris AJ, Whitlow CT, American College of Radiology Head Injury Institute. Imaging evidence and recommendations for traumatic brain injury: advanced neuro- and neurovascular imaging techniques. *AJNR Am J Neuroradiol*. 2015;36(2):E1-E11. doi:10.3174/ajnr.A4181
169. Lipton ML, Kim N, Park YK, et al. Robust detection of traumatic axonal injury in individual mild traumatic brain injury patients: intersubject variation, change over time and bidirectional changes in anisotropy. *Brain Imaging Behav*. 2012;6(2):329-342. doi:10.1007/s11682-012-9175-2
170. Tang-Schomer MD, Patel AR, Baas PW, Smith DH. Mechanical breaking of microtubules in axons during dynamic stretch injury underlies delayed elasticity, microtubule disassembly, and axon degeneration. *FASEB J Off Publ Fed Am Soc Exp Biol*. 2010;24(5):1401-1410. doi:10.1096/fj.09-142844
171. Siedler DG, Chuah MI, Kirkcaldie MTK, Vickers JC, King AE. Diffuse axonal injury in brain trauma: insights from alterations in neurofilaments. *Front Cell Neurosci*. 2014;8:429. doi:10.3389/fncel.2014.00429
172. Johnson VE, Stewart W, Smith DH. Axonal pathology in traumatic brain injury. *Exp Neurol*. 2013;246:35-43. doi:10.1016/j.expneurol.2012.01.013
173. Meaney DF, Smith DH. Biomechanics of concussion. *Clin Sports Med*. 2011;30(1):19-31, vii. doi:10.1016/j.csm.2010.08.009
174. Mukherjee P, Berman JI, Chung SW, Hess CP, Henry RG. Diffusion tensor MR imaging and fiber tractography: theoretic underpinnings. *AJNR Am J Neuroradiol*. 2008;29(4):632-641. doi:10.3174/ajnr.A1051
175. Shin W, Mahmoud SY, Sakaie K, et al. Diffusion measures indicate fight exposure-related damage to cerebral white matter in boxers and mixed martial arts fighters. *AJNR Am J Neuroradiol*. 2014;35(2):285-290. doi:10.3174/ajnr.A3676
176. Bennett RE, Mac Donald CL, Brody DL. Diffusion tensor imaging detects axonal injury in a mouse model of repetitive closed-skull traumatic brain injury. *Neurosci Lett*. 2012;513(2):160-165. doi:10.1016/j.neulet.2012.02.024
177. Wang S, Wu EX, Qiu D, Leung LHT, Lau H-F, Khong P-L. Longitudinal diffusion tensor magnetic resonance imaging study of radiation-induced white matter damage in a rat model. *Cancer Res*. 2009;69(3):1190-1198. doi:10.1158/0008-5472.CAN-08-2661

178. Hasan KM, Wilde EA, Miller ER, et al. Serial atlas-based diffusion tensor imaging study of uncomplicated mild traumatic brain injury in adults. *J Neurotrauma*. 2014;31(5):466-475. doi:10.1089/neu.2013.3085
179. Bazarian JJ, Zhong J, Blyth B, Zhu T, Kavcic V, Peterson D. Diffusion tensor imaging detects clinically important axonal damage after mild traumatic brain injury: a pilot study. *J Neurotrauma*. 2007;24(9):1447-1459. doi:10.1089/neu.2007.0241
180. Eierud C, Craddock RC, Fletcher S, et al. Neuroimaging after mild traumatic brain injury: review and meta-analysis. *NeuroImage Clin*. 2014;4:283-294. doi:10.1016/j.nicl.2013.12.009
181. Lo C, Shifteh K, Gold T, Bello JA, Lipton ML. Diffusion tensor imaging abnormalities in patients with mild traumatic brain injury and neurocognitive impairment. *J Comput Assist Tomogr*. 2009;33(2):293-297. doi:10.1097/RCT.0b013e31817579d1
182. Alhilali LM, Yaeger K, Collins M, Fakhran S. Detection of central white matter injury underlying vestibulopathy after mild traumatic brain injury. *Radiology*. 2014;272(1):224-232. doi:10.1148/radiol.14132670
183. Fakhran S, Yaeger K, Alhilali L. Symptomatic white matter changes in mild traumatic brain injury resemble pathologic features of early Alzheimer dementia. *Radiology*. 2013;269(1):249-257. doi:10.1148/radiol.13122343
184. Chung H-W, Chou M-C, Chen C-Y. Principles and limitations of computational algorithms in clinical diffusion tensor MR tractography. *AJNR Am J Neuroradiol*. 2011;32(1):3-13. doi:10.3174/ajnr.A2041
185. Steven AJ, Zhuo J, Melhem ER. Diffusion kurtosis imaging: an emerging technique for evaluating the microstructural environment of the brain. *AJR Am J Roentgenol*. 2014;202(1):W26-33. doi:10.2214/AJR.13.11365
186. Matthies S, Rüsçh N, Weber M, et al. Small amygdala – high aggression? The role of the amygdala in modulating aggression in healthy subjects. *World J Biol Psychiatry*. 2012;13(1):75-81. doi:10.3109/15622975.2010.541282
187. Blatter DD, Bigler ED, Gale SD, et al. MR-based brain and cerebrospinal fluid measurement after traumatic brain injury: correlation with neuropsychological outcome. *AJNR Am J Neuroradiol*. 1997;18(1):1-10.
188. Ding K, de la Plata CM, Wang JY, et al. Cerebral Atrophy after Traumatic White Matter Injury: Correlation with Acute Neuroimaging and Outcome. *J Neurotrauma*. 2008;25(12):1433-1440. doi:10.1089/neu.2008.0683
189. Hofman PA, Stapert SZ, van Kroonenburgh MJ, Jolles J, de Kruijk J, Wilmink JT. MR imaging, single-photon emission CT, and neurocognitive performance after mild traumatic brain injury. *AJNR Am J Neuroradiol*. 2001;22(3):441-449.

190. Misquitta K, Dadar M, Tarazi A, et al. The relationship between brain atrophy and cognitive-behavioural symptoms in retired Canadian football players with multiple concussions. *NeuroImage Clin.* 2018;19:551-558. doi:10.1016/j.nicl.2018.05.014
191. Tate DF, York GE, Reid MW, et al. Preliminary findings of cortical thickness abnormalities in blast injured service members and their relationship to clinical findings. *Brain Imaging Behav.* 2014;8(1):102-109. doi:10.1007/s11682-013-9257-9
192. Wilde EA, Hunter JV, Li X, et al. Chronic Effects of Boxing: Diffusion Tensor Imaging and Cognitive Findings. *J Neurotrauma.* 2016;33(7):672-680. doi:10.1089/neu.2015.4035
193. Kornguth S, Rutledge N, Perlaza G, Bray J, Hardin A. A Proposed Mechanism for Development of CTE Following Concussive Events: Head Impact, Water Hammer Injury, Neurofilament Release, and Autoimmune Processes. *Brain Sci.* 2017;7(12):164. doi:10.3390/brainsci7120164
194. Churchill N, Hutchison M, Richards D, Leung G, Graham S, Schweizer TA. Brain Structure and Function Associated with a History of Sport Concussion: A Multi-Modal Magnetic Resonance Imaging Study. *J Neurotrauma.* 2017;34(4):765-771. doi:10.1089/neu.2016.4531
195. Raji CA, Merrill DA, Barrio JR, Omalu B, Small GW. Progressive Focal Gray Matter Volume Loss in a Former High School Football Player: A Possible Magnetic Resonance Imaging Volumetric Signature for Chronic Traumatic Encephalopathy. *Am J Geriatr Psychiatry.* 2016;24(10):784-790. doi:10.1016/j.jagp.2016.07.018
196. Zhou Y, Kierans A, Kenul D, et al. Mild traumatic brain injury: longitudinal regional brain volume changes. *Radiology.* 2013;267(3):880-890. doi:10.1148/radiol.13122542
197. Monti JM, Voss MW, Pence A, McAuley E, Kramer AF, Cohen NJ. History of mild traumatic brain injury is associated with deficits in relational memory, reduced hippocampal volume, and less neural activity later in life. *Front Aging Neurosci.* 2013;5:41. doi:10.3389/fnagi.2013.00041
198. Smith DH, Meaney DF, Shull WH. Diffuse Axonal Injury in Head Trauma: *J Head Trauma Rehabil.* 2003;18(4):307-316. doi:10.1097/00001199-200307000-00003
199. Zanier ER, Marchesi F, Ortolano F, et al. Fractalkine Receptor Deficiency Is Associated with Early Protection but Late Worsening of Outcome following Brain Trauma in Mice. *J Neurotrauma.* 2016;33(11):1060-1072. doi:10.1089/neu.2015.4041
200. Shelton SB, Pettigrew DB, Hermann AD, et al. A simple, efficient tool for assessment of mice after unilateral cortex injury. *J Neurosci Methods.* 2008;168(2):431-442. doi:10.1016/j.jneumeth.2007.11.003
201. Todd D. Gould, David T. Dao, Colleen E. Kovacsics. *The Open Field Test, Mood and Anxiety Related Phenotypes in Mice, Neuromethods 42, Doi: 10.1007/978-1-60761-303-9_1, 2009.*

202. Santamaria G, Brandi E, Vitola PL, et al. Intranasal delivery of mesenchymal stem cell secretome repairs the brain of Alzheimer's mice. *Cell Death Differ.* 2021;28(1):203-218. doi:10.1038/s41418-020-0592-2
203. Lueptow LM. Novel Object Recognition Test for the Investigation of Learning and Memory in Mice. *J Vis Exp JoVE.* 2017;(126). doi:10.3791/55718
204. Smith SM, Jenkinson M, Johansen-Berg H, et al. Tract-based spatial statistics: voxelwise analysis of multi-subject diffusion data. *NeuroImage.* 2006;31(4):1487-1505. doi:10.1016/j.neuroimage.2006.02.024
205. Jenkinson M, Beckmann CF, Behrens TEJ, Woolrich MW, Smith SM. FSL. *NeuroImage.* 2012;62(2):782-790. doi:10.1016/j.neuroimage.2011.09.015
206. Bai J, Trinh TLH, Chuang K-H, Qiu A. Atlas-based automatic mouse brain image segmentation revisited: model complexity vs. image registration. *Magn Reson Imaging.* 2012;30(6):789-798. doi:10.1016/j.mri.2012.02.010
207. Ma D, Cardoso MJ, Modat M, et al. Automatic structural parcellation of mouse brain MRI using multi-atlas label fusion. *PloS One.* 2014;9(1):e86576. doi:10.1371/journal.pone.0086576
208. Nie J, Shen D. Automated segmentation of mouse brain images using multi-atlas multi-ROI deformation and label fusion. *Neuroinformatics.* 2013;11(1):35-45. doi:10.1007/s12021-012-9163-0
209. Wang H, Yushkevich PA. Multi-atlas segmentation with joint label fusion and corrective learning—an open source implementation. *Front Neuroinformatics.* 2013;7. doi:10.3389/fninf.2013.00027
210. Avants BB, Tustison NJ, Stauffer M, Song G, Wu B, Gee JC. The Insight ToolKit image registration framework. *Front Neuroinformatics.* 2014;8:44. doi:10.3389/fninf.2014.00044
211. Dorr AE, Lerch JP, Spring S, Kabani N, Henkelman RM. High resolution three-dimensional brain atlas using an average magnetic resonance image of 40 adult C57Bl/6J mice. *NeuroImage.* 2008;42(1):60-69. doi:10.1016/j.neuroimage.2008.03.037
212. Das SR, Avants BB, Grossman M, Gee JC. Registration based cortical thickness measurement. *NeuroImage.* 2009;45(3):867-879. doi:10.1016/j.neuroimage.2008.12.016
213. Pagani M, Bifone A, Gozzi A. Structural covariance networks in the mouse brain. *NeuroImage.* 2016;129:55-63. doi:10.1016/j.neuroimage.2016.01.025
214. Namjoshi DR, Good C, Cheng WH, et al. Towards clinical management of traumatic brain injury: a review of models and mechanisms from a biomechanical perspective. *Dis Model Mech.* 2013;6(6):1325-1338. doi:10.1242/dmm.011320

215. Mouzon BC, Bachmeier C, Ojo JO, et al. Lifelong behavioral and neuropathological consequences of repetitive mild traumatic brain injury. *Ann Clin Transl Neurol.* 2018;5(1):64-80. doi:10.1002/acn3.510
216. Jolly AE, Bălăeș M, Azor A, et al. Detecting axonal injury in individual patients after traumatic brain injury. *Brain.* 2021;144(1):92-113. doi:10.1093/brain/awaa372
217. Blennow K, Brody DL, Kochanek PM, et al. Traumatic brain injuries. *Nat Rev Dis Primer.* 2016;2(1):16084. doi:10.1038/nrdp.2016.84